Thesis for MSc Transport, Infrastructure and Logistics

A capacity-effective scheduling approach for Virtual Coupling train operations

Rui Miao

2021

TU Delft

A CAPACITY-EFFECTIVE SCHEDULING APPROACH FOR VIRTUAL COUPLING TRAIN OPERATIONS

A thesis submitted to the Delft University of Technology in partial fulfillment
of the requirements for the degree of

Master of Science
in Transportation, Infrastructure & Logistics

by

Rui Miao

2021

Supervisors: Prof.dr. R.M.P. (Rob) Goverde - CITG
Dr.ir. E. (Egidio) Quaglietta - CITG
Dr. N. (Nikola) Bešinović - CITG
Dr.ir. A.J.J. van den Boom (Ton) - 3ME

CONTENTS

1 INTRODUCTION

Rapid urbanization and population growth worldwide have profound implications for the future world of railway operation, and passenger demand is expected to increase under this trend. Meanwhile, due to global targets for energy conservation and pollution reduction, the rail freight model is expected to be greener than other models, so it has more policy support to accept future demand. Rotoli et al. [2016] Sessa and Isis [2010] To meet the increasing travel demand and release transportation pressure, railway researchers have updated the signal control system early from fixed blocked line-side signals under National Automatic Train Protection systems (ATP) to ETCS L1, 2 and 3 which is still under investigation and development. By further application of radio communications the ETCS Level 3 (L3) with moving block (MB) has now been developed.

Recent studies have proposed the concept of virtual coupling (VC) based on the concept of moving block to to allow trains to move closer to each other than the absolute braking distance to further gain capacity. Several researchers (MOVINGRAIL [2019], Felez et al. [2019]) as well as international research projects (like the EC Shift2Rail MOVINGRAIL) have investigated potential benefits and ways to implement it. In virtual coupling, trains run in rows and can be treated as a single train, thus saving railway capacity, especially at bottlenecks. For trains that share the same section of track, they can line up at the same speed and acceleration, keeping relatively short distances apart. However, as a new topic, virtual coupling is still in its infancy, and there is no research on service planning under virtual coupling. This research is going to propose a service plan acquisition model based on virtual coupling operation to optimize the utilization of track capacity.

2 LITERATURE REVIEW

2.1 Literature review on railway timetable scheduling

As defined by Caimi et al. [2017], railway schedules are usually arranged in the following process. Timetables are designed for a given time period, and the periodic timetables refer to 1 hour. This can be achieved by many methods and different optimization objectives, which will be explained latter. Then a generic weekly timetable is generated by rolling out the single period for one week time. Secondly, the generic weekly timetable is updated by non-periodic elements, such as such as eliminating night train service, planning different operation times on weekdays and weekends, as well as planning different frequencies during peak hours and off-peak hours. The result of this step is to generate a partial cycle schedule in which the passenger-related descriptions act as an influencing factor for the train operating schedule. Next, the partially periodic timetable is going to be detailed into a daily timetable for each calendar day. In this procedure, the timetable is adjusted according to the specific date. For example, on the infrastructure maintenance day some trains need to be canceled or rerouted. Another example is if a special public event is expected to increase the load, the train service for that day should be rescheduled. After these steps, the daily schedule is fixed, with vehicle circulation and crew schedules being the next matching plan.

The timetable models in the study have two main objectives. One is to schedule the timetable including routing the train and scheduling the events to meet service levels, such as minimum running time, minimum transfer time and maximize transport demand. The other is to increase the timetable's robustness, such as minimizing delayed propagation and maintaining punctuality. Setyawan and Diah Damayanti [2018] Especially when the infrastructure capacity is saturated, the robustness of the trains should be cared to face any random interrupts. The robustness of schedules can be improved by optimally allocating the supplementary time between a single train operation (e.g., run time recovery) and a continuous train operation (e.g., buffer time). The timetable models are realized by means of analytical models, which can describe the trains' events such as dwelling, arrival, departure times.The schedule should clearly specify the departure time and arrival time, which satisfies the requirement of dwell time and running time, and without conflict. The classic periodic timetable model proposed by Serafini and Ukovich [1989] uses a mathematical model to describe the Periodic Event Scheduling Problem (PESP). In PESP, the trains events such as departure and arrival are constrained by time, such as minimum dwell time, minimum running time as well as buffer time.

Researchers use many variants to update the PESP model to adapt to different conditions, with various solutions, such as MIP, constraint programming, genetic algorithm. Geraets et al. [2007] To promote the transfer fluency, a so-called integrated fixed-interval timetable (IFIT) was developed by (FGSV,2001), and it chooses specific stations as hubs and the train lines arriving in and departing from these hubs are concentrated in the same time window. Corman et al. [2011] constructed a graph model to solve the minimum delay problem in multi-level networks, which was solved by train sequence and time schedules, in which trains with higher priority were guaranteed first to maintain the quality of the solution, while trains with lower priority were given less consideration. Pellegrini et al. [2017] established a

saturated timetable model, in which the network has two types of trains, existing scheduled saturation trains and new added freight trains. This problem is also solved by means of a MILP model. Bešinović et al. [2019] addressed the problem of timetable instability by using a heuristic method to solve a MILP model, which develops a stable timetable. Meanwhile, it maximizes the satisfaction of transportation demand within a limited railway capacity.

In addition to the PESP based model, there are some other timetabling models such as Feasible Differential Problem (FDP) model, Train Timetabling Problem (TTP), as well as individual trip scheduling problem (ITSP). The TTP model requires an ideal train path as input. It is now a popular practice for infrastructure managers to develop train schedules that best meet the train service requirements of train operators. By post-processing, the intermeshed network timetable ban be combined with corridor timetables for infrastructure managers. Caprara et al. [2002] This research formulates the problem in MILP based on graph theory, adopts Lagrange relaxation method, and uses heuristic algorithm to solve it. The FDP model has the characteristic pre-defining train sequence and taking it as the model input,, which means that the optimal solution provided does not take the service order as a decision variable. Vansteenwegen and Oudheusden [2006] In addition, to consider the transfer between trains, it should also Determine in advance which pairs of trains can transfer. Compared with the FDP and TTP, the ITSP model is suitable for networks with small scale and shorter time. It does not require prepossessed inputs such as train sequence and can start from a completely empty network, as mentioned in Caimi et al. [2017]. Therefore, it is suitable for a new network or for a network with a new operation control mode, such as upgrading the train control system for a part of the network. There are also many ways to improve the robustness of the schedule model. As listed in Caimi et al. [2017], there are many robust transfer penalty function methods, stochastic programming methods for redistributive relaxation, light robust modeling frameworks, delay-resistant scheduling methods, event flexibility methods and recoverability robust methods.

Although researchers have proposed many methods for the timetable scheduling, the timetable research focusing on the virtual coupling is still a new topic and how does the virtual coupling affect the timetable scheduling as well as the capacity of the new timetables is still unknown.

2.2 Literature review on railway capacity evaluation

A consolidated method to assess railway capacity defined in the UIC Code 406 introduces the concept of timetable compression to identify the total rate of infrastructure occupation and the overall amount of time allowances to help timetable stability and robustness rather than daily statistical changes in train operating times, see UIC [2013]. Landex et al. [2008] expounded and explained the method of UIC 406, including dividing railway lines into line segments, analyzing intersections and stations with overtaking, crossing and ending line plans, and analyzing multiple lines. In addition to UIC 406, the Capacity Utilization Index (CUI) method is another way to compress the timetable and obtain the updated occupancy time. The difference is that the UIC 406 divides the lines into blocks between signals while the CUI method takes into account less detail and is based on headway values. Therefore, the CUI method can analyze longer corridors. For more comparative details, see Sameni [2012]. The UIC 406 method is widely used in Dutch railways, cooperating with block time timetable method. For example, in Goverde et al. [2013], the method of UIC 406 is applied to compare the capacity consumption between conventional Dutch NS'54/ATB signal system and the ETCS L2, and concludes that the ETCS L2 saves more braking distance and has a stabilizing effect on headway times, delay propagation and throughtput. There are several programs that use compression methods for schedule estimation, such as RailSys, EGTRAIN, and OpenTrack.

2.3 Literature review on the control of moving block and virtual coupling

Ning [1998] explained two modes in moving block systems, including absolute braking distance and relative braking distance, which are the distance maintained in the vehicle following model. It has been clarified that the braking distance is affected by the two trains' locations, speeds, safe protection distance, fluctuation protection distance, braking capacity, as well as the line conditions and environment factors. According to the theoretical calculation, with the support of communication technology, the moving block operation has more advantages than the fixed block operation, and the relative braking distance method saves more space than the absolute braking distance method. To further develop this idea from the perspective of simulations, there a number of studies have been done on moving blocks. For example, Ho et al. [1998] developed a multi-train motion simulator with moving signal blocks. It enables railway operators to obtain minimum headway and check conflicts with different speed limits and priorities, different track geometry and locomotive parameters. This research explained the details of headway calculation method. Another example is in Zhang et al. [2005]. This simulation method explained the delay calculation under moving block, and then showed the simulator interface and the simulation result. Basile et al. [2019] simulated the ETCS L3 communication system on Simulink and Uppaal SMC, verified that the message communication between satellite, trains and radio block centre is safe for the moving block.

Virtual coupling advances the concept of moving block by reducing even further train separation to less than an absolute braking distance. Xu et al. [2012] simulated the rail traffic flow under moving block with minimum instantaneous distance. In this paper, the relative braking distance mode is called "hit soft wall" tracking operation mode, which is the preliminary idea of the virtual coupling. Afterwards, the clear operational principles and running modes of trains under virtual coupling were defined by Quaglietta et al. [2020] as well as the EC Shift2Rail project MOVINGRAIL. Quaglietta [2019] ddefined preliminary operational principles of train operation under virtual coupling.

As for the practicability and the operational expenses, as indicated in MOVINGRAIL [2019], it needs to upgrade some necessary infrastructure, such as overhead line systems, platforms, and possibly switch technologies, but based on the developing on-board automatic operation devices and V2V communication architectures, this part of the investigation costs can be the same. In addition, according to the survey in this report, if the cost of travel remains the same, most people expect virtual companion to provide higher frequency of service. MOVINGRAIL [2019] It is also pointed out that the current switch technology cannot switch quickly to support the virtual coupling, so the follower still needs to keep the absolute braking distance with the front vehicle at the diverging junction.

2.4 Literature review on moving block and virtual coupling's timetable model and capacity evaluation

The proposed scheduling models mainly deal with the traditional fixed block train separation, but there is no relevant literature for the moving block and virtual coupling. A qualitative study is carried out and a method is proposed to analyze the potential improvement on capacity with the line operation changed from fixed block system to moving block system. This is a rapid qualitative evaluation method based on the number of trains, average speed, stability and heterogeneity.Ying [2014] However, this method does not form a timetable for train control guidance at the operating level. Duan and Schmid [2019] simulated the moving block under relative

braking distance with optimal headway distance. The results show that the moving block with relative braking distance has smaller headway and higher theoretical capacity than the traditional moving block and the fixed block signal system. Liu and Han [2017] focused on the headway's effect on timetables, and extended the MIP model to column generation model to consider all the time slots, thus finding the optimal timetable. This study only studies the headway effect from a mesoscopic perspective, ignoring the signal system mechanism during train operation. Dick et al. [2019] compared the capacity and punctuality performance between fixed block three-aspect signal system and moving-block absolute braking distance control system under different service levels (percentage of using the second main track) in a north American cargo passenger hybrid corridor. Its result shows a greater capacity benefit for a higher level of service. Schumann [2017] simulated the virtual coupling operation on Shinkansen high-speed lines and verified the capacity benefit, and the reasons are as follow: First of all, the virtual coupling combines several trains on the main line together, thus saving the number of rolling stocks, because it is the number of vehicles rather than the length that affects railway capacity; Secondly, due to the low speed near the station, the braking distance of the intermodal train after departure is shorter; Thirdly, another benefit of virtual coupling is that when a train needs to wait to overtake, coupling an overtaking train can save waiting time.

In conclusion, as the next step in moving block development, virtual coupling has been shown to reduce train capacity utilization, thus providing the opportunity to run more trains within less time and increasing flexibility to make it more tailored to customer travel needs. However, so far, the railway traffic scheduling model under virtual coupling has not been determined, and it is crucial to determine the operation plan that can be executed under virtual coupling to improve the capability bottleneck.

3 RESEARCH PROBLEM

3.1 Problem description

As introduced in Caimi et al. [2017], adjusting the frequency of train routes during peak and off-peak hours is an important step in daily schedule design. Virtual coupling is an alternative operation way for trains running in peak hours which can improve network capacity and make train services more flexible and more responsive to travel needs. This research is going to propose a model to design the timetable with the objective of maxmizing capacity utilisation, which is going to save the infrastructure occupation time for a given timetable pattern, and to observe the trains operation under virtual coupling. A convoy is a list of trains which departs from the same station under the mode of virtual coupling. It can be called as a platoon when they are coupled, running in the minimum distance and same speed. The process of the platoon forming in a convoy will be analyzed,

The advent of virtual coupling will revolutionize the way in which trains are rescheduled, because the operation of a train will depend on the operation of other trains that they will couple to when forming platoons. In the optimal capacity timetable schedule, the train's behaviour on an intermesh network is unknown, especially some bottlenecks such as merging at the junctions or departure from a station. For example, a train at a platform might wait for a longer time resulting in a later departing time to couple with the next trains, or it also might partially accelerating to let the next trains couple and result in a late arrival time, or it might not consider the following trains. Thus up to now, how to optimally forming a platoon is unknown. Also, it would be crucial to understand when and where trains shall form or decompose platoons, for example at a diverging junction, before stop or after departure and how far away. Meanwhile, it is expected that coupling the trains departing in batch for a same route can increase the capacity but will couple the trains departing in turns, which need to split for different destination, also have this benefit. How much such capacity benefit can be obtained compared to the moving block also requires investment. These questions will be answered in this research by establishing a model with the goal of optimal capacity utilization.

The main question of this research is **How can Virtual Coupling railway operation be optimally scheduled to maximize capacity utilization by forming platoons?** The sub-questions of this research are as follows:

- 1.How will the operation of the trains be adjusted in a convoy to form a platoon under virtual coupling, comparing to moving block?
- 2.How can train running times and headway be adjusted to satisfy an optimized formation of virtually coupled platoons?
- 3.What and where are the actual capacity gains that Virtual Coupling can provide over plain moving Block if an optimized platoon formation is considered?

Taking the Y-shape network as the studied case, this paper carries out theoretical experiments on the network, under different timetable patterns, verified by changing the number of trains,to study the benefit brought from virtual coupling, compared with the moving blocks so as to answer the above questions. The sensitivity analysis on the speed limit and the service braking rate will also be conducted.

3.2 Network introduction

The following is the Y-shape network to be studied by this research. It consists of three sections connected by one transfer station. In this example, all trains depart from Station A, stop at Station B for a predefined dwell time, then one part of the trains go to Station C, while the others go to Station D. Location R is the switching point in front of Station B, where the trains diverge to different destinations. The details of the layout and how the layout is modelled will be introduced in Section 5.1, Case study set up.

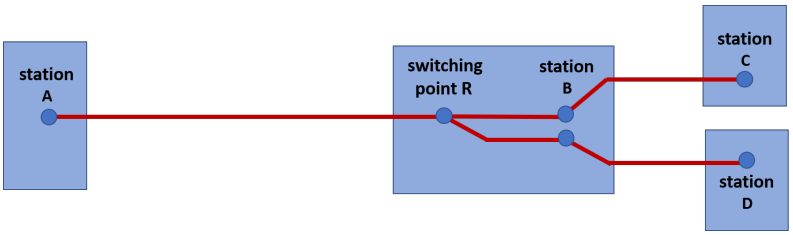

Figure 3.1: Network demonstration

4 METHODOLOGY

The method used to compute the timetable and observe the trains operation is to build a multi-objective mixed integer quadratic programming(MIQP) model. The overview of the model is shown in Figure 4.1. The input of the model contains the trains information and the route information. The output of the model gives the the optimal solution of the trains operation and timetable results including the information as trains' headway, time and speed at each location, and the speed difference. The objective of the model is to form a platoon and making the most utilization of the capacity. The model is constraint by the kinematic motion and dynamic equations for single train and the convoys running principles for adjacent trains.

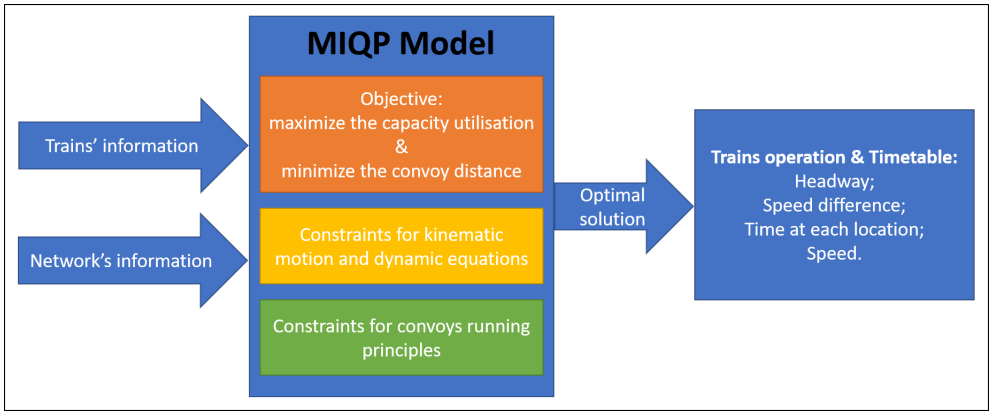

Figure 4.1: Illustration of the model

4.1 convoy's running principles under virtual coupling

The following is the trains' running principles in a convoy under virtual coupling, defined in Quaglietta et al. [2020] which is also the trains' running principles in this research. The following will call a couple of trains leader and follower, referring to two trains under virtual coupling. For the operation mode of virtual coupling, the trains in a convoy are defined to have the state of coupling, state of coupled, and state of decoupling. The operation principles of these states will be explained in this section and the model of these states will be explained in section 4.3.

For the trains sharing the same route or the same part of the route, the trains will always start running in the coupling state. Coupling state is a state in which a convoy's followers try to catch up with the leader, trying to maintain the same speed, and trying to keep a minimum safety distance. Under the coupling state, if the follower in the convoy has a speed larger than the leader, the follower will brake to decrease its speed. The distance between two trains is the distance covered by the follower braking to a same speed as the leader. Considering the distance between the head of the leader and the follower, this safety distance shall plus the clearing time of the leader. If the follower's speed is smaller than that of the leader, the follower will increase its speed. To keep a minimum distance, the follower tends to accelerate to have a higher speed than the leader, and then slows down to the same

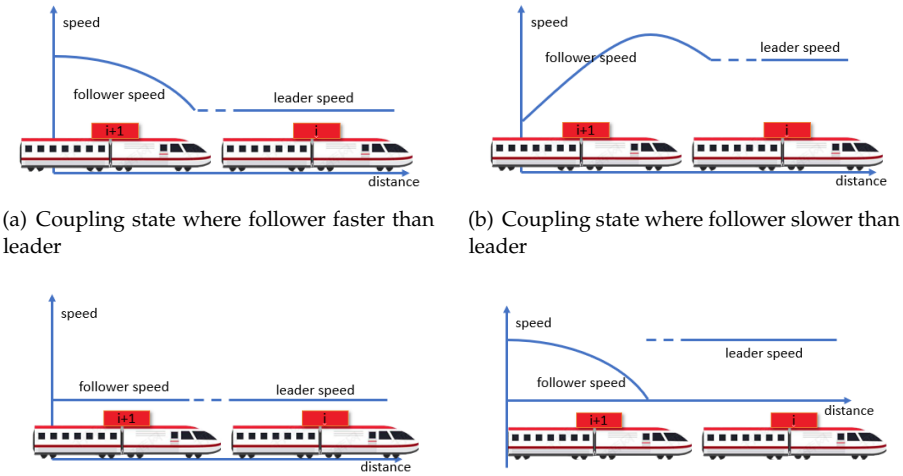

(a) Coupling state where follower faster than leader

(b) Coupling state where follower slower than leader

(c) Coupled state

(d) decoupling state

Figure 4.2: Operation states under Virtual coupling

speed as the leader in a minimum safety distance. The minimum safety distance is the distance of the follower passing through when changing its speed plus an extra safety distance, as well as the clearing time of the leader.

The coupled state is the result and objective of the coupling state. The leader and the follower have the same speed and a minimum safety margin. Once the trains are coupled, the convoy can be called a platoon, and the control of the trains in a platoon can have the same speed, same acceleration, same traction force. The platoon can be seen as a separate train, which improves the capacity utilization.

The decoupling state occurs in two situations. Firstly, it happens when the trains cannot maintain the coupled state. For example, the traction force or the power cannot support the follower to closely follow the leader. Secondly, it happens at the diverging junctions, where if the trains are going to different routes, there must be enough time for the switch to operate. In the decoupling state, the trains in the convoy keep an absolute braking distance, which is the same as the moving block operation.

4.2 Modelling assumptions

The inter-station sections are divided into N space-discrete train behavioral intervals, which will be named as **intervals** in the following description. The length of each interval can be unequal, as shown in Figure 4.3. A distance of 30km between Station A and Station B is divided into 40 intervals, where the first 28 intervals are 1000m each followed by a 500m interval, and the 10 intervals before the switching point R are 100m for each. The reason why the section is divided in this way will be explained in Section 4.5, "Headway model for decoupling state". It is assumed that the trains in each interval are accelerating and decelerating at a uniform speed in each interval. Therefore, the trains' motions in each interval have the attributes of initial speed, end speed and constant acceleration, where the end speed of one interval is the initial speed of another interval.

These attributes will be addressed by a Multi-objective Mixed Integer Quadratic Programming (MIQP) Model to maximize the utilization of the track's capacity. This model aims at an optimal speed profile of the platoons to take full advantage of the capacity, in which departure time, arrival time and running time constitute the key factors of the schedule.

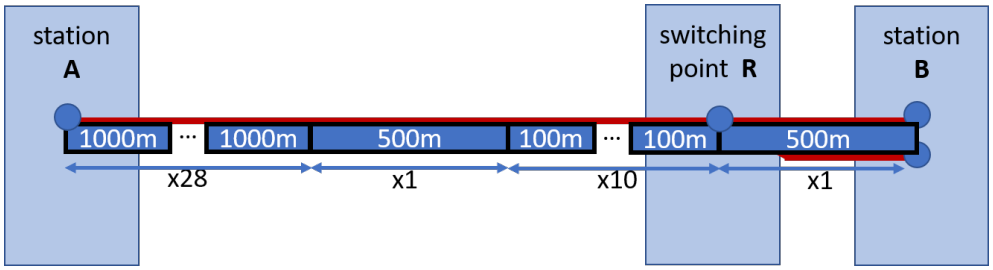

Figure 4.3: Example of the space-discrete train behavioral intervals on a section

4.2.1 Equation term Nomenclature

Sets

I The set of all the trains

I_r The set of trains operating route r.

J The set of sections.

K_j The set of space-discrete train behavioral intervals in section j.

Indexes

i Index of train

j Index of sections

k_j Index of space-discrete train behavioral intervals belonging to section j.

Decision Variables

a_{i,k_j} The acceleration of the train i over interval k_j. The positive value means acceleration. The negative value means deceleration.

τ_{i,k_j} The running time of the train i over interval k_j

v_{i,k_j} The speed of the train i at location k_j

v_{b',i,k_j} The speed to approach the leader, which is the speed needed by the follower to catch up and approach the leader for coupling to it.

y_{i,k_j} Binary variable, which reflects the coupling state of the train. y_{i,k_j} equals to 0 means the following train with index i's speed is smaller than the leading train with index i-1.

γ_i Binary variable. It equals 1 means the train i can be scheduled within the period, and equalling to 0 means the train cannot be scheduled in the period.

Indirect Variables

R_{i,k_j} The forces exerted of affecting the train i at the start node of the interval k_j.

T_{i,k_j} The traction force of the train i at the start node of interval k_j. If it gives a negative value, it means the braking force.

t_{i,k_j} The time of train i crosses location k_j

t'_{i,k_j} The middle time of train i crosses interval k_j

v'_{i,k_j} The multiplicative inverse of v_{i,k_j}

$\bar{v}_{i,k_j}$ The average speed if the train i over interval k

$\bar{v}'_{i,k}$ The multiplicative inverse of $\bar{v}_{i,k_j}$

Parameters

$a_{\max}$ Maximum acceleration

$b_{s,i}$ Service braking rate for train i

c_1, c_2, c_3 The resistance coefficient of the Davis equation

d_{k_j} The length (e.g., 500m) of the space-discrete train behavioral interval k_j. The space-discrete train behavioral intervals will be called as intervals in the following description.

f_p Rotating mass factor

L_j The distance between the stations for section j (e.g., 30km).

l_i The length of the train i

m_i The mass of train i

s_m An extra safety margin with respect to the relative or absolute braking distance.
$v_{\max,k_j}$ Maximum speed over interval k_j
N The number of space-discrete train behavioral intervals.
$T_{\max,i}$ Maximum traction force
M An extremely big value used in the big M method for optimization problem formulation
B An extremely small positive value used in the big M method for optimization problem formulation

4.3 Model for single train's operation

4.3.1 Constraints describing Kinematic Motion Equations

For each train i, assuming the trains in each interval move in uniform acceleration and deceleration, the speed of the start and end node of the interval is described as (4.1), where a_{i,k_j} is the acceleration or deceleration at interval k_j and τ_{i,k_j} is the time cost over the interval k_j.

$$v_{i,k_j+1} = v_{i,k_j} + a_{i,k_j} \cdot \tau_{i,k_j} \quad \forall i \in I, \forall j \in J, \forall k_j \in K_j \tag{4.1}$$

The start node of interval $k_j + 1$ is also the end node of interval k_j, so the time of train i crossing it can be calculated as below.

$$t_{i,k_j+1} = t_{i,k_j} + \tau_{i,k_j} \quad \forall i \in I, \forall j \in J, \forall k_j \in K_j \tag{4.2}$$

The average speed over the interval k_j can be calculated as (4.3), assuming a constant acceleration.

$$\bar{v}_{i,k_j} = \frac{v_{i,k_j} + v_{i,k_j+1}}{2} \quad \forall i \in I, \forall j \in J, \forall k_j \in K_j \tag{4.3}$$

Thus the relationship between the train's moving distance and the time cost is shown in (4.4), where the train's moving distance the train moves is the length of interval d_{k_j}.

$$\bar{v}_{i,k_j} \cdot \tau_{i,k_j} = d_{k_j} \quad \forall i \in I, \forall j \in J, \forall k_j \in K_j \tag{4.4}$$

The acceleration of train i has the following range. For the positive value, the train i increases its speed at that interval, the upper bound of which is the maximum acceleration. For the negative value, the train i brakes to decrease its speed, and the maximum deceleration is the service braking rate b_s.

$$-b_s \leq a_{i,k_j} \leq a_{max} \quad \forall i \in I, \forall j \in J, \forall k_j \in K_j \tag{4.5}$$

It also requires the speed, v_{i,k_j}, time t_{i,k_j} and time costτ_{i,k_j} to be non-negative.

$$v_{i,k_j} \geq 0 \quad \forall i \in I, \forall j \in J, \forall k_j \in K_j \tag{4.6}$$

$$t_{i,k_j} \geq 0 \quad \forall i \in I, \forall j \in J, \forall k_j \in K_j \tag{4.7}$$

$$\tau_{i,k_j} \geq 0 \quad \forall i \in I, \forall j \in J, \forall k_j \in K_j \tag{4.8}$$

4.3.2 Constraints describing the Dynamic Equations

The trains' motion is restricted by the Newton's law, thus it has the following relationship between the acceleration and the force. a_{i,k_j} is the acceleration of train i at interval k_j, f_p is the rotating factor for the moving train with a mass m_i. T_{i,k_j} is the traction force the engines in train apply, and the R_{i,k_j} is the force exerted or affecting the train i over interval k_j.

$$a_{i,k_j} \cdot f_p \cdot m_i = T_{i,k_j} - R_{i,k_j} \quad \forall i \in I, \forall j \in J, \forall k_j \in K_j \tag{4.9}$$

Where the force R_{i,k_j} is the approximate resistance, coming from the average speed of the interval.

$$R_{i,k_j} = c_1 + c_2 \cdot \bar{v}_{i,k_j} + c_3 \cdot \bar{v}^2_{i,k_j} \quad \forall i \in I, \forall j \in J, \forall k_j \in K_j \tag{4.10}$$

The traction force sourced from engine is limited by the maximum power and maximum force. The constraint of it is shown in (4.11) and (4.12). The figure of this relation is shown in Figure 4.4.

$$T_{i,k_j} \cdot \bar{v}_{i,k_j} \leq P_{max,i} \quad \forall i \in I, \forall j \in J, \forall k_j \in K_j \tag{4.11}$$

$$T_{i,k_j} \leq T_{max,i} \quad \forall i \in I, \forall j \in J, \forall k_j \in K_j \tag{4.12}$$

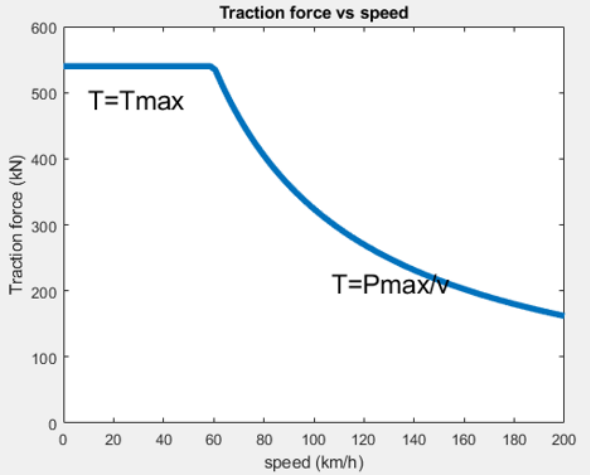

Figure 4.4: Illustration of the traction force versus the speed

4.4 Model for trains' headway

In this model, the trains have two modes of running operation, moving block and virtual coupling. In the mode of moving block, the adjacent trains keep an safety distance of absolute braking distance plus an extra distance margin. In virtual coupling, the trains have three states, coupling, coupled, and decoupling. In the coupling state, the trains keep an safety distance of relative braking distance plus an additional safety distance margin. In the coupled state, the adjacent trains have the same speed so the trains keep the distance of only the safety distance. When approaching the diverging area, the trains need to change to the decoupling state to leave enough distance and time for the point switching, where the follower is required to maintain an absolute braking distance and to be able to fully stop in front of the switch plus a safety margin.

4.4.1 Headway model for Moving Block

Considering the headway, of which the adjacent trains passing same location, the trains arriving this location keep the safety time gap including the approaching time plus the clearing time. The approaching time in the moving block is the absolute braking time of the followers added by an extra time margin the for the follower. $\frac{v_{i,k_j}}{b_s} + \frac{s_m}{v_{i,k_j}}$ gives the approaching time. $\frac{l_{i-1}}{v_{i-1,k_j}}$ gives the clearing time. The clearing time is the time for the leader to run over a distance of its length. This relation is showing in the constraint (4.13), where the train i is the follower and the train $i-1$ is the leader. The first two items on the right hand side give the approaching time and the last item gives the time for the leader fully leaving the location k, which is the clearing time.

$$t_{i,k_j} - t_{i-1,k_j} \geq \frac{v_{i,k_j}}{b_s} + \frac{s_m}{v_{i,k_j}} + \frac{l_{i-1}}{v_{i-1,k_j}} \quad \forall i \in I, \forall j \in J, \forall k_j \in K_j \tag{4.13}$$

The above constraint (4.13) cannot works for the departure and arrival intervals, where the initial and final speed of which are 0km/h and cannot be put in the denominator. To include the departure and arrival intervals in station area,the middle time of a interval can be considered of which the speed is non-zero. As introduced in section 4.2,there is a linear relationship listed in (4.14), and the speed at this middle time is the average speed of the interval, calculated by formular (4.3). The t'_{i,k_j} is the speed at the middle time of the interval k_j.

$$t'_{i,k_j} = \frac{t_{i,k_j} + t_{i,k_j+1}}{2} \tag{4.14}$$

$$t'_{i,k_j} - t'_{i-1,k_j} \geq \frac{\bar{v}_{i,k_j}}{b_{s,i}} + \frac{s_m}{\bar{v}_{i,k_j}} + \frac{l_{i-1}}{\bar{v}_{i-1,k_j}} \quad \forall i \in I, \forall j \in J, \forall k_j \in K_j \tag{4.15}$$

To write the constraint in the MIQP format, a variable $\bar{v}'_{i,k}$ is used to represent the multiplicative inverse value of speed $\bar{v}_{i,k}$.

$$\bar{v}_{i,k_j} \times \bar{v}'_{i,k_j} = 1 \quad \forall i \in I, \forall j \in J, \forall k_j \in K_j \tag{4.16}$$

The constraint (4.15) is updated to be (4.17).

$$t'_{i,k_j} - t'_{i-1,k_j} \geq \frac{\bar{v}_{i,k_j}}{b_{s,i}} + s_m \cdot \bar{v}'_{i,k_j} + l_{i-1} \cdot \bar{v}'_{i-1,k_j} \quad \forall i \in I, \forall j \in J, \forall k_j \in K_j \tag{4.17}$$

4.4.2 Headway model for Coupling State under Virtual Coupling

Under the virtual coupling, three states will be considered for the time difference between two adjacent trains. State 1 refers to the coupling state with the follower's speed higher than the leader. In this circumstance, the follower shall decelerate the speed to the same speed as the leader. This state can be described as

$$\begin{aligned} &\text{State 1: } If \quad v_{i,k_j} > v_{i-1,k_j} \quad holds, \\ &\qquad t_{i,k_j} - t_{i-1,k_j} \geq \frac{v_{i,k_j} - v_{i-1,k_j}}{b_s} + \frac{s_m}{v_{i,k_j}} + \frac{l_{i-1}}{v_{i-1,k_j}} \quad must \quad hold. \end{aligned} \tag{4.18}$$

This $if - then$ sentence can be realized using an extremely big value M, an extremely small positive value B, and a series of 0-1 binary variables $y_{i,k}$, written as (4.19), (4.20) and (4.21). The (4.19) makes the $y_{i-1,k}$ equals to 0 if $v_{i,k}$ is larger than

the $v_{i-1,k}$. The (4.20) makes the $y_{i-1,k}$ equals to 1 if $v_{i,k}$ is smaller than or equal to the $v_{i-1,k}$. Together these inequalities determine whether y is 0 or 1. The extremely small positive value B is used when $v_{i,k}$ equals to $v_{i-1,k}$. The $if - then$ sentence is realized in (4.21) by $y_{i-1,k}$ equals to 0 or 1.

$$v_{i,k_j} \leq v_{i-1,k_j} + M(1 - y_{i-1,k_j}) \quad \forall i \in I, \forall k_j \in K_j \tag{4.19}$$

$$v_{i,k_j} \geq v_{i-1,k_j} - M \cdot y_{i-1,k_j} + B \quad \forall i \in I, \forall k_j \in K_j \tag{4.20}$$

$$t_{i,k_j} - t_{i-1,k_j} \geq \frac{v_{i,k_j} - v_{i-1,k_j}}{b_s} + \frac{s_m}{v_{i,k_j}} + \frac{l_{i-1}}{v_{i-1,k_j}} - M \cdot y_{i-1,k_j} \quad \forall i \in I, \forall k_j \in K_j \tag{4.21}$$

To write in the quadratic form and considering the station area, the constraint (4.21) is written as in (4.22).

$$t'_{i,k_j} - t'_{i-1,k_j} \geq \frac{\bar{v}_{i,k_j} - \bar{v}_{i-1,k_j}}{b_s} + s_m \cdot \bar{v}'_{i,k_j} + l_{i-1} \cdot \bar{v}'_{i-1,k_j} - M \cdot y_{i-1,k_j} \quad \forall i \in I, \forall k_j \in K_j \tag{4.22}$$

State 2 refers to the coupling state with the follower's speed lower than the leader. The follower shall increase the speed up to $v_{b'}$ then decrease the speed from $v_{b'}$ to the leader's speed. $v_{b'}$ is a speed for the follower to reach to justify and maintain a minimum distance between the leader, introduced in Quaglietta et al. [2020]. The approaching time is the time it takes to first increase the speed then decrease the speed.

State 2: $If \quad v_{i,k_j} < v_{i-1,k_j} \quad holds,$

$$t_{i,k_j} - t_{i-1,k_j} \geq \frac{v_{b',i-1,kj} - v_{i,k_j}}{a_{max}} + \frac{v_{b',i-1,k_j} - v_{i-1,k_j}}{b_s} + \frac{s_m}{v_{i,k_j}} + \frac{l_{i-1}}{v_{i-1,k_j}} \quad must \quad hold. \tag{4.23}$$

As in (4.19) and (4.20) explained in state 1, the $y_{i-1,k}$ equals to 1 if the follower's speed $v_{i,k}$ is smaller than the leader's speed $v_{i-1,k}$. Since the $y_{i-1,k}$ equals to 1, the constraint (4.24) limits the safety gap as the expected (4.23).

$$\begin{aligned} t_{i,k_j} - t_{i-1,k_j} \geq & \frac{v_{b',i-1,k_j} - v_{i,k_j}}{a_{max}} + \frac{v_{b',i-1,k_j} - v_{i-1,k_j}}{b_s} + \frac{s_m}{v_{i,k_j}} \\ & + \frac{l_{i-1}}{v_{i-1,k_j}} - M \cdot (1 - y_{i-1,k_j}) \quad \forall i \in I, \forall k_j \in K_j \end{aligned} \tag{4.24}$$

To write in the quadratic form and considering the station area, the constraint (4.24) is written as in (4.25).

$$\begin{aligned} t'_{i,k_j} - t'_{i-1,k_j} \geq & \frac{v_{b',i-1,k_j} - \bar{v}_{i,k_j}}{a_{max}} + \frac{v_{b',i-1,k_j} - \bar{v}_{i-1,k_j}}{b_s} + s_m \cdot \bar{v}'_{i,k_j} \\ & + l_{i-1} \cdot \bar{v}'_{i-1,k_j} - M \cdot (1 - y_{i-1,k_j}) \quad \forall i \in I, \forall k_j \in K_j \end{aligned} \tag{4.25}$$

4.4.3 Headway model for Coupled State under Virtual Coupling

The state 3 of the VC is the coupled state, where the adjacent trains' have the same speed and keep a distance of the short safety margin. The state can be described as

$$\begin{aligned} &\text{State 3: } If \quad v_{i+1,k} = v_{i,k} \quad holds, \\ &\qquad t_{i+1,k} - t_{i,k} \geq \frac{s_m}{v_{i+1,k}} + \frac{l_i}{v_{i,k}} \quad must \quad hold. \end{aligned} \tag{4.26}$$

As the items on the right side also work for the state 1 and state 2, this constraint is modelled as

$$t_{i+1,k} - t_{i,k} \geq \frac{s_m}{v_{i+1,k}} + \frac{l_i}{v_{i,k}} \quad \forall i \in I, \forall k_j \in K_j \tag{4.27}$$

The constraint (4.27) is written as (4.28) in the quadratic form considering the station area.

$$t'_{i,k_j} - t'_{i-1,k_j} \geq s_m \cdot \bar{v}'_{i,k_j} + l_{i-1} \cdot \bar{v}'_{i-1,k_j} \quad \forall i \in I, \forall k_j \in K_j \tag{4.28}$$

4.4.4 Headway model for the Decoupling State

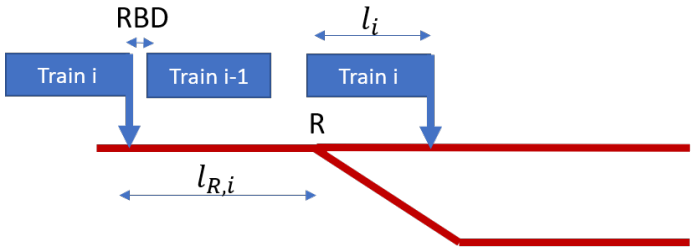

Figure 4.5: Decoupling state demonstration before the divergence

When a convoy approaching the divergence, if the turnout needs to switch for the trains going to different sections, the safety distance and the safety time between the trains should allow enough space for the turnout switching, and leave enough space for the train i to fully brake down after the leader before the switching point. As shown in the Figure 4.5, the R point representing the location of the switch, the fully braking down distance for the following train i marked in $l_{R,i}$, consists of the absolute braking distance, the distance covered by the follower when the turnout switching, and the safety margin. The formula of it is in 4.29. For train i, before entering its fully braking distance $l_{R,i}$, it keeps an relative braking distance with its front car, marked as RBD in the figure. Once the train i's head crossing the $l_{R,i}$, the distance to the front car should be adjusted to keep an absolute braking distance, or said the headway between train i and train $i+1$ should allow fully braking before the switch. This relation ship is written in

$$l_{R,i} = \frac{v_i^2}{2b_s} + v_i \cdot T_{sw} + s_m \tag{4.29}$$

The decoupling state in front of the divergence can be summarized as the following state 4 in 4.30.

State 4: *If*

Train i has a different route with train $i-1$

and

train i's head is in the position of $[R - l_{R,i}\ ,\ R]$

Then

the distance between has a requirement that (4.30)

$$(x_{i-1} - l_{i-1}) - (x_i + v_i \cdot T_{sw}) \geq \frac{v_i^2}{2b} + s_m$$

which is

$$x_{i-1} - x_i \geq \frac{v_i^2}{2b} + s_m + l_{i-1} + v_i \cdot T_{sw}$$

The above $if - then$ logic can be written as a mathematical programming model, in (4.31) - (4.33).

$$\sum_{k'=0}^{k} \Delta d_{k'} - [R - (\frac{v_i^2}{2b_s} + v_i \cdot T_{sw} + s_m)] + B \leq M \cdot z_{i,j,k} \quad \forall i \in I, \forall k_j \in K_j \tag{4.31}$$

$$\sum_{k'=0}^{k} \Delta d_{k'} - [R - \frac{v_i^2}{2b_s} + v_i \cdot T_{sw} + s_m] \geq M \cdot (z_{i,j,k} - 1) \quad \forall i \in I, \forall k_j \in K_j \tag{4.32}$$

$$t_{i,k_j} - t_{i-1,k_j} \geq z_{i,j,k} \cdot (T_{sw} + \frac{v_{i,k_j}}{b} + \frac{s_m}{v_{i,k_j}} + \frac{l_{i-1}}{v_{i-1,k_j}}) \quad \forall i \in I, \forall k_j \in K_j \tag{4.33}$$

The term $\sum_{k'=0}^{k} \Delta d_{k'}$ gives the location of the head of the train i, which is the sum of the intervals from the starting $k' = 0$ to the current location $k' = k$.

4.5 Modelling objective

The following objective 1 - 3 are possible ways to maximize the timetable capacity, by minimizing the trains arrival time, running time ,or scheduling as many trains as possible in a given period. The objective 4 minimizes the train's safety distance under the moving block and form platoons under virtual coupling, by minimizing the headway of the trains at each interval.

Objective 1: minimizing the trains arrival time

$$min \sum_{i \in I_r} (t_{i,N_r}) \tag{4.34}$$

N_j is the last interval of section j. For section j, t_{i,N_j} is the arrival time of train i. This objective minimizes all trains' arrival time over all the routes.

Objective 2: minimizing the trains running time

$$min \sum_{i \in I_r} (t_{i,N_r} - t_{i,0}) \tag{4.35}$$

$t_{i,0}$ is the departure time of each train. The arrival time minusing it gives the trains operating time on each routes. This objective sums all train's running time over all the routes.

Objective 3: maximizing the number of trains

$$max \sum_{i=1}^{N} \gamma_i \tag{4.36}$$

γ_i equals to 1 means the train i can arrive within a period, where P is the ending time of the period, assuming 0 is the starting time of the period. 4.36 is the sum of the gamma, which gives the number of trains scheduled within the period.

$$\gamma_i = \begin{cases} 1 & 0 \leq t_{i,N_r} \leq P \\ 0 & t_{i,N_r} > P \end{cases}$$

This relationship equals to the constraint4.37 and 4.38. M is an big value and B is an extremely small positive value. The B in constraint4.37 works when $t = P$, the small B makes the right hand side larger than left, thus the γ must be 1.

$$t_{i,N_r} \geq P - \gamma_i \cdot M + B \quad \forall i \in Ir \tag{4.37}$$

$$t_{i,N_r} \leq P + M(1 - \gamma_i) \quad \forall i \in Ir \tag{4.38}$$

Objective 4: minimizing the safety distance

$$min \sum_{j \in J} \sum_{i \in I} \sum_{k_j \in K_J} (t_{i,k_j} - t_{i-1,k_j}) \tag{4.39}$$

This objective minimizes the headway of all adjacent trains at each location of each section. It is expected that under moving block, the trains have a distance of the absolute braking distance and under virtual coupling, the trains have a distance of the relative braking distance. Before the divergence on both the virtual coupling and moving block, the trains have a safety distance that can fully brake down before the point during the switching time.

The model cannot give solution if including only the objective 4. This is because if only having this minimizing distance objective, the possible solutions for the trains are infinite. Thus the MIQP model is designed to be a multi-objective model, which has the first objective of 1. minimizing the arrival times, 2.minimizing the running times or 3.maximizing the number of trains for a given period, and has the second objective 4.minimizing the safety distance. The hierarchical model will be used. It first solves the optimal objective result of the fist objective. Then under the first result of the first objective, it searches for the optimal result of the second objective, which not affects the first objectives optimal value.

A case study of three combinations is conducted in this study, as shown below. The names in parentheses are abbreviations for each one.

- 1.Obj: To minimize Arrival times & safety distance (ATMIN MODEL)
- 2.Obj: To minimize Running times & safety distance (RTMIN MODEL)
- 3.Obj: To maximize Train number & minimize safety distance (NUMMAX MODEL)

4.6 Hhierarchical optimization model

The multiple objective is realized by hierarchical approach on the Gurobi solver. The hierarchical approach is a method giving priority to the multiple objectives, The objective with higher priority will be solved first. And the objective solved later

will not affect the optimization value for the solved objectives. The calibration test of the priority is shown in the appendix A.

The hierarchical model is used because this model can optimize the second objective without costing the optimal result of the first objective, since it is not expected if coupling the trains can affect the overall timetable efficiency, which is possible by the weight-and-sum method.

4.7 Time, speed difference and headway calculation

The output of the model gives the optimized solution of each variables, listed in 4.2.1. The speed of each interval gives the timetable pattern a guide of operation. The solution of the time gives the timetable's departure and arrival times of each train. The time difference at each location gives the headway of the trains over the route, the speed difference is calculated in the same way, shown in Figure 4.6.

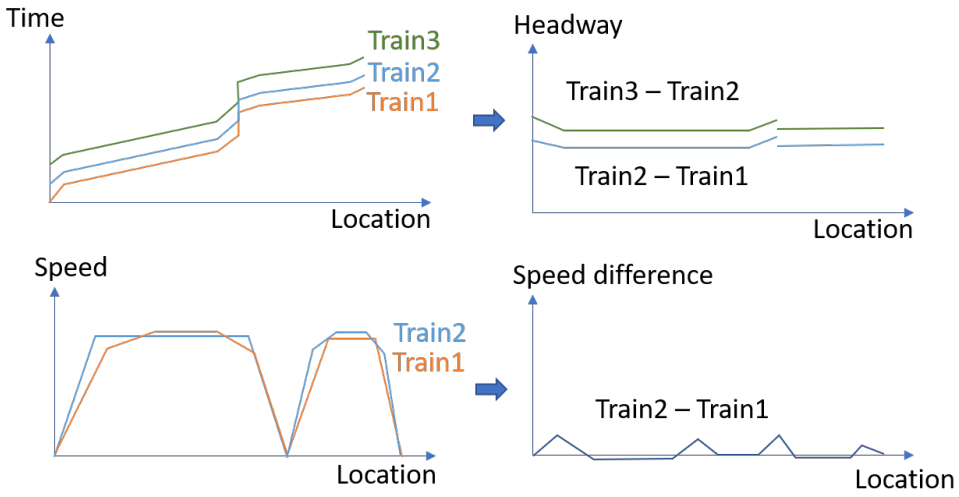

Figure 4.6: Demonstration of the calculation of headway and speed difference

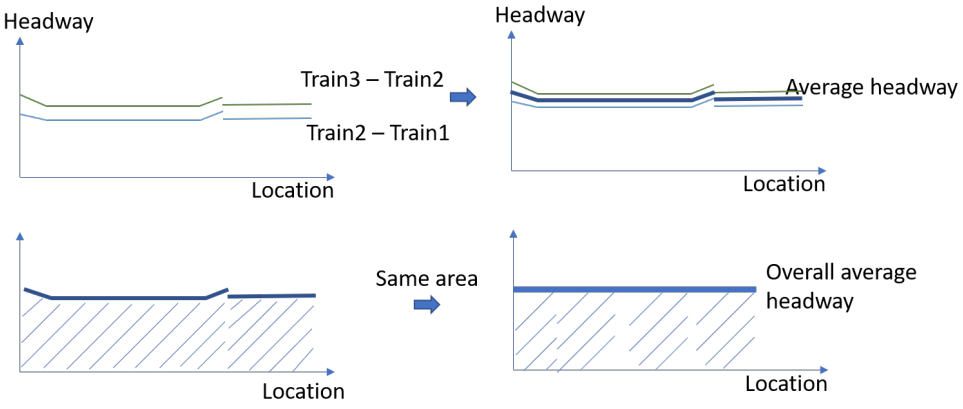

Figure 4.7: Demonstration of average headway calculating on routes

The headway of each train at each location is obtained according to the result by the above process. The average headway of each location is calculated by averaging the headway of all the trains at this interval, like the demonstration of the first step in Figure 4.7. After obtaining the average headway of each interval on the route, the overall average headway of the route can be calculated by the method of "equal area

averaging". As shown in the Figure 4.7, the area of the shadows is the same. The area under the curve of the average headway on the left-hand side is formed by a set of trapezoids. On the right-hand side, the value of the overall average headway is the height of the square area.

5 CASE STUDY

5.1 case study setup

5.1.1 Layout setup

This research studies the case with the layout shown in Figure 5.1. It consists with three sections, where section 0 in 30 km, section 1 in 15 km and section 2 in 10 km. Station A is the departure station. Station B is the dwell station. Station C and D are the arrival stations. The switching point is 500 m in front of Station B.

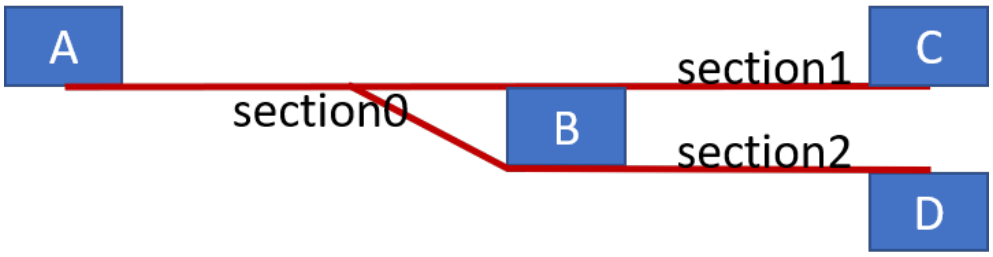

Figure 5.1: Layout of the case study

The Y-shape network is divided into the following space-discrete train behavioural intervals, in Figure 5.2. The section 0 is unevenly divided into 40 intervals, where are loose at the open lines but tight before the switch. The section 1 and section 2 are divided equally into 15 intervals and 10 intervals respectively.

The space-discrete train behavioural intervals in front of the switch are designed to be compact, in 500m and 100m. This is because the trains decoupling in this area have a relatively more complex decision making, which has been explained in section 4.5, and the trains will brake to leave the platoons. It is supposed that the maximum speed is $v = 150km/h$. The service braking rate is $b_s = 0.8m/s^2$. The fully braking distance is $v^2/2b_s = 1082m$. The switching time of the turnouts is supposed as $T_{sw} = 10s$, which gives the running distance during the switching is $v \cdot T_{sw} = 417m$. Therefore, the maximum length for the trains fully stopped before the switch is $1499m$. In this case study, we set the $1.5km$ in front of the switch in compact intervals.

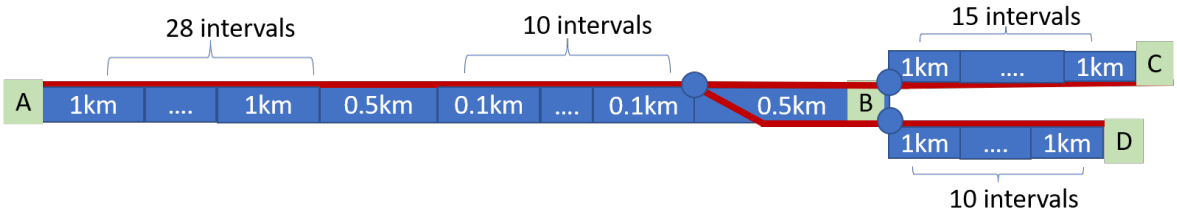

Figure 5.2: The space-discrete train behavioural intervals division on the layout

5.1.2 Timetable pattern

The two routes are defined as the following table. Route 1 is composed of section 0 and section 1, which departs from staton A, dwells at station B and arrives in station C. Route 2 is composed of section 0 and section 2, which departs from staton A, dwells at station B and arrives in station D.

Table 5.1: Route composition

Route #	section composition	Stop station
route 1	section 0 + section 1	A-B-C
route 2	section 0 + section 2	A-B-D

The trains are scheduled in two timetable patterns, departing in batch and depart in turns. For 4 trains, 6 trains, 8 trains, the trains are scheduled on each route as follow. The trains always leave the station A in the sequence of train 1 departing first, train 2 departing secondly, train3 departing thirdly...

Table 5.2: Timetable patterns and train schedule

Route #	Train #	Depart in batch	Depart in turns
route 1	4 trains	Train 1,Train 2	Train 1,Train 3
route 2		Train 3,Train 4	Train 2,Train 4
Route #	**Train #**	**Depart in batch**	**Depart in turns**
route 1	6 trains	Train 1,Train 2,Train 3	Train 1,Train 3,Train 5
route 2		Train 4,Train 5,Train 6	Train 2,Train 4,Train 6
Route #	**Train #**	**Depart in batch**	**Depart in turns**
route 1	8 trains	Train 1,Train 2,Train 3,Train 4	Train 1,Train 3,Train 5,Train 7
route 2		Train 5,Train 6,Train 7,Train 8	Train 2,Train 4,Train 6,Train 8

This case study works on three combinations of objectives by hierarchical optimization. The first objective is minimizing the arrival times and the safety distance, which is abbreviated below as the ATMIN model. The second is minimizing the running time and safety distance, called the RTMIN Model. The third is maximizing the number of trains and safety distance, hereinafter referred to as NUMMAX model.

5.1.3 Parameter setup

Table 5.3: Parameter and value

Parameter	Value
Train mass (m_i)	$480ton$
Rotating mass factor (f_p)	1.07
Resistance Coefficient (c_1, c_2, c_3)	$c_1 = 10.689, c_2 = 0.28906, c_3 = 0.011282$
Maximum acceleration (a_{max})	$1m/s^2$
Service braking rate (b_s)	$0.8m/s^2$
Maximum traction force (T_{max})	$450kN$
Maximum power (P_{max})	$900kW$
Maximum speed (v_{max})	$150km/h$
Length of train (l_i)	$180m$
Additional safety margin (s_m)	$100m$
Big value (M)	9999999
small positive value (B)	0.0001

5.2 case study result

The following shows the comparison of the RTMIN, ATMIN, NUMMAX model's result, from the aspect of the capacity utilization and the headway. The most capacity efficiency model is the RTMIN. Thus computed by the RTMIN model, the optimal operation of 6 trains in two timetable patterns under moving block and under virtual coupling will be presented. According to this, the operation of the trains adjusted from moving block to virtual coupling can be observed. The results of the ATMIN and NUMMAX models as well as the 4 trains and 8 trains results of the RTMIN model are shown in the appendix. In the legends of the following figures, the VC stands for virtual coupling and the MB stands for moving block.

5.2.1 Result of capacity utilisation of RTMIN, ATMIN, NUMMAX model.

The capacity utilisation is studied and evaluated from the aspect of infrastructure occupation time and headway. The shortest infrastructure occupation time means the best capacity utilisation efficiency. The headway over the route is also an important factor affecting the timetable efficiency.

Infrastructure occupation time comparison

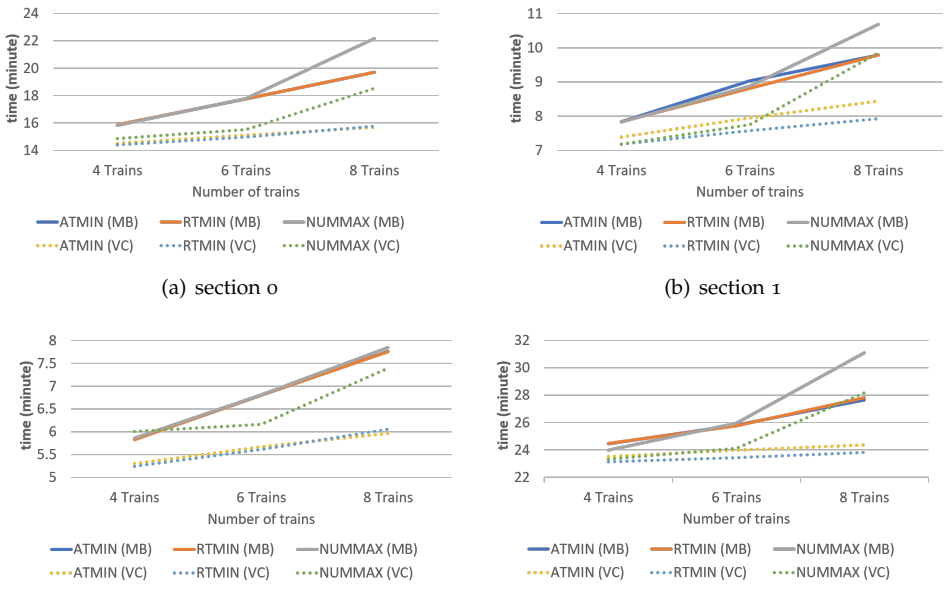

(a) section 0

(b) section 1

(c) section 2

(d) the entire network

Figure 5.3: Infrastructure occupation time for trains in batch

The infrastructure occupation time of the RTMIN, ATMIN, NUMMAX model for the two timetable patterns are plotted in the Figure 5.3 and Figure 5.4. The infrastructure occupation time on each sections are in each sub-figure (a)-(c). The sub-figure (d) shows the infrastructure occupation time over the entire network, which is the overall time of the timetable. It is calculated by the last arrival trains arriving time at station C or D, minus the first train's departing time from station A. Comparing the timetable patterns, the trains departing in batch always give the minimum infrastructure occupation time. Comparing the three model, RTMIN, ATMIN and NUMMAX, the NUMMAX model gives the longest occupation time, because the objective of this model is to arrange as many trains as possible in the time period, while for the trains within the period, the infrastructure occupation

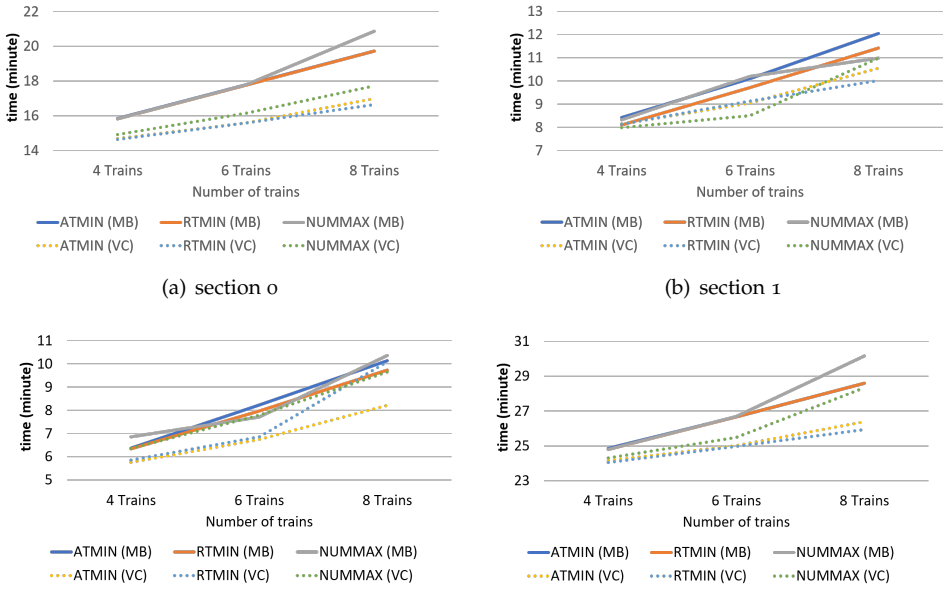

(a) section 0 (b) section 1

(c) section 2 (d) the entire network

Figure 5.4: Infrastructure occupation time for trains in turns

time is not further squeezed. The RTMIN always gives the minimum occupation time, which means the RTMIN Model is the most efficient on capacity utilization. The magnitude of the infrastructure occupancy time in details as well as the improving percentage on each scenarios are shown in the Table 5.4, analyzed in the next section.

Headway comparison

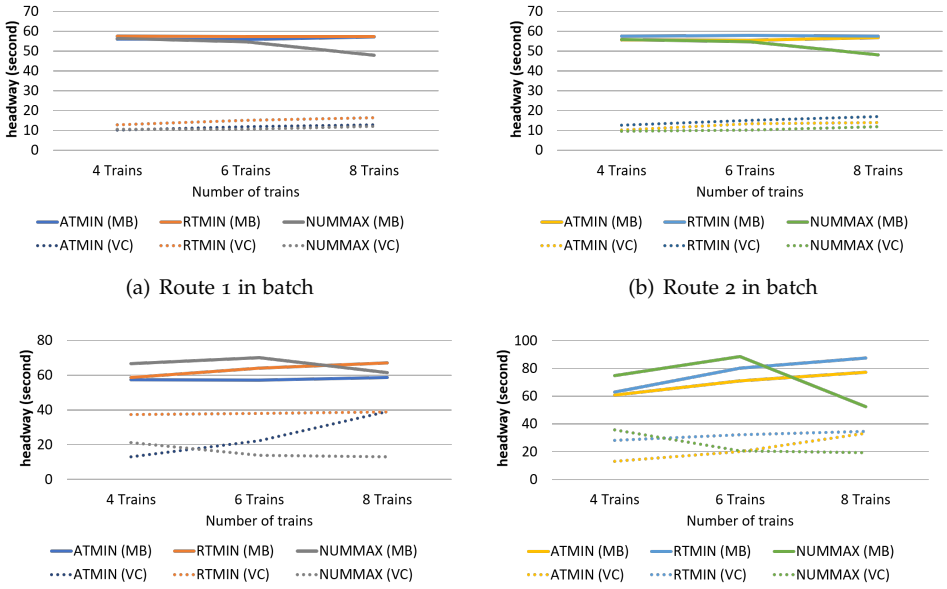

(a) Route 1 in batch (b) Route 2 in batch

(c) Route 1 in turns (d) Route 2 in turns

Figure 5.5: Headway of trains

The headway of the three models are shown in Figure 5.5. According to the figures, the virtual coupling brings more benefit of headway shortening to the trains

departing in batch than in turns. The figures of (a) and (b) show that the trains in batch has an average headway of 55.56 sec under moving block and of 12.61 sec under virtual coupling, which is 77.31% less. The figures of (c) and (d) show that the trains in turns has an average headway of 67.54 sec under moving block and of 26.30 sec under virtual coupling, which is 61.06% less. The magnitude of the headway as well as the improving percentage on each scenarios in details are shown in the Table 5.5 in the next section.

Among the RTMIN, ATMIN and NUMMAX models, the NUMMAX model optimizes the headway most, but it does not provide the most time saving result, looking back to Figure 5.3 and Figure 5.4. This is because the NUMMAX model allows frequent accelerating and braking, and by this the headway of the trains can be adjusted and optimized most. Consequently, it is proved that minimum headway doesn't mean the best capacity utilisation efficiency, although saving the headway can saving the capacity using.

The RTMIN model does not show the minimum headway optimization result, because this model gives a higher priority on minimizing all the trains running time and it will not minimize headway at the cost of total time.

Capacity utilisation efficiency improvement by VC, comparing to MB.

The percentage of infrastructure occupation time saving and the headway shortening is shown in Table 5.4 and 5.5.

Table 5.4: The infrastructure occupation time saving percentage by VC, comparing to MB.

Occ_Time (min)		**Timetable pattern: In batch**								
		4 Trains			**6 Trains**			**8 Trains**		
		MB	**VC**	**Impr***	**MB**	**VC**	**Impr***	**MB**	**VC**	**Impr***
ATMIN	section 0	15.853	14.510	8.5%	17.770	15.118	14.9%	19.703	15.677	20.4%
RTMIN	section 0	15.869	14.401	9.2%	17.755	14.965	15.7%	19.711	15.753	20.1%
NUMMAX	section 0	15.810	14.872	5.9%	17.783	15.517	12.7%	22.173	18.526	16.5%
ATMIN	section 1	7.836	7.395	5.6%	9.030	7.949	12.0%	9.792	8.438	13.8%
RTMIN	section 1	7.843	7.182	8.4%	8.817	7.573	14.1%	9.790	7.930	19.0%
NUMMAX	section 1	7.832	7.182	8.3%	8.877	7.751	12.7%	10.689	9.852	7.8%
ATMIN	section 2	5.835	5.304	9.1%	6.803	5.673	16.6%	7.769	5.971	23.1%
RTMIN	section 2	5.832	5.248	10.0%	6.803	5.616	17.4%	7.759	6.062	21.9%
NUMMAX	section 2	5.860	6.007	-2.5%	6.815	6.163	9.6%	7.847	7.399	5.7%
ATMIN	**entire***	**24.439**	**23.521**	**3.8%**	**25.813**	**23.973**	**7.1%**	**27.660**	**24.360**	**11.9%**
RTMIN	**entire***	**24.473**	**23.137**	**5.5%**	**25.753**	**23.437**	**9.0%**	**27.803**	**23.821**	**14.3%**
NUMMAX	**entire***	**23.980**	**23.333**	**2.7%**	**25.962**	**24.106**	**7.1%**	**31.092**	**28.166**	**9.4%**
Occ_Time (min)		**Timetable pattern: In turns**								
		4 Trains			**6 Trains**			**8 Trains**		
		MB	**VC**	**Impr***	**MB**	**VC**	**Impr***	**MB**	**VC**	**Impr***
ATMIN	section 0	15.846	14.679	7.4%	17.780	15.592	12.3%	19.723	16.987	13.9%
RTMIN	section 0	15.821	14.640	7.5%	17.768	15.579	12.3%	19.726	16.640	15.6%
NUMMAX	section 0	15.824	14.926	5.7%	17.778	16.146	9.2%	20.863	17.731	15.0%
ATMIN	section 1	8.421	8.147	3.3%	10.102	9.059	10.3%	12.050	10.549	12.5%
RTMIN	section 1	8.096	8.137	-0.5%	9.708	9.127	6.0%	11.427	10.027	12.3%
NUMMAX	section 1	8.321	7.993	3.9%	10.205	8.510	16.6%	10.988	10.994	0.0%
ATMIN	section 2	6.367	5.756	9.6%	8.222	6.742	18.0%	10.127	8.219	18.8%
RTMIN	section 2	6.341	5.854	7.7%	7.971	6.860	13.9%	9.724	10.084	-3.7%
NUMMAX	section 2	6.852	6.363	7.1%	7.713	7.789	-1.0%	10.355	9.647	6.8%
ATMIN	**entire***	**24.858**	**24.155**	**2.8%**	**26.661**	**25.012**	**6.2%**	**28.597**	**26.394**	**7.7%**
RTMIN	**entire***	**24.789**	**24.039**	**3.0%**	**26.663**	**24.975**	**6.3%**	**28.602**	**25.929**	**9.3%**
NUMMAX	**entire***	**24.802**	**24.301**	**2.0%**	**26.686**	**25.474**	**4.5%**	**30.167**	**28.333**	**6.1%**
Impr*: VC improvement over MB										
entire*: The infrastructure occupation time over the entire network										

In the Table 5.4, the percentage of the single section is saved more than the total time of the entire network, which because the trains on the Y-style network including the entire network are more complex than a single section. According to the saving percentage of the entire network of the ATMIN, RTMIN, NUMMAX model in Table 5.4, the infrastructure occupancy time saving increases in percentage for more trains. The result of the entire network comes starting from the departure time of the first train on section 0, and ending at the latest train arriving in station

Table 5.5: Headway shortening percentage by VC, comparing to MB

Headway (sec)		Timetable pattern: In batch								
		4 Trains			6 Trains			8 Trains		
		MB	VC	save	MB	VC	save	MB	VC	save
ATMIN	Route1	55.982	**10.165**	**81.8%**	55.772	**11.968**	**78.5%**	57.244	**12.925**	**77.4%**
ATMIN	Route2	55.628	**10.217**	**81.6%**	55.399	**13.390**	**75.8%**	56.720	**14.020**	**75.3%**
RTMIN	Route1	57.615	**12.797**	**77.8%**	57.533	**15.130**	**73.7%**	57.533	**16.499**	**71.3%**
RTMIN	Route2	57.514	**12.714**	**77.9%**	57.834	**15.181**	**73.8%**	57.623	**17.064**	**70.4%**
NUMMAX	Route1	56.491	**10.634**	**81.2%**	54.736	**10.509**	**80.8%**	47.841	**12.108**	**74.7%**
NUMMAX	Route2	55.747	**9.587**	**82.8%**	54.676	**10.125**	**81.5%**	48.165	**11.892**	**75.3%**
Headway (sec)		Timetable pattern: In turns								
		4 Trains			6 Trains			8 Trains		
		MB	VC	save	MB	VC	save	MB	VC	save
ATMIN	Route1	57.388	**12.961**	**77.4%**	57.177	**22.363**	**60.9%**	58.604	**39.160**	**33.2%**
ATMIN	Route2	60.683	**13.219**	**78.2%**	70.918	**19.984**	**71.8%**	77.210	**33.159**	**57.1%**
RTMIN	Route1	58.621	**37.414**	**36.2%**	64.065	**37.905**	**40.8%**	66.996	**38.797**	**42.1%**
RTMIN	Route2	62.897	**28.214**	**55.1%**	80.068	**32.127**	**59.9%**	87.391	**34.533**	**60.5%**
NUMMAX	Route1	66.540	**21.110**	**68.3%**	70.180	**13.768**	**80.4%**	61.451	**13.083**	**78.7%**
NUMMAX	Route2	74.657	**35.829**	**52.0%**	88.369	**20.602**	**76.7%**	52.493	**19.201**	**63.4%**

C or station D. The RTMIN model shorten the time of the timetable pattern in batch averagely in 7.9%, which is 9.6% in batch and 6.2% in turns. The ATMIN model has the time saved averagely in 6.6%, which is 7.6% in batch and 5.6 % in turns. The NUMMAX saves the least infrastructure occupation time, which is 5.3% on average, which is 6.4% in batch and 4.2% in turns. Among the three model, RTMIN gives the most infrastructure occupancy time saving percentage, which means this model performs best to saving the capacity, for timetable pattern of in batch an in turns. Thus, the results presented in the following are from RTMIN model. The results of the ATMIN and NUMMAX models are shown in the appendix C and D.

According to Table 5.5, it is observed that the headway saving percentage is decreasing when adding in more trains, by ATMIN and RTMIN model. This is because if adding in more trains, the trains brake more to adjust the distance, and such braking can be propagated among the platoon. For example, at the departing area the leading trains brake to decrease the speed more than the following trains, if observing the Figure 5.8(d) in the following results. Thus for a convoy to form a platoon, how much the trains brake are different, where for more trains, such average headway shall be enlarged. In the NUMMAX model, the headway for 8 trains is higher than 6 trains, which contradicts the previous finding. This is because in the optimization result of the 8 trains, the trains frequently brake and accelerate all along the sections to minimize the distance, shown in Figure D.12(b). Such frequent speed changing is not practical in the industry and leads to longer infrastructure occupation time.

Also, the saving percentage of the trains in batch is higher than in turns, which means the VC bings more benefit on the timetable pattern of departing in batch than in turns. On average, the headway is shortened by the RTMIN in 61.62%, which is 74.14% in batch and 49.10% in batch, by ATMIN in 70.75%, which is 78.4% in batch and 63.10% in turns, and by NUMMAX in 74.65%, which is 79.38% in batch and 69.91% in turns. In the NUMMAX model, it is possible that the headway shortening for 8 trains is more than that for 6 trains, because the NUMMAX model tried to squeeze the train operation into one period and the last train's arrival time is exactly the period's ending time. It cares only last train's arrival time and the trains before the last one can be scheduled with some uncertainty, which might lead to an uncertainty on the headway.

5.2.2 Result of trains departing in batch

Average headway and speed difference of trains departing in batch

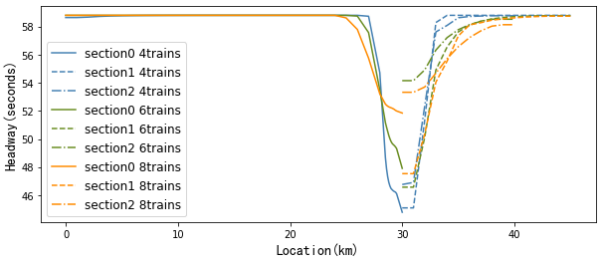

(a) Average headway of trains under MB

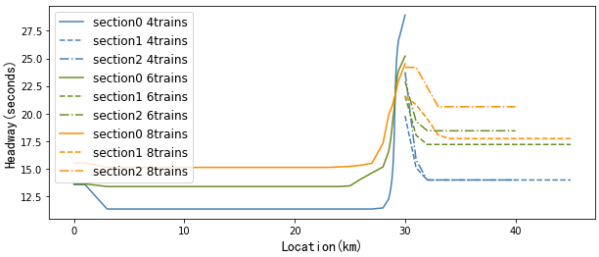

(b) Average headway of trains under VC

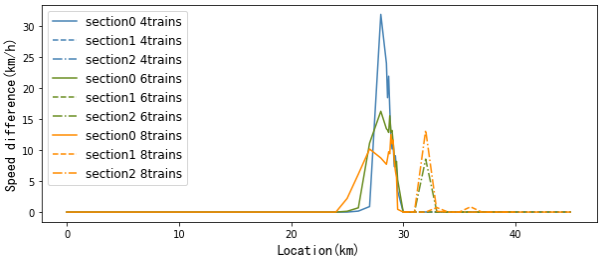

(c) Speed difference of trains under MB

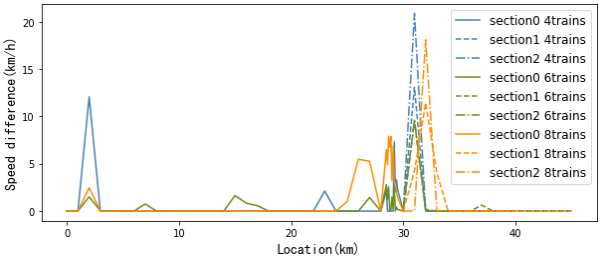

(d) Speed difference of trains under VC

Figure 5.6: Average headway and speed difference of 4, 6, 8 trains in batch (RTMIN)

For the timetable pattern of trains in batch, the average headway of 4, 6, 8 trains under MB and VC are plotted in the following Figure 5.6(a) and 5.6(b) and the average speed difference at each location of the trains are plotted in Figure 5.6(c) and 5.6(d).

By comparing the headway of MB and VC, the most benefit brought from the VC is at the open track area, On this area, the headway at this area under moving block is 59 second, while under virtual coupling, it is improved to 11, 13, 15 seconds for 4 trains, 6 trains and 8trains, saving 81.4%, 78.0% and 74.6%. The bottleneck of the operation is still at the divergence area, but improved from 45, 48 and 52 seconds to 30, 26 and 24 seconds by virtual coupling for 4, 6, 8 trains, improving the percentage

of 33.3%, 45.8%, and 53.8%. These are reflected in Figure 5.6(a) for moving block and Figure 5.6(b) for virtual coupling.

The speed difference of the trains over the network in Figure 5.6(c) for moving block and Figure 5.6(d) for virtual coupling shows that under the virtual coupling, the speeds of the trains in a convoy have peak speed difference after departing from station and at the divergence area, where is the trains to couple and decouple. It is because the trains adjust the speed after departing in coupling state and at the diverging area in the decoupling state. Similar characteristics are also shown in the ATMIN model and NUMMAX model, in appendix C and D.

Result of 6 trains departing in batch under moving block and virtual coupling

The operation adjustment of the trains updated from moving block to virtual coupling will be analysed based on the headway between adjacent trains and the speed profile of each train on time and on location. For 6 trains departing in batch, train 1, train 2 and train 3 go through the section 0 and section 1, followed by train 4, train 5 and train 6 through the section 0 and section 2. The results of the 4 trains and the 8 trains are shown in the appendix B, which shows the same characteristics described as below.

The **headway** between the adjacent trains over the routes are shown in Figure 5.7(a) under MB and Figure 5.7(b) under VC. It is observed that the headway is improved when under virtual coupling. The average headway in Figure 5.6(a) and Figure 5.6(b) before were calculated from the detailed headway of every adjacent trains shown below. The headway is shortened more at the open area than at the diverging area. The bottleneck is still at the diverging area, and the largest headway occurs between the first train of the second batch and the last train of the first batch, observed in Figure 5.7(b),

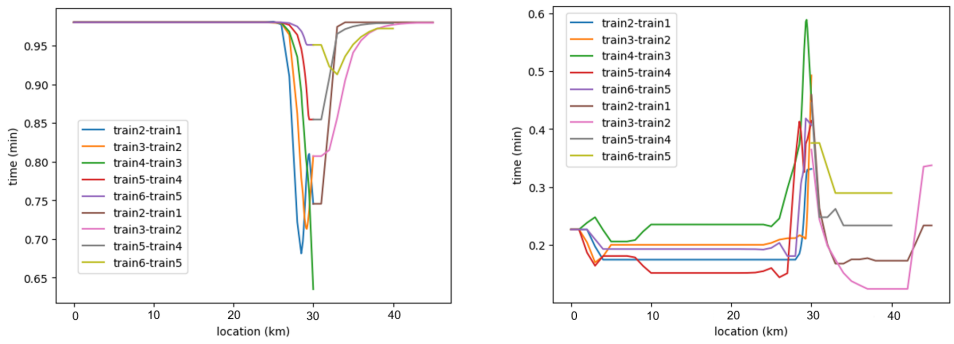

(a) Headway of 6 trains under MB

(b) Headway of 6 trains under VC

Figure 5.7: Headway of 6 trains in batch (RTMIN model)

The **speed profile** is shown below, where Figure 5.8(a) and Figure 5.8(c) is for moving block and Figure 5.8(b) and Figure 5.8(d) is for virtual coupling.

It shows that the convoy starts with a coupling state, where they adjust the speed and shorten the safety distance, and they decelerate together in front of the switch, comparing the virtual coupling on the right column to the moving block on the left column. It can be observed that under virtual coupling, the leading train brakes to shorten the distance with the follower, after departing from the station.

Before arriving a station, the followers brake to keep the safety distance with their leaders. It is clearer in the speed-time profile comparing Figure 5.8(c) for moving block with Figure 5.8(d) to observe the trains' operation adjustment from moving

block to virtual coupling. When approaching the switch, under virtual coupling, the trains in the first batch fully brake to stop, and the trains in the second batch adjusts the speed by braking and accelerating to keep a safety distance with the leader and finally stop, where under virtual coupling the trains in second batch brakes frequently, comparing Figure 5.8(d) to Figure 5.8(c).

It is also observed that the time distance between the curves are denser in the virtual coupling, Figure 5.8(d) than in the moving block, Figure 5.8(c). The time-location profiles in Figure 5.9(b) under virtual coupling is also denser than the one for moving block, in Figure 5.9(a). The time-location profile reflects the timetable scheduling of each train, without conflict under moving block and virtual coupling.

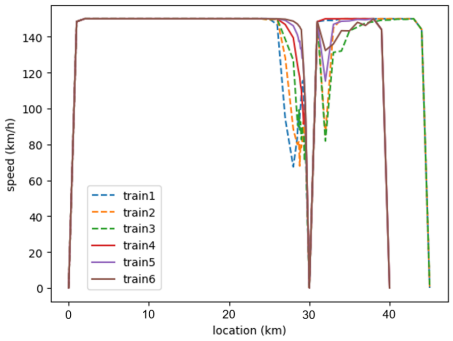

(a) Speed-location profile of 6 trains under MB

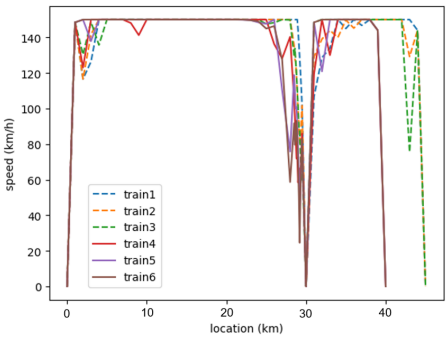

(b) Speed-location profile of 6 trains under VC

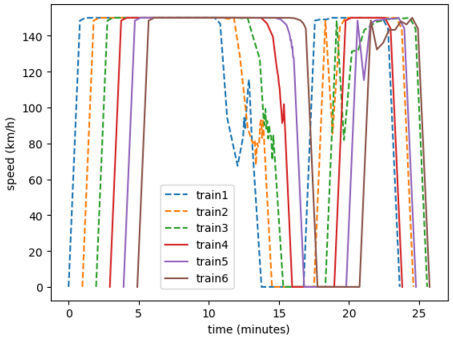

(c) Speed-time profile of 6 trains under MB

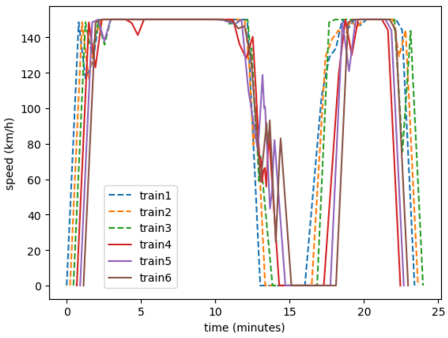

(d) Speed-time profile of 6 trains under VC

Figure 5.8: Speed profile of 6 trains in batch (RTMIN model)

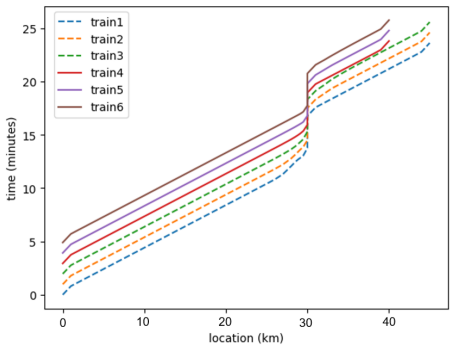

(a) Time-location profile of 6 trains under MB

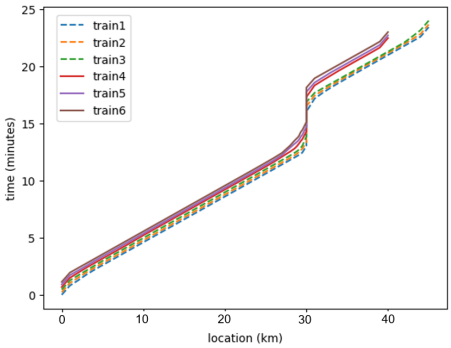

(b) Time-location profile of 6 trains under VC

Figure 5.9: Time-location profile of 6 trains in batch (RTMIN model)

5.2.3 Result of trains departing in Turns

Average headway and speed difference of trains departing in turns

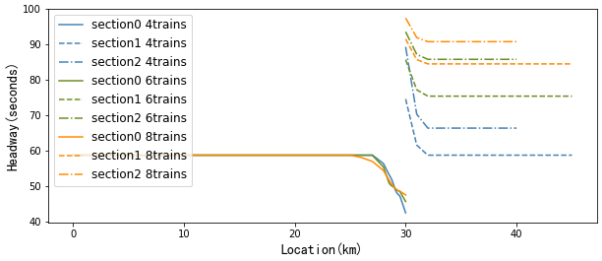

(a) Average headway of trains under MB

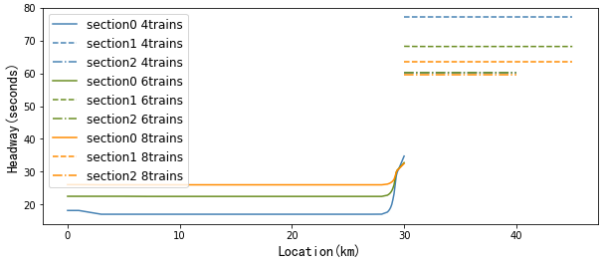

(b) Average headway of trains under VC

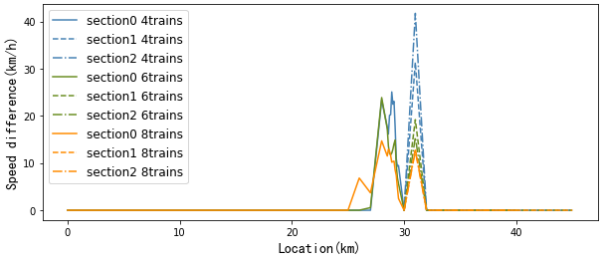

(c) Speed difference of trains under MB

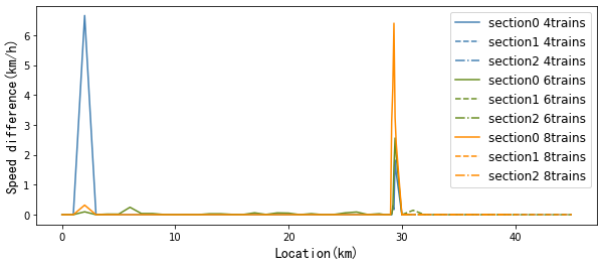

(d) Speed difference of trains under VC

Figure 5.10: Average headway and speed difference of 4, 6, 8 trains in turns (RTMIN)

For the timetable pattern of trains in turns, the average headway of 4, 6, 8 trains under MB and VC are plotted in the following Figure 5.10(a) and 5.10(b) and the average speed difference at each location of the trains are plotted in Figure 5.10(c) and 5.10(d).

For the trains in the timetable pattern of departing in turns, by comparing the headway of MB and VC, the headway at the open track area is also saved more than the diverging area. On the open track area, the 4, 6, 8trains have an improvement from 59 seconds to 18, 23, 26 seconds, saving 69.5%, 61.0% and 55.9%. The bottleneck of the operation is still at the divergence area, but improved from 43, 46

and 48 seconds to a lower headway in 35, 33, 32 second, improving the percentage of 18.6%, 28.2%, 33.3%.

According to the results in Figure 5.10(a) and Figure5.10(b), the headway on the section 0 is minimized under the RTMIN model, where is the shared section for all trains. Similar as the trains in batch, the trains on the section 0 shortened their distance and coupled in the open track area. However, the headway of the trains at the section 1 and section 2 is not squeezed. This is because, the trains at same section when departing in turns has a larger departure headway than the timetable pattern of departing in batch. If focusing the trains to couple, it must take the cost of the running time of the trains. It also shows in the speed difference of the moving block and the virtual coupling, in Figure 5.10(c) and in Figure 5.10(d). After the station B, under virtual coupling ,the trains no longer have speed difference, which means all the trains have the same operation over their second sections.

Result of 6 trains departing in turns under moving block and virtual coupling

For 6 trains departing in turns, train 1, train 2 train 3, train 4, train 5, and train 6 departing in turns from the station A, start of the section 0, where train 1 departs first and train 6 departs last. Train 1, train 3 and train 5 go through the section 0 and section 1, and train 2, train 4 and train 6 through the section 0 and section 2. The results of the 4 trains and the 8 trains are also shown in the appendix B, which present the same characteristics described as below.

The **headway** between the adjacent trains over the routes are shown in Figure 5.11(a) under MB and Figure 5.11(b) under VC. After departing from station B, the trains go to different destinations over the different sections so the departure time between two adjacent trains are longer than the trains in batch. Under the moving block, in Figure 5.11(a), there is still capacity allowed for the trains to squeeze the headway and distance to the absolute braking distance, so as to minimizing the running time. While under the virtual coupling, in Figure 5.11(b), in this timetable pattern, squeezing the headway and distance cannot further minimizing the running time. Thus on the second section, the section 1&2, the trains operates in their minimum running time from departure to arrival, and do not couple with each other. The details of the operation will be seen in next section.

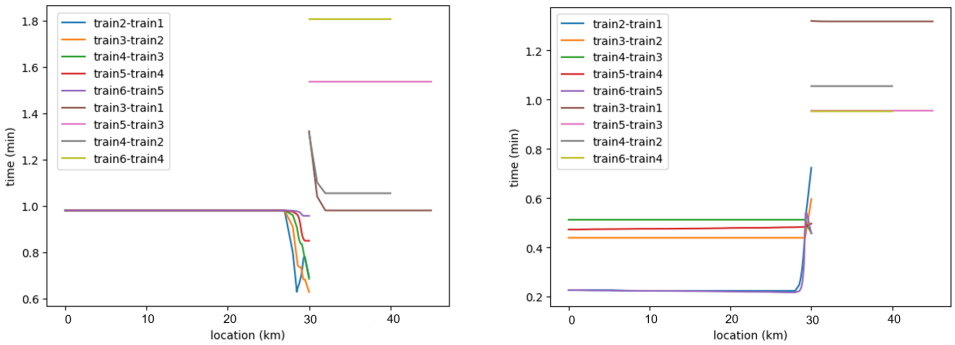

(a) Headway of 6 trains under MB

(b) Headway of 6 trains under VC

Figure 5.11: Headway of 6 trains in turns (RTMIN model)

The **speed profile** is shown below, where Figure 5.12(a) and Figure 5.12(c) is for moving block and Figure 5.12(b) and Figure 5.12(d) is for virtual coupling.

Comparing the section 0 in this departing in turns scenario to the departing in batch scenario before, now only the first train brakes to shorten its distance with

the followers, according to the speed profile. This is because the other trains need to brake at the diverging area, thus if they brake after departing immediately to shorten the headway, the time would be wasted. When entering a station, the first train fully brakes until stop while the other trains brakes in turns before the switching point so as to maintain the safety distance at the diverging area.

At the second sections of the routes, section 1&2, it shows no braking behaviour. In the sections after station B, the trains are expected to arrive in a minimum time, under the RTMIN model. Since coupling the trains takes the cost of the running time here, the trains run in their minimum running time operation in their second sections.

Comparing the operation on the second sections on this timetable pattern and the operation on the timetable pattern of departing in batch before, it can be concluded that if the trains is inevitable to have a large headway on the sections, the trains will run in its minimum running time operation and might not couple. For example, in this timetable pattern, all the trains brakes before the switch so the arrival headway of the trains at the station B is larger than the one of the trains arriving together with same destinations. The different operation at the diverging area between the trains in batch and in turns causes the difference of the operation on the open track area, with the same objective of minimizing the running time.

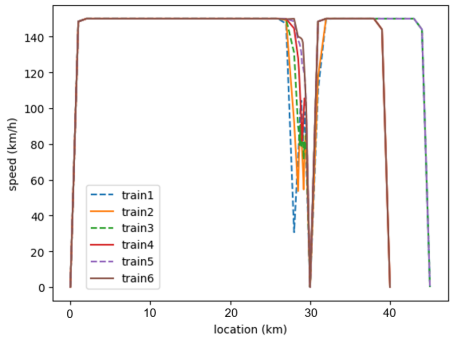

(a) Speed-location profile of 6 trains under MB

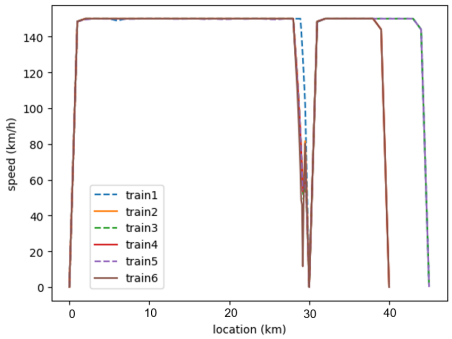

(b) Speed-location profile of 6 trains under VC

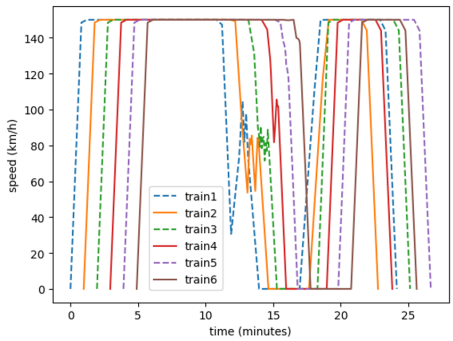

(c) Speed-time profile of 6 trains under MB

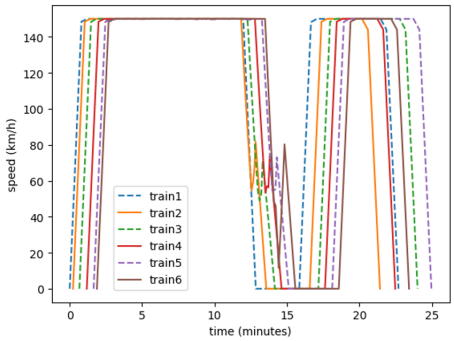

(d) Speed-time profile of 6 trains under VC

Figure 5.12: Speed profile of 6 trains in turns (RTMIN model)

The time-location profile is shown in Figure 5.13(a) and Figure 5.13(b). The profile for the virtual coupling, especially the section 0, is more crowded than the moving block, which means the virtual coupling squeezes the trains headway to improve the capacity utilization.

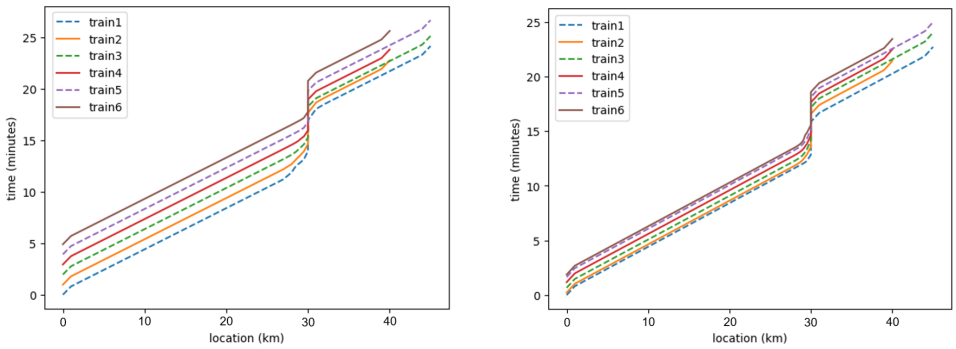

(a) Time-location profile of 6 trains under MB (b) Time-location profile of 6 trains under VC

Figure 5.13: Time-location profile of 6 trains in batch (RTMIN model)

5.3 sensitivity analysis on service braking rate

5.3.1 Set up of the Service braking rate

This sensitivity analysis is studied on the RTMIN model for 6 trains under virtual coupling, under the timetable pattern of departing in turns and departing in batch. The braking service rate are set up as in the Table 5.6, where the scenario 1-0 and scenario 2-0 with all trains' braking rate same in $0.8 m/s^2$ were done above in Section 5.2.2 and Section 5.2.3. The scenario 1-1, 1-2, 2-1, 2-2 are designed to see how are the headway and the trains speed adjusted under virtual coupling,if the trains have different service braking rate.

Table 5.6: Service braking rate varying setup

	Timetable pattern 1: Departing in batch		Scenario 1-0	Scenario 1-1	Scenario 1-2
	Route	Station	$b_s \quad (m/s^2)$	$b_s \quad (m/s^2)$	$b_s \quad (m/s^2)$
Train 1	section 0 + section 1	A-B-C	0.8	0.6	0.8
Train 2	section 0 + section 1	A-B-C	0.8	0.8	0.6
Train 3	section 0 + section 1	A-B-C	0.8	0.6	0.8
Train 4	section 0 + section 2	A-B-D	0.8	0.8	0.6
Train 5	section 0 + section 2	A-B-D	0.8	0.6	0.8
Train 6	section 0 + section 2	A-B-D	0.8	0.8	0.6
	Timetable pattern 2: Departing in turns		Scenario 2-0	Scenario 2-1	Scenario 2-2
	Route	Station	$b_s \quad (m/s^2)$	$b_s \quad (m/s^2)$	$b_s \quad (m/s^2)$
Train 1	section 0 + section 1	A-B-C	0.8	0.6	0.8
Train 2	section 0 + section 2	A-B-D	0.8	0.8	0.6
Train 3	section 0 + section 1	A-B-C	0.8	0.6	0.8
Train 4	section 0 + section 2	A-B-D	0.8	0.8	0.6
Train 5	section 0 + section 1	A-B-C	0.8	0.6	0.8
Train 6	section 0 + section 2	A-B-D	0.8	0.8	0.6

5.3.2 Result of varying the Service braking rate

Infrastructure occupation time

The infrastructure occupation time of the scenarios are shown in Table 5.7. For trains in batch, the longest time on route 1 comes from the scenario 1-1 and on

route 2 comes from the scenario 1-2, and in the set up there are two trains on these routes has the service braking rate of 0.6 m/s^2. For trains in turns, the longest time on route 1 comes from the scenario 2-1 and on route 2 comes from the scenario 2-2, where all the three trains in the routes have the service braking rates of 0.6 m/s^2. Also, the scenario 1-0 and scenario 2-0, where the service braking rates of all the trains are $0.8m/s^2$, give the shortest infrastructure occupation time. Thus it can be concluded that for a convoy on a route, the lower the service braking rate is, the longer infrastructure occupation time the convoy has.

Table 5.7: Infrastructure occupation time of varying service braking rate, by virtual coupling

			scenario 1-0		scenario 1-1		scenario 1-2	
			b_s (m/s^2)	Occ_Time (min)	b_s (m/s^2)	Occ_Time (min)	b_s (m/s^2)	Occ_Time (min)
In batch	Route 1	Train 1	0.8	23.437	0.6	23.733	0.8	23.533
		Train 2	0.8		0.8		0.6	
		Train 3	0.8		0.6		0.8	
	Route 2	Train 4	0.8	22.133	0.8	22.232	0.6	22.432
		Train 5	0.8		0.6		0.8	
		Train 6	0.8		0.8		0.6	
			scenario 2-0		scenario 2-1		scenario 2-2	
			b_s (m/s^2)	Occ_Time (min)	b_s (m/s^2)	Occ_Time (min)	b_s (m/s^2)	Occ_Time (min)
In turns	Route 1	Train 1	0.8	24.975	0.6	25.329	0.8	25.095
		Train 3	0.8		0.6		0.8	
		Train 5	0.8		0.6		0.8	
	Route 2	Train 2	0.8	23.205	0.8	23.450	0.6	23.675
		Train 4	0.8		0.8		0.6	
		Train 6	0.8		0.8		0.6	

Headway of varying the Service braking rate

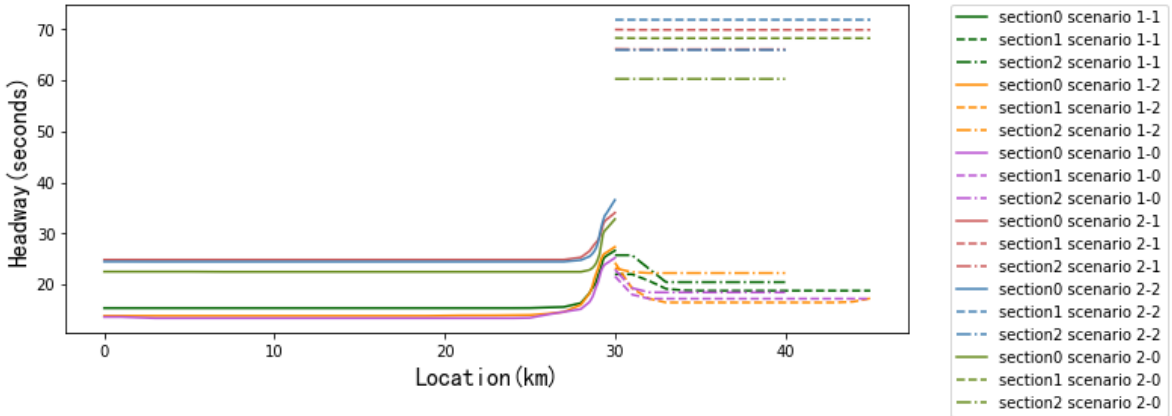

Figure 5.14: Headway of the 6 trains varying service braking rate

It can be observed according to Figure 5.14 that when varying the service braking rate from $0.8m/s^2$ of all the trains to $0.6m/s^2$ for every other trains, the headway between the trains gets increased. As shown in the figure in section 0, the scenario of 2-0 and 1-0 is at the bottom of the group of in turns and in batch. This is because the service braking rate is on the denominator when calculating the safety distance, the formular of which was explained in section 4.4.2 and 4.5. The higher the service braking rate is, the shorter the safety distance and the minimum headway are.

For the section 0, the convoys in scenario 1-1 and in scenario 2-1 with leading trains having braking rate of 0.6 have the largest headway, comparing to the convoys with leading trains having braking rate of 0.8 in scenario 1-2 and scenario 2-2. This is also shown for the trains in batch at section 2 and section 3, seen from the bottom right curves in the figure. For the trains in turns in section 2 and section 3, of which the curves in the upper right, because they run in its minimum running time and is difficult to couple, the headway are maintained same from departing. Details of the value of the headway is shown in the Table 5.8. In the table, the headway for the whole section refers to the overall headway of each trains over the section 0 from station A to station B, and the headway at the diverging area refers to the headway of the trains at the diverging area, which is the last 2 km before station B, and is where the model gets tense in Figure 5.2. According to the result, comparing the headway at the diverging area, if the follower has a higher braking rate, the convoy of which the follower has a higher braking rate gives a better headway at the diverging area. This is because if the second train has a better braking rate than the first train,the the headway can be shortened at the diverging area where needs flexible braking. This characteristic is also discovered by Quaglietta et al. [2021]. Comparing the headway for the whole section, for the convoy in which the leader has a higher braking rate, the overall headway is better. This is consistent with the infrastructure occupation time result in section 5.3.2, which shows the convoy in which the leader has a higher braking rate has a shorter infrastructure occupation time. It reflects that if the headway at the diverging area is restricted by different service braking rate, it could still be compensated at the open track area by optimization.

Table 5.8: Headway of each train

	In batch						
		scenario 1-0		scenario 1-1		scenario 1-2	
Headway for the whole section (min)	Train2-Train1	0.8 0.8	0.21312	0.6 0.8	0.37015	0.8 0.6	0.24622
	Train3-Train2	0.8 0.8	0.23397	0.8 0.6	0.23474	0.6 0.8	0.23982
	Train4-Train3	0.8 0.8	0.26819	0.6 0.8	0.24142	0.8 0.6	0.26941
	Train5-Train4	0.8 0.8	0.20849	0.8 0.6	0.23487	0.6 0.8	0.25269
	Train6-Train5	0.8 0.8	0.24180	0.6 0.8	0.23862	0.8 0.6	0.20190
	average		0.23311		0.26396		**0.24201**
Headway at the diverging area (min)	Train2-Train1	0.8 0.8	0.28563	0.6 0.8	0.39563	0.8 0.6	0.28236
	Train3-Train2	0.8 0.8	0.26360	0.8 0.6	0.28317	0.6 0.8	0.31143
	Train4-Train3	0.8 0.8	0.47022	0.6 0.8	0.41111	0.8 0.6	0.58913
	Train5-Train4	0.8 0.8	0.32289	0.8 0.6	0.34061	0.6 0.8	0.36412
	Train6-Train5	0.8 0.8	0.35716	0.6 0.8	0.38570	0.8 0.6	0.32067
	average		0.33990		**0.36324**		0.37354
	In turns						
		scenario 2-0		scenario 2-1		scenario 2-2	
Headway for the whole section (min)	Train2-Train1	0.8 0.8	0.23654	0.6 0.8	0.23836	0.8 0.6	0.24311
	Train3-Train2	0.8 0.8	0.44077	0.8 0.6	0.45558	0.6 0.8	0.46061
	Train4-Train3	0.8 0.8	0.51137	0.6 0.8	0.55388	0.8 0.6	0.55102
	Train5-Train4	0.8 0.8	0.47718	0.8 0.6	0.58031	0.6 0.8	0.57217
	Train6-Train5	0.8 0.8	0.23082	0.6 0.8	0.26847	0.8 0.6	0.24121
	average		0.37933		0.41932		**0.41362**
Headway at the diverging area (min)	Train2-Train1	0.8 0.8	0.41336	0.6 0.8	0.39303	0.8 0.6	0.49195
	Train3-Train2	0.8 0.8	0.46821	0.8 0.6	0.54281	0.6 0.8	0.44004
	Train4-Train3	0.8 0.8	0.50059	0.6 0.8	0.49083	0.8 0.6	0.58028
	Train5-Train4	0.8 0.8	0.48528	0.8 0.6	0.62036	0.6 0.8	0.51149
	Train6-Train5	0.8 0.8	0.35231	0.6 0.8	0.40578	0.8 0.6	0.44278
	average		0.44395		**0.49056**		0.49331

Speed difference of varying the Service braking rate

The speed difference of the scenarios is shown in Figure 5.15. It can be observed that after leaving the station B, on the second sections (section 1 and section 2), the trains departing in batch adjust their speeds to couple and the convoy with different service braking rate has a higher speed difference, which reflected in the figure is the scenario 1-1 and scenario 1-2 has a higher peak than the scenario 1-0 after leaving the station B, the 30km. The trains are in the coupling state where they trying to minimize the safety distance at the section 2 and section 3. It can be seen in the location-speed and time-speed profile that the train 1 and train 2 brakes in turns to couple with train 3, in Figure E.1(b) and E.2(b), in the appendix.

It is observed that for the trains in batch, at the arriving area of section 1 and section 2, the trains have a large speed difference, because this is where the trains need to brake while under different rate. The large speed difference is where the trains brakes or accelerate in different rates to minimize the trains' distance. It does not show in the in-turns scenario, because the trains at the section 2 and section 3 have the same braking rate.

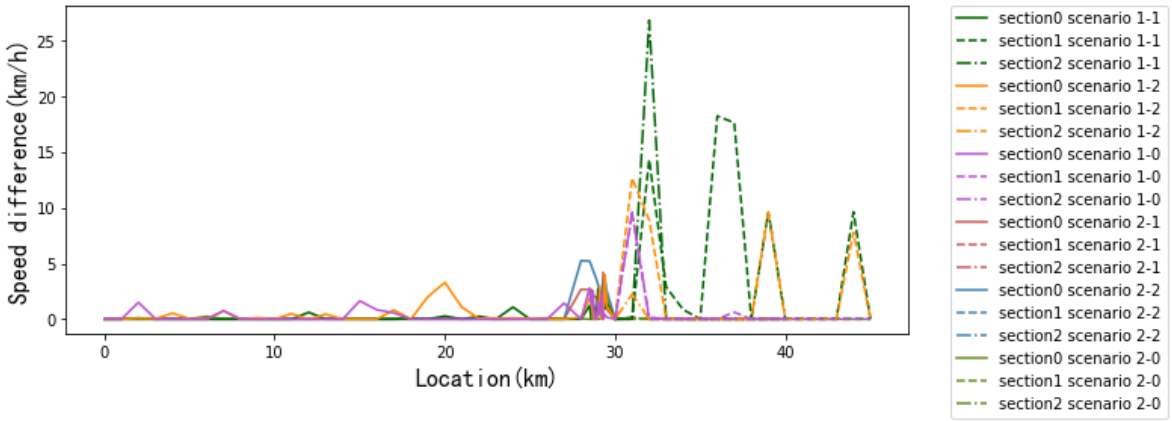

Figure 5.15: Speed difference of the 6 trains varying service braking rate

5.4 sensitivity analysis on speed limit

5.4.1 Set up of the speed limit

The speed limit on the trains are set up in Figure F. The maximum speed allowed at the open track, is 150km/h. At the end of the section 0, 28-29 km, it is set to 80 km/h, for approaching the switching point, and at 29-30 km, it is set up to 60 km, where the switching point is at the 29.5 km. For section 1 and section 2, it is set to be 80 km/h as the maximum speed, from 3 km before the station until the end.

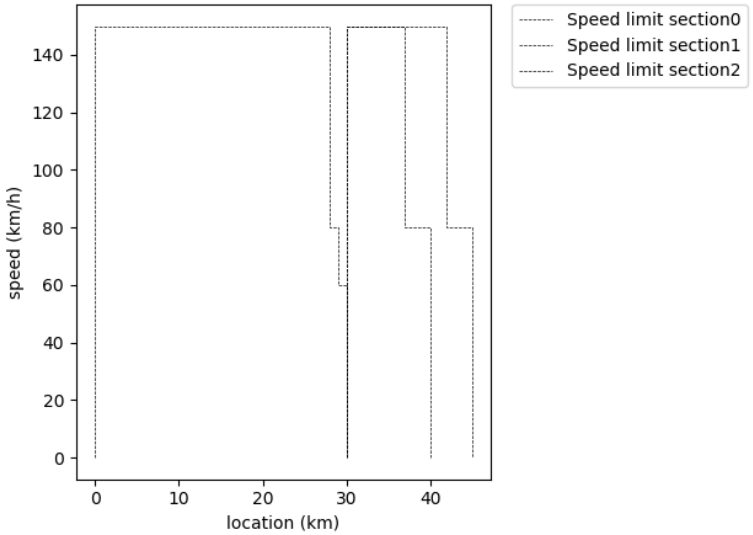

Figure 5.16: Speed limit setup

This sensitivity analysis applies the above speed limit on trains departing in batch and departing in turns. It will be analyzed how does the trains perform if add in the speed limit, and comparing the moving block and the virtual coupling.

5.4.2 Headway and infrastructure occupation time with and without speed limit

Table 5.9: Headway and infrastrucute occupation time improvement

Headway (Sec)	With speed limit			Without speed limit			
	MB	VC	Impr*	MB	VC	Impr*	
In batch	56.313	21.253	62.3%	57.533	15.130	73.7%	Route 1
In batch	34.356	17.153	50.1%	57.834	15.181	73.8%	Route 2
In turns	62.657	31.749	49.3%	64.065	37.905	40.8%	Route 1
In turns	47.615	34.325	27.9%	80.068	32.127	59.9%	Route 2
		Average:	**47.4%**		**Average:**	**62.0%**	
Occ_Time (min)	With speed limit			Without speed limit			
	MB	VC	Impr*	MB	VC	Impr*	
In batch	28.204	26.451	6.2%	25.5793	23.43729	8.4%	Route 1
In batch	28.387	26.131	7.9%	25.7532	22.81731	11.4%	Route 2
In turns	29.276	27.571	5.8%	26.6635	24.97496	6.3%	Route 1
In turns	28.234	26.131	7.4%	25.6201	23.43119	8.5%	Route 2
		Average:	**6.9%**		**Average:**	**8.7%**	
Impr*:VC improvement over MB							
Occ_Time:Infrastructure occupation time							

The results of the headway and the infrastructure occupation time are shown in the following table. Generally, the improvement of the headway and the infrastructure occupation time are smaller than the scenarios without speed limit. The average headway without speed limit is 62.0% and with speed limit is 47.4%. The infrastructure occupation time without speed limit is 8.7% and with speed limit is 6.9%. Thus, if adding speed limit on the diverging area, the capacity utilization efficiency is affected.

5.4.3 Optimization result for trains in batch and in turns with speed limit

The trains under moving block and virtual coupling with speed limit has the following result, for 6 trains in batch and in turns.

Headway with speed limit

If add in the speed limit set up as above, the optimization result shows the following headway, in Figure 5.17. Comparing the virtual coupling to the moving block, the headway is shortened. It shows with the speed limit, the VC departing in batch gives the shortest headway. The VC in turns is ranked second. The MB in batch is ranked third. The MB in turns gives the largest headway. It also shows the virtual coupling brings more benefit on the open track area and the trains decouples at the diverging area, and such capacity efficiency benefit is obvious by comparing the virtual coupling to the moving block.

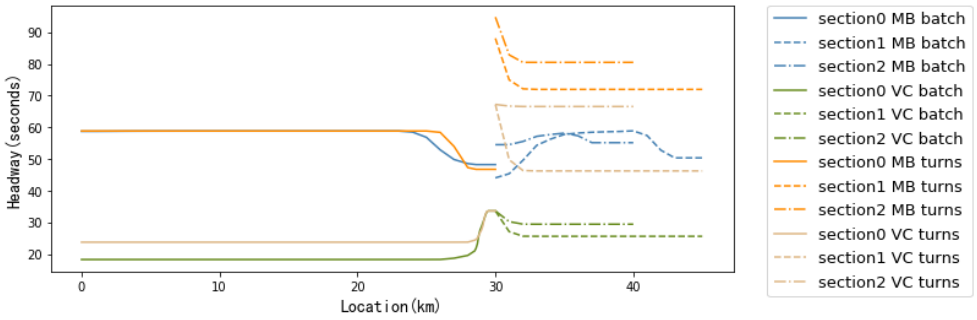

Figure 5.17: Headway of the 6 trains with speed limit

speed difference with speed limit

The speed difference for the trains moving with speed limit are shown in Figure 5.18. The trains have less speed difference after departing from the station A, and still have much speed difference at the arriving area of the station B, where the diverging area is.

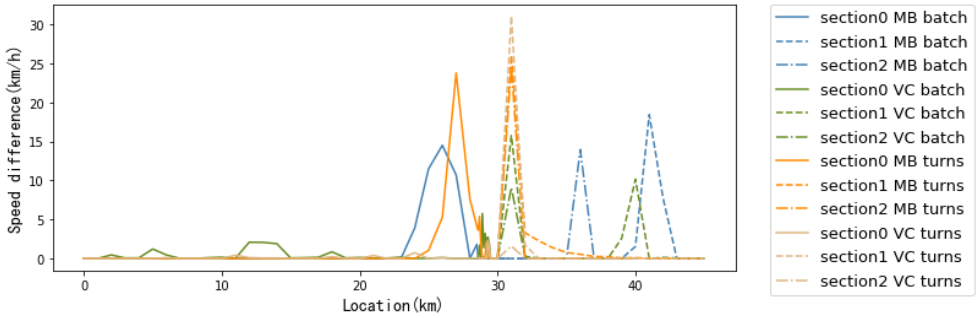

Figure 5.18: Speed difference of the 6 trains with speed limit

5.4.4 Result of operation with speed limit test for trains in batch and in turns

The location-speed profile of the 6 trains under moving block and virtual coupling, in batch and in turns are shown in the following Figure. It shows the trains moving under the speed limit and under the minimum running time objective.

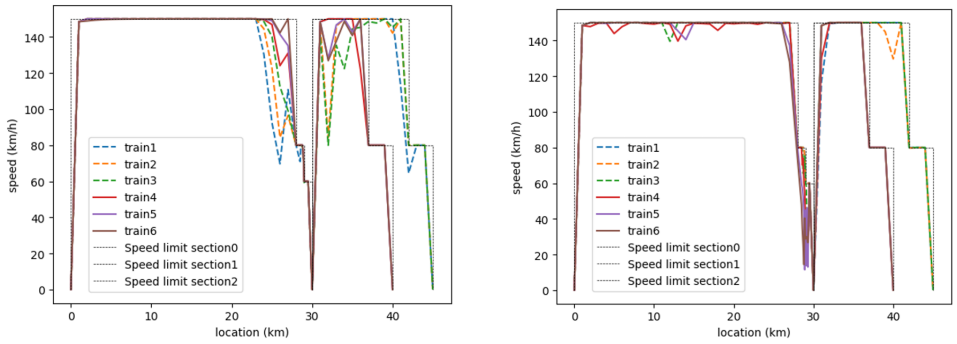

(a) Location-speed profile of 6 trains under MB (b) Location-speed profile of 6 trains under VC

Figure 5.19: Location-speed profile of 6 trains in batch (RTMIN model)

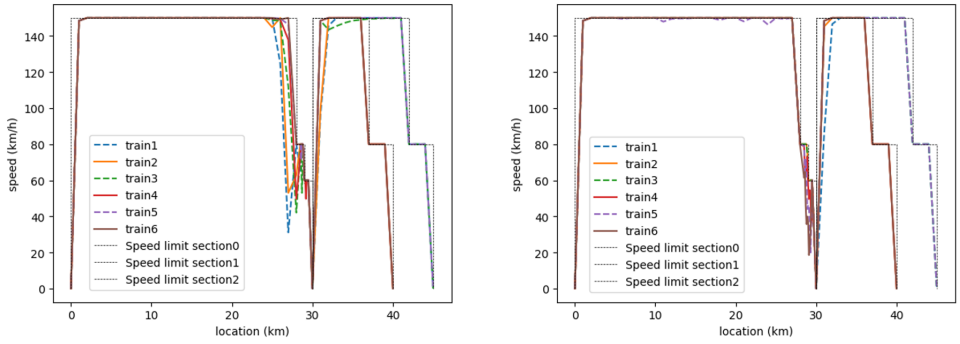

(a) Location-speed profile of 6 trains under MB (b) Location-speed profile of 6 trains under VC

Figure 5.20: Location-speed profile of 6 trains in turns (RTMIN model)

It can be observed that comparing the **Location-speed profile** to the scenarios' without speed limit before, the trains now have less braking behaviour after departing from the station. This is because adding in the speed limit, the trains are forced to braking before entering the speed limit area. Especially for the leading train in the first batch, if without speed limit, it does not need to brake at the diverging area in the scenarios before, so it has some space to brake after departing to shorten

its distance with the follower. However in this scenario with speed limit, it must decelerate at the arriving area, so the optimization result does not show braking behaviour after leaving the station, otherwise the running time would be wasted.

Comparing the virtual coupling and the moving block with speed limit, it is found that under moving block the leading train brakes before entering the speed limit area, and under the virtual coupling the following train brakes at this area. This characteristic under moving block is because the leading train must decelerate at this area and decelerating here can further minimize the distance between adjacent trains. While under virtual coupling, the following trains brakes because the safety distance is enlarged to the absolute braking distance, thus the following trains should brake to satisfy it.

The figures of the speed-time profile and time-location profile are shown in the appendix F.

6 DISCUSSION

The questions proposed in Chapter 3.1 will be discussed, to see how Virtual Coupling railway operation can be optimally scheduled to maximize capacity utilization by forming platoons. By comparing the RTMIN, ATMIN, and NUMMAX model, the RTMIN gives the most capacity utilization efficiency and the NUMMAX gives the most headway saving results at the cost of running time.

Since the RTMIN model gives the best balance between the headway shortening and the infrastructure occupancy time saving, as this model only couple the trains when the coupling will improve or at least not affect the running time. Thus, the following questions are discussed based on the results mainly from the RTMIN model, which has minimizing the trains running time as the first objective. The different optimization result by ATMIN and by NUMMAX will be explained.

6.1 How will the operation of the trains be adjusted in a convoy to form a platoon?

When departing from a station, the trains can start couple to form a platoon by departing in a small headway, then braking or accelerating at different rate to further shorten the headway. For trains departing in batch, on section 0, the trains in first batch brakes after reaching the maximum speed. On section 1 and section 2, the trains accelerate in different acceleration rate. It is observed that after acceleration from a station, the leader of a convoy can brake to shorten the distance with its follower, and all the leading trains with followers have this operation. For trains departing in turns, the trains on the shared section 0 also start with similar characteristic as the trains in batch. The train brakes to shorten the headway but only the first train brakes. This is because the trains departing in turns excluding the first train need to brake to maintain a large distance at the diverging area, so braking after acceleration would take some cost of the running time. On section 1 and section 2, the trains fully accelerate without coupling, since the two trains departing in turns are too far away to couple. For the routes with speed limit at the diverging area, all the train including the first leader should brakes here. In this circumstance, the trains in batch or in turns are optimized to fully accelerate with a small headway when departing, without braking to further shorten the distance. It can be summarized that the leading trains can shorten the headway by braking after acceleration from a station, but if they must brake in the following, they are optimized to not brake, in case of wasting time.

When arriving in a station, the followers brake to maintain the safety distance. For the trains in batch, the first batch fully brakes to stop at the station B and the trains in second batch brakes to main the safety distance, which is the absolute braking distance, safety margin, the lead plus the distance covered by the switching time. For the trains in turns, the first train fully brakes, and the followers are all brakes in turns to leave the platoon and keep a safety distance.

For trains under different service braking rate, the trains operation has the same characteristics as described before, but fully brakes in their service braking rate. The headway is changed, analyzed in the sub question 2. In the scenarios with speed limit, the trains under virtual coupling have more deceleration than under

the moving block, because when entering this speed limit area, the trains under virtual coupling has a short headway which needs to be enlarged.

The RTMIN model couples the trains only if the capacity efficiency can improve or at least not affect. The ATMIN and the NUMMAX model give a different optimal solution in some circumstance. For the trains in batch, all the three models can couple the trains, but for the trains departing in turns, the RTMIN model does not couple the trains in the second sections. The ATMIN and the NUMMAX model can couple the trains, by the leading train departing in a smaller acceleration and braking to adjust the train distance to couple. The results of the NUMMAX and the ATMIN model show a larger infrastructure occupancy time and a lower capacity efficiency, while the RTMIN gives the minimum infrastructure occupancy time and the best capacity efficiency. It reflects that minimizing the headway or the trains' distance cannot always improve the railway's capacity utilization efficiency.

6.2 How can train running times and the headway be adjusted to satisfy an optimized formation of virtually coupled platoons?

Comparing the running time of the three model, the NUMMAX gives the longest running time of the trains and the RTMIN gives the minimum running time. In the RTMIN model, the running time of all the trains is not changed and maintained in minimum, comparing the virtual coupling and the moving block. The trains are coupled under the objective of minimum running time.

About the headway, all of the RTMIN, ATMIN and NUMMAX model show the improved headway by virtual coupling. On average, the headway can be shortened by the RTMIN in 61.62%, which is 74.14% in batch and 49.10% in batch, by ATMIN in 70.57%, which is 78.05% in batch and 63.10% in turns, and by NUMMAX in 74.65%, which is 79.38% in batch and 69.91% in turns. The NUMMAX and the ATMIN show more headway shortening, but the platoon does not run in the most efficient way, due to adjusting speed and distance frequently in operation.

In the RTMIN, ATMIN and NUMMAX model, the trains departing the station in a short headway. For the trains in batch, the trains can further minimizing the headway in the open track area, and the headway is enlarged at the diverging area. For the trains in turns, the first train brakes to further shorten the headway and the other trains keep a same headway as the short departing headway, until the diverging area. In the second sections, in the RTMIN, the trains in batch can further decrease the headway, while the trains in turns in this section run in a small headway and is not changed till stop. In the ATMIN and the NUMMAX, all the trains in batch and in turns in the second section can further decrease the headway after leaving station B, by adjusting the speed, where the NUMMAX shows more speed changing behaviour than the ATMIN.

For trains under different service braking rate, the trains fully brakes in their service braking rate, and such different rate result in different headway for both in batch and in turns. The trains has the shortest arriving headway when the service braking rate are same in $0.8m/s^2$, the maximal headway come from the scenarios of service braking rate in $0.6m/s^2$ for first train and $0.8m/s^2$ for the second. The scenarios of $0.8m/s^2$ for first train and $0.6m/s^2$ for the second gives the headway in middle.

In the scenarios with speed limit, the headway improvement by the virtual coupling is 47.4% on average, smaller than 62.0%, the average headway of the scenarios without speed limit. This is mainly because the operation of the leading train is changed, which should also decrease the speed at the diverging area, and the followers should further braking to maintain the safety distance.

6.3 what and where are the actual capacity gains that virtual coupling can provide over plain moving block if an optimised platoon formation is considered?

The most capacity improvement benefit comes from the RTMIN mode, which saves the infrastructure occupation time averagely in 7.9%, which is 9.6% in batch and 6.2% in turns. The ATMIN model has the time saved averagely in 6.6%, which is 7.6% in batch and 5.6 % in turns. The NUMMAX saves the least infrastructure occupation time, which is 5.3% on average, which is 6.4% in batch and 4.2% in turns.

The most beneficial improvement seen from the headway profile is at the open track area. At this area, for 4,6 and 8 trains departing in batch, the headway under moving block is 59 seconds, while under virtual coupling, it is improved to 11, 13, 15 seconds for 4 trains, 6 trains and 8trains, saving 81.4%, 78.0% and 74.6% respectively. For trains in turns, the 4, 6, 8trains has an improvement from 59 seconds to 18, 23, 26 seconds, saving 69.5%, 61.0% and 55.9% respectively. The bottleneck is still at the diverging area, but it is also improved. On this area, the 4,6 and 8 trains departing in batch under moving block have the headway of 45, 48 and 52 seconds, which were improved to 30, 26 and 24 seconds by virtual coupling, improving the percentage of 33.3%, 45.8%, and 53.8%. For trains in turns, the 4, 6, 8 trains has an improvement from 43, 46 and 48 seconds to a lower headway in 35, 33, 32 seconds, improving the percentage of 18.6%, 28.2%, 33.3%. The results also show that the trains departing in batch can save more headway and capacity by virtual coupling, on the entire track including the open area and the diverging area.

Thus, comparing the virtual coupling to the plain moving block, the capacity gain it provides is that it can shorten the headway, especially at the open track area and also especially when trains are operated in batches rather than in turns. And the bottleneck at the diverging area, the headway is also improved, so as to improve the capacity utilization efficiency for timetable scheduling.

The service braking rate can have an effect on the results. In the scenarios of varying the service braking rate, the convoy of which the leader has a higher braking rate gives a shorter infrastructure occupation time, because if the headway at the diverging area is restricted by different service braking rate, it could still be compensated at the open track area by optimization.

Comparing the scenarios with speed limit and without speed limit, more benefit are brought without speed limit, where the average infrastructure occupation time for the scenarios without speed limit is 8.7% and with speed limit is 6.9%, on average for trains in batch and in turns.

6.4 current limitations and further research

One current limitations of this MIQP model is that if more trains are scheduled in the timetable, the computation time will get increased. This is because the model solves all trains' variable at each location at the same time. Future research shall look at a multi-layer model for computing more trains timetable. For extending the model to schedule more trains, it could be possible to put two or three trains as a group, calculate the trains in each group first, then to minimize the distance between each group.

Another characteristic of this model is that it considered only one train can stop in a station at a time, where all the trains shall stop with the head exactly at the ending interval of the sections, which means the follower shall cannot stop until the leading trains leaving that stop location. The current space-discrete MIQP model can only have the trains stop at the node of each space-discrete train behavioural

intervals. To allow more trains stopping in one station, it might need a continuous model, since the trains head can stop at any location within the station area.

7 CONCLUSION

This study constructed an MIQP model to schedule the railway service under virtual coupling. A case study on a Y-shape network was conducted to see how virtual coupling railway operation can be optimally scheduled. The virtual coupling and the moving block is compared, on two timetable patterns, departing in batch and departing in turns, by RTMIN, ATMIN and NUMMAX model. It also conducted the sensitivity analysis on service braking rate and on speed limit. The headway of each scenarios are compared between virtual coupling and the moving bock, which intuitively reflects the headway of the trains in a timetable. It is verified that the benefit brought by virtual coupling is mostly for trains in batch, on the open track area, and can improve the performance at the diverging area where the bottleneck is. To form a platoon, the leading trains can brake to minimize the trains' distance after departing from the station. To leave a platoon, the following trains brakes at the approach to the diverging junction.

The RTMIN gives the most capacity utilization efficiency, which gives the shortest infrastructure occupation time in all the scenarios, although the RTMIN does not shorten the headway most, comparing to ATMIN and NUMMAX. The infrastructure occupation time can be improved on average in 7.9% by RTMIN, in 6.6% by ATMIN, and in 5.3% by NUMMAX.The headway can be improved on average in 61.62% by RTMIN, in 70.57% by ATMIN and in 74.65%by NUMMAX.

According to the sensitivity analysis on the service braking rate, comparing the headway under virtual coupling, the trains with the same service braking rate gives the minimum headway, among the three scenarios. And the leading train with lower service braking rate gives a higher headway than the platoon with the leader having a higher service braking rate. About the infrastructure occupation time, the convoys with more trains in higher service braking rate give shorter infrastructure occupation time on their routes.

For the trains running with the limit on speed, because this constraint works for all the trains including the leading trains strictly, trains in the platoon brake more frequently when approaching the diverging area if imposing a speed limit on the tracks. In this circumstance, the trains would not further shorten the headway after departing from a station.

For future research, the RTMIN model can be further developed for other research objectives, because this model synthesizes the running time and the headway of each trains. It gives the most capacity efficiency results, as it couples the trains only when it can shorten the overall time to improve the capacity utilization efficiency. The RTMIN model is flexible to be adjusted for different research objectives, such as to schedule the train services on demand by assigning different weights to the network's sections or routes based on demand. In all the scenarios, the virtual coupling can shorten the headway and improve the capacity, but the scenarios with same service braking rate, without speed limit and departing in batch gives the maximum capacity improvement. This scenario is more worth considering to get the most out of the virtual coupling capacity gains. To increase the ability of scheduling more trains, a multi-layer model could be build using the RTMIN model as the base layer, which could compute the train schedules in groups of trains.

BIBLIOGRAPHY

Basile, D., ter Beek, M. H., Ferrari, A., and Legay, A. (2019). Modelling and Analysing ERTMS L3 Moving Block Railway Signalling with Simulink and Uppaal SMC. *Lecture Notes in Computer Science (including subseries Lecture Notes in Artificial Intelligence and Lecture Notes in Bioinformatics)*, 11687 LNCS(September):1–21.

Bešinović, N., Quaglietta, E., and Goverde, R. M. (2019). Resolving instability in railway timetabling problems. *EURO Journal on Transportation and Logistics*, 8(5):833–861.

Caimi, G., Kroon, L., and Liebchen, C. (2017). Models for railway timetable optimization: Applicability and applications in practice. *Journal of Rail Transport Planning and Management*, 6(4):285–312.

Caprara, A., Fischetti, M., and Toth, P. (2002). Modeling and solving the train timetabling problem. *Operations Research*, 50(5).

Corman, F., D'Ariano, A., Hansen, I. A., and Pacciarelli, D. (2011). Optimal multi-class rescheduling of railway traffic. *Journal of Rail Transport Planning and Management*, 1(1):14–24.

Dick, C. T., Mussanov, D., Evans, L. E., Roscoe, G. S., and Chang, T. Y. (2019). Relative Capacity and Performance of Fixed- and Moving-Block Control Systems on North American Freight Railway Lines and Shared Passenger Corridors. *Transportation Research Record*, 2673(5):250–261.

Duan, H. and Schmid, F. (2019). Optimised Headway Distance Moving Block with Capacity Analysis. *2018 International Conference on Intelligent Rail Transportation, ICIRT 2018*.

Felez, J., Kim, Y., and Borrelli, F. (2019). A Model Predictive Control Approach for Virtual Coupling in Railways. *IEEE Transactions on Intelligent Transportation Systems*, 20(7):2728–2739.

Geraets, F., Kroon, L., Schöbel, A., Wagner, D., Zaroliagis, C., Liebchen, C., and Möhring, R. (2007). The Modeling Power of the Periodic Event Scheduling Problem: Railway Timetables — and Beyond. In *Lecture Notes in Economics and Mathematical Systems*, volume 600, pages 117–150.

Goverde, R. M., Corman, F., and D'Ariano, A. (2013). Railway line capacity consumption of different railway signalling systems under scheduled and disturbed conditions. *Journal of Rail Transport Planning and Management*, 3(3):78–94.

Ho, M., Mao, B., and Yang, Z. (1998). Multi-train movement simulator with moving block signalling. *Proceedings of the International Conference on Computer Aided Design, Manufacture and Operation in The Railway and Other Advanced Mass Transit Systems*, 34:783–792.

Landex, A., Schittenhelm, B., Kaas, A. H., and Schneider-Tilli, J. (2008). *Capacity measurement with the UIC 406 capacity method*, volume 103.

Liu, P. and Han, B. (2017). Optimizing the train timetable with consideration of different kinds of headway time. *Journal of Algorithms and Computational Technology*, 11(2):148–162.

MOVINGRAIL (2019). Market Potential and Operational Scenarios for Virtual Coupling. Technical report, Shift2Rail.

Ning, B. (1998). Absolute braking and relative distance braking - train operation control modes in moving block systems. *Proceedings of the International Conference on Computer Aided Design, Manufacture and Operation in The Railway and Other Advanced Mass Transit Systems*, 34:991–1001.

Pellegrini, P., Marlière, G., and Rodriguez, J. (2017). RECIFE-SAT: A MILP-based algorithm for the railway saturation problem. *Journal of Rail Transport Planning and Management*, 7(1-2):19–32.

Quaglietta, E. (2019). Analysis of Plooning Train Operations under V2V Communication-based Signaling:Fundamental Modelling and Capacity Impacts of Virtual Coupling. In *Transportation Research Board 98th Annual Meeting*, number April, pages 1–17.

Quaglietta, E., Spartalis, P., Wang, M., Goverde, Rob, M. P., and van Koningsbruggen, P. (2021). Modelling and analysis of Virtual Coupling with dynamic safety margin considering risk factors in railway operations. *RailBeijing, 9th International Conference on Railway Operations Modelling and Analysis (ICROMA)*, (2015).

Quaglietta, E., Wang, M., and Goverde, R. M. (2020). A multi-state train-following model for the analysis of virtual coupling railway operations. *Journal of Rail Transport Planning and Management*, 15(April):100195.

Rotoli, F., Cawood, E. N., and Soria, A. (2016). Capacity assessment of railway infrastructure tools, methodologies and policy relevance in the EU context. Technical report, Joint Research Centre (JRC), Luxembourg.

Sameni, M. K. (2012). *Railway track capacity: measuring and managing*. PhD thesis, University of Southampton.

Schumann, T. (2017). Increase of capacity on the shinkansen high-speed line using virtual coupling. *International Journal of Transport Development and Integration*, 1(4):666–676.

Serafini, P. and Ukovich, W. (1989). A Mathematical Model for Periodic Scheduling Problems. *SIAM Journal on Discrete Mathematics*, 2(4):550–581.

Sessa, C. and Isis, R. E. (2010). EU transport demand: Trends and drivers. (March):1–46.

Setyawan, E. B. and Diah Damayanti, D. (2018). Integrated railway timetable scheduling optimization model and rescheduling recovery optimization model: A systematic literature review. *2018 5th International Conference on Industrial Engineering and Applications, ICIEA 2018*, pages 226–230.

UIC (2013). Capacity (UIC Code 406). (2nd edition):56.

Vansteenwegen, P. and Oudheusden, D. V. (2006). Developing railway timetables which guarantee a better service. *European Journal of Operational Research*, 173(1):337–350.

Xu, Y., Cao, C. X., Li, M. H., and Luo, J. L. (2012). Modeling and simulation for urban rail traffic problem based on cellular automata. *Communications in Theoretical Physics*, 58(6):847–855.

Ying, C. (2014). Impact of Moving Block System on Railway Timetable Planning: a qualitative study on existing timetables. *International Journal of Scientific & Engineering Research*, 5(6):1162–1166.

Zhang, L. Y., Li, P., Jia, L. M., and Yang, F. Y. (2005). Study on the simulation for train operation adjustment under moving block. *IEEE Conference on Intelligent Transportation Systems, Proceedings, ITSC*, 2005:807–812.

A CALIBRATION ON THE HIERARCHICAL MODEL

A.1 CALIBRATION TEST

The multiple objectives are optimised by hierarchical approach, which assigns a priority to each objectives. Gurobi optimizer requires that the priority is an integral, not continuous. The attribute of of priority is different from the attribute of weight, which is used in the blended approach, or said the weight and sum method. The attribute of a weight can be negative, which means to minimize the maximization objective or on contrary. The priority attribute only means the order of saving objective. The hiechachical approach can only solve the minimizing objectives, and the solution of lower priority objective should not enlarge the the optimization result of the higher priority objective. To test which priority to use for this study, the following tests were done, on RTMIN model for trains in turns. The first three columns are the priority set up of the model, and the last two columns are the two objectives' value of the result in each test.

A.2 TEST RESULT

Table A.1: Objective value of priority calibrating test

Test	Priority for obj1	Priority for obj2	Optimizaiton value of Obj1	Optimizaiton value of Obj2
1	1	1	5673.394	1908.364
2	2	1	5337.408	4254.855
3	5	1	5337.408	4254.320
4	10	1	5337.408	4254.320
6	15	1	5337.408	4254.320
7	20	1	5337.408	4254.320
8	200	1	5337.408	4254.320
9	2000	1	5337.408	4254.320

The result of test 3-9 give the same result, and the obj1 result is maintained optimal. Thus the set up of the priority in test 3-9 are suitable for this model. The priority of 20:1 are used in this research, which is from the official example of the Gurobi.

Result of test 1

In this test, the priority of the two objectives are set in same. The obj1 result is 5673.394 second.The obj2 result is 1908.364 second. It also shows that sacrificing some running time can further shorten the headway, but brings more braking behaviour to the platoon.

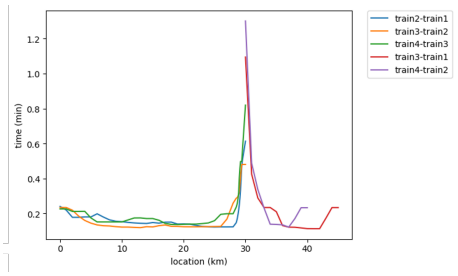

(a) Headway of test 1

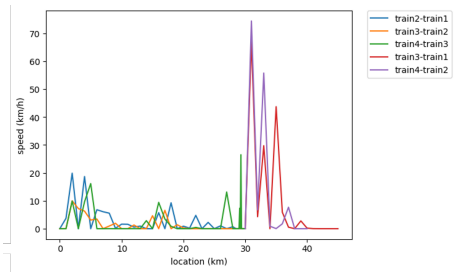

(b) Speed-difference profile of test 1

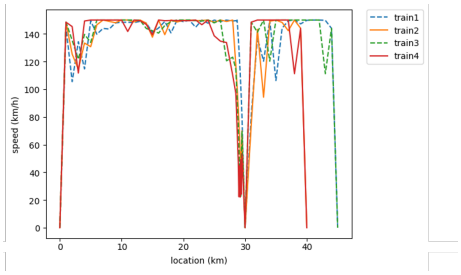

(c) Location-speed profile of test 1

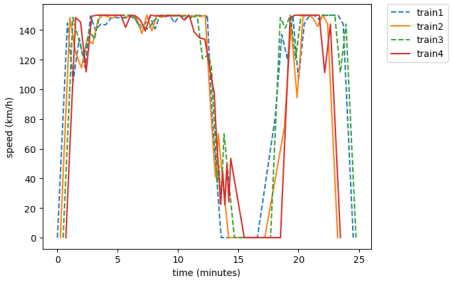

(d) Time-speed profile of test 1

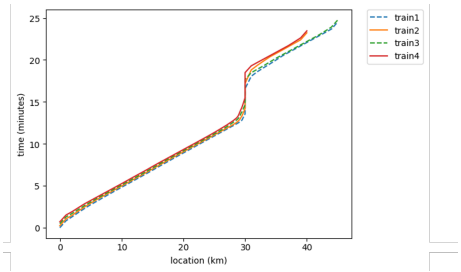

(e) Location-time profile of test 1

Figure A.1: Optimization result of test 1

Result of test 2

The obj1 result is 5337.408 second.The obj2 result is 4252.855 second.

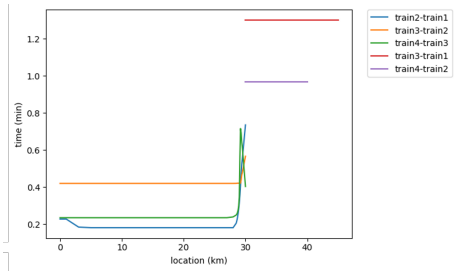

(a) Headway of test 2

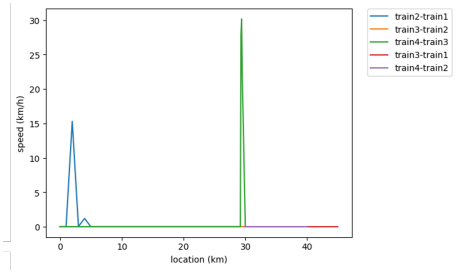

(b) Speed-difference profile of test 2

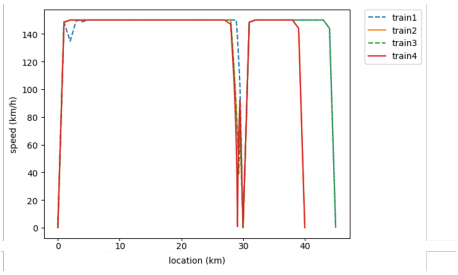

(c) Location-speed profile of test 2

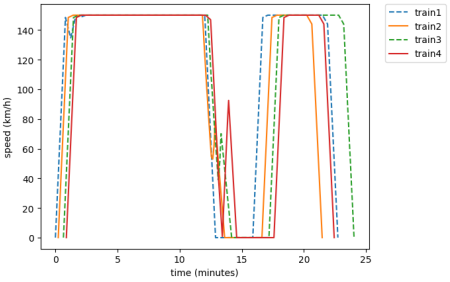

(d) Time-speed profile of test 2

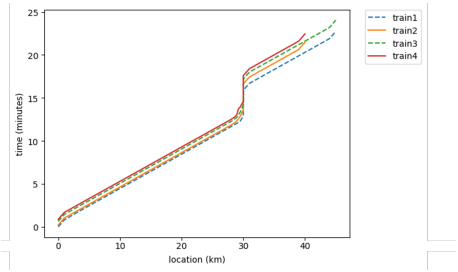

(e) Location-time profile of test 2

Figure A.2: Optimization result of test 2

Result of test 3,4,5

The optimization result of test 3,4 5 are same. The obj1 result is 5337.408 second in same.The obj2 result is 4252.320 second.

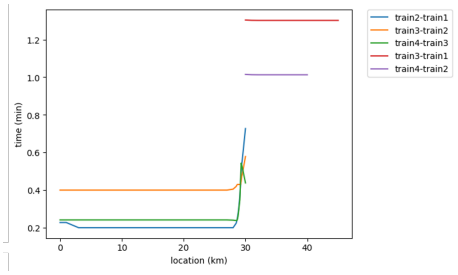

(a) Headway of test 3

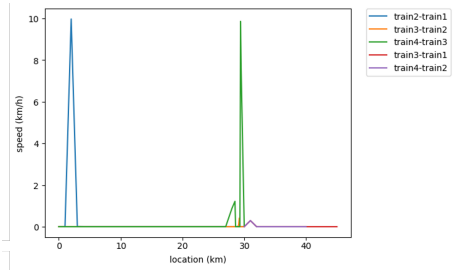

(b) Speed-difference profile of test 3

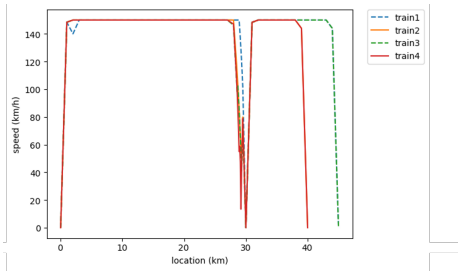

(c) Location-speed profile of test 3

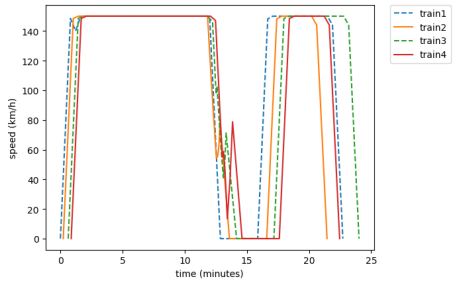

(d) Time-speed profile of test 3

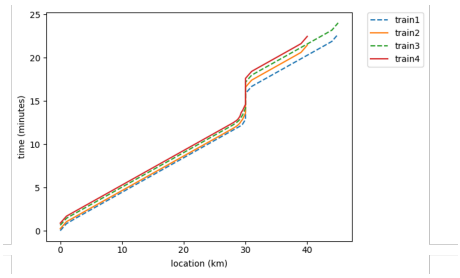

(e) Location-time profile of test 3

Figure A.3: Optimization result of test 3

B RTMIN MODEL

B.1 RESULT OF RTMIN MODEL

B.1.1 Result of trains departing in batch

Result of 4 trains under moving block and virtual coupling

For 4 trains departing in batch, train 1 and train 2 go through the section 0 and section 1, followed by train 3 and train 4 through the section 0 and section 2. The distance from 0 to 30km is the section 0, covered by 4 trains. From 30km to 45km is the section 1 and another track from 30km to 40km is the section 2. The headway, speed-location profile, speed-time profile and time-location profile are shown in the following figures. The figures under moving block are on the left column and the ones under virtual coupling are on the right column.

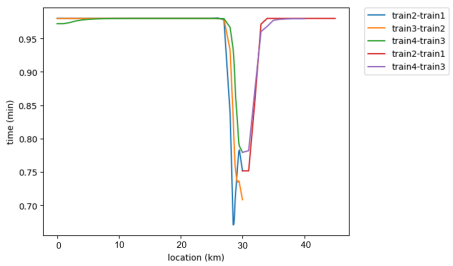

(a) Headway of 4 trains (in batch) (MB) (RTMIN model)

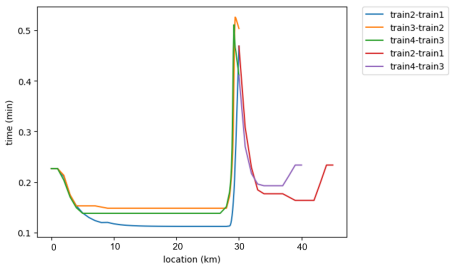

(b) Headway of 4 trains (in batch) (VC) (RTMIN model)

Figure B.1: Headway of 4 trains in batch (RTMIN model)

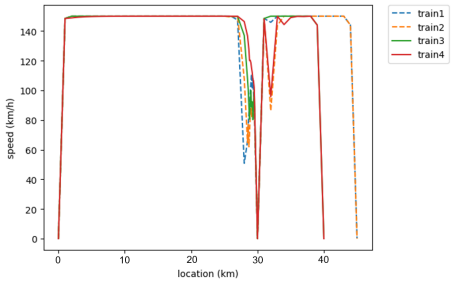

(a) Speed-location profile of 4 trains (in batch) (MB) (RTMIN model)

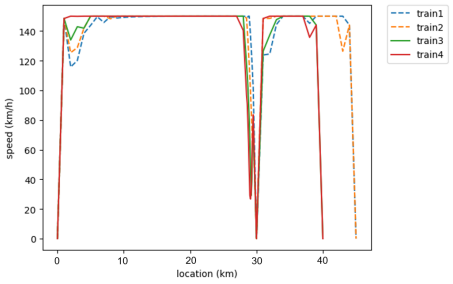

(b) Speed-location profile of 4 trains (in batch) (VC) (RTMIN model)

Figure B.2: Speed-location profile of 4 trains in batch (RTMIN model)

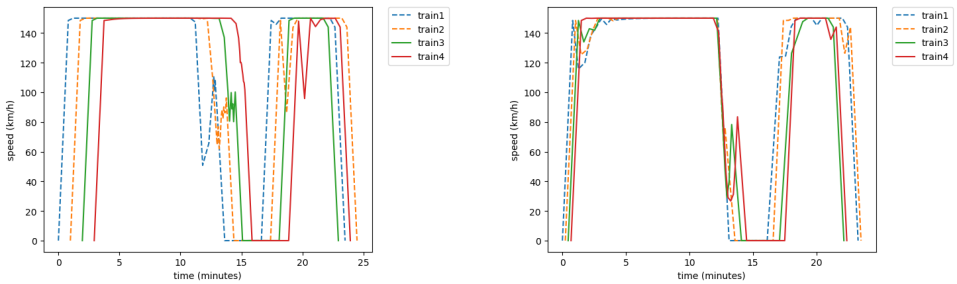

(a) Speed-time profile of 4 trains (in batch) (MB) (RTMIN model)

(b) Speed-time profile of 4 trains (in batch) (VC) (RTMIN model)

Figure B.3: Speed-time profile of 6 trains in batch (RTMIN model)

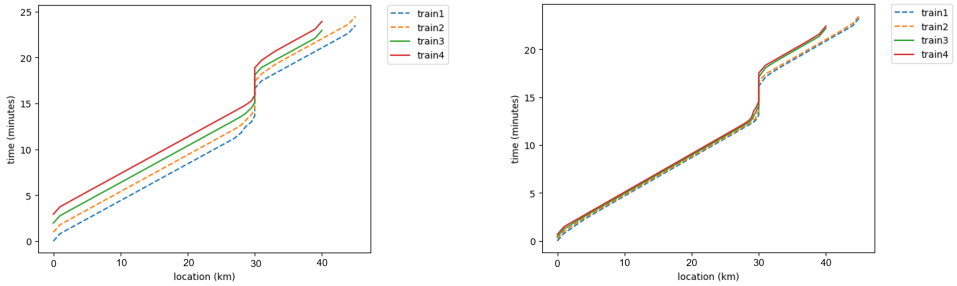

(a) Time-location profile of 4 trains (in batch) (MB) (RTMIN model)

(b) Time-location profile of 4 trains (in batch) (VC) (RTMIN model)

Figure B.4: Time-location profile of 4 trains in batch (RTMIN model)

Result of 8 trains under moving block and virtual coupling

For 8 trains departing in batch, train 1, train 2, train 3 and train 4 go through the section 0 and section 1, followed by train 5, train 6, train 7 and train 8 through the section 0 and section 2. The following is the results output from the RTMIN model for 8 trains. However, the finally optimization result stops at the optimization gap of 60%, which means the results can be further minimizing in concept, while the computation ability does not support it to continue. This reflects the drawback of this model, that if put in too many trains, the variables add in are explosively growing.

The headway, speed-location profile, speed-time profile and time-location profile are shown in the following figures. The figures under moving block are on the left column and the ones under virtual coupling are on the right column.

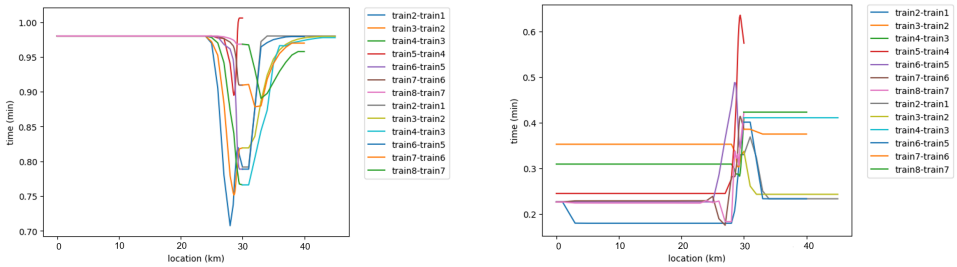

(a) Headway of 8 trains (in batch) (MB) (RTMIN model)

(b) Headway of 8 trains (in batch) (VC) (RTMIN model)

Figure B.5: Headway of 8 trains in batch (RTMIN model)

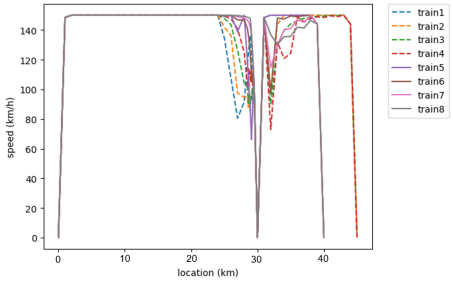

(a) Speed-location profile of 8 trains (in batch) (MB) (RTMIN model)

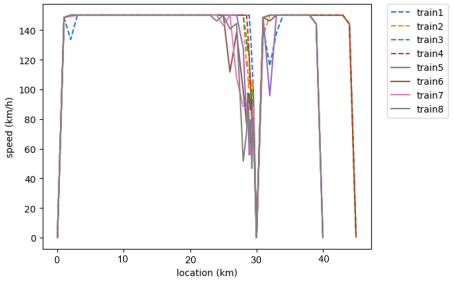

(b) Speed-location profile of 8 trains (in batch) (VC) (RTMIN model)

Figure B.6: Speed-location profile of 8 trains in batch (RTMIN model)

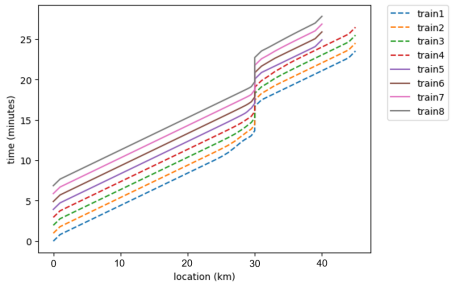

(a) Time-location profile of 8 trains (in batch) (MB) (RTMIN model)

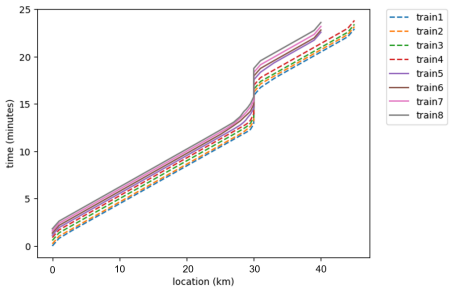

(b) Time-location profile of 8 trains (in batch) (VC) (RTMIN model)

Figure B.7: Time-location profile of 8 trains in batch (RTMIN model)

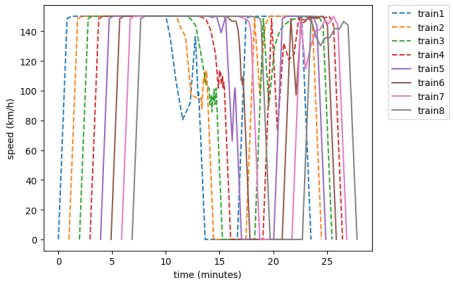

(a) Speed-time profile of 8 trains (in batch) (MB) (RTMIN model)

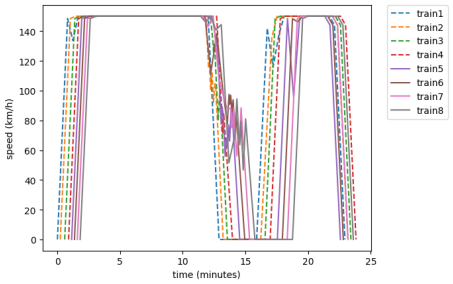

(b) Speed-time profile of 8 trains (in batch) (VC) (RTMIN model)

Figure B.8: Speed-location profile of 8 trains in batch (RTMIN model)

B.1.2 Result of trains departing in turns

Result of 4 trains under moving block and virtual coupling

For 4 trains departing in turns, train 1, train 2, train 3 and train 4 departing in turns. Train 1 and train 3 go through the section 0 and section 1, and train 2 and train 4 go through the section 0 and section 2. The headway, speed-location profile, speed-time profile and time-location profile are shown in the following figures. The figures under moving block are on the left column and the ones under virtual coupling are on the right column.

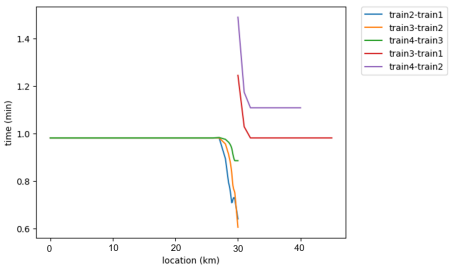

(a) Headway of 4 trains (in turns) (MB) (RTMIN model)

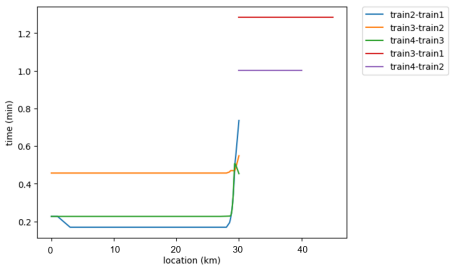

(b) Headway of 4 trains (in turns) (VC) (RTMIN model)

Figure B.9: Headway of 4 trains in turns (RTMIN model)

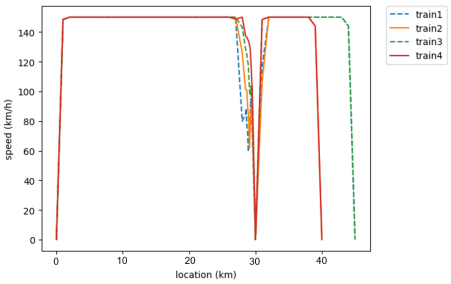

(a) Speed-location profile of 4 trains (in turns) (MB) (RTMIN model)

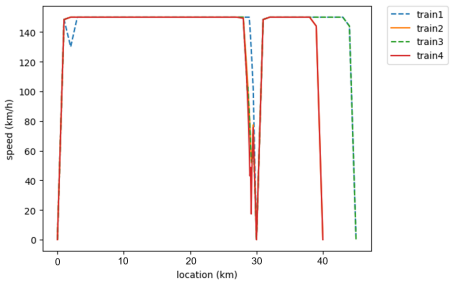

(b) Speed-location profile of 4 trains (in turns) (VC) (RTMIN model)

Figure B.10: Speed-location profile of 4 trains in turns (RTMIN model)

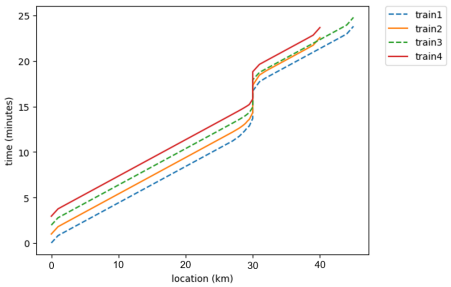

(a) Time-location profile of 4 trains (in turns) (MB) (RTMIN model)

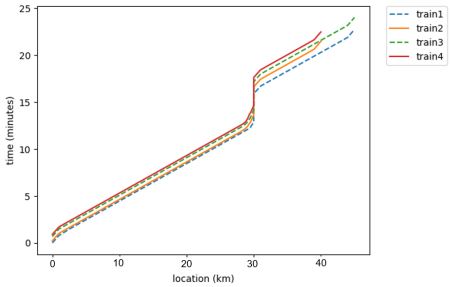

(b) Time-location profile of 4 trains (in turns) (VC) (RTMIN model)

Figure B.11: Speed-location profile of 4 trains in turns (RTMIN model)

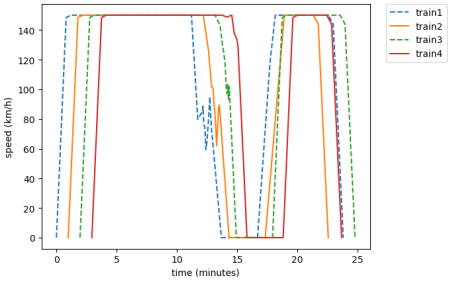

(a) Speed-time profile of 4 trains (in turns) (MB) (RTMIN model)

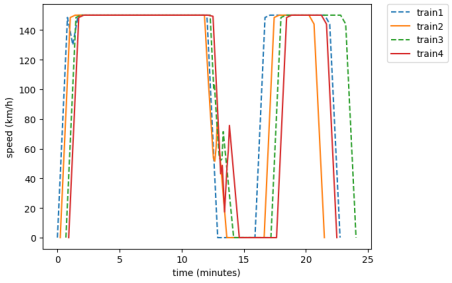

(b) Speed-time profile of 4 trains (in turns) (VC) (RTMIN model)

Figure B.12: Speed-time profile of 4 trains in turns (RTMIN model)

Result of 8 trains under moving block and virtual coupling

For 6 trains departing in turns, train 1, train 2 train 3, train 4, train 5, train 6, train 7 and train 8 departing in turns. Train 1, train 3, train 5 and train 7 go through the section 0 and section 1, and train 2, train 4, train 6 and train 8 through the section 0 and section 2. The headway, speed-location profile, speed-time profile and time-location profile are shown in the following figures. The figures under moving block are on the left column and the ones under virtual coupling are on the right column.

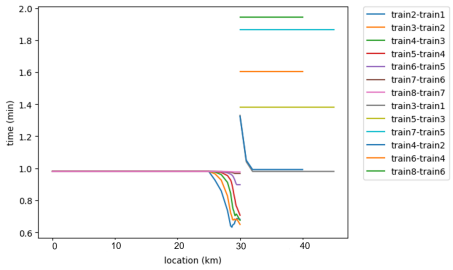

(a) Headway of 8 trains (in turns) (MB) (RTMIN model)

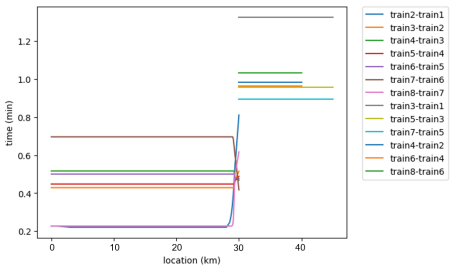

(b) Headway of 8 trains (in turns) (VC) (RTMIN model)

Figure B.13: Headway of 8 trains in turns (RTMIN model)

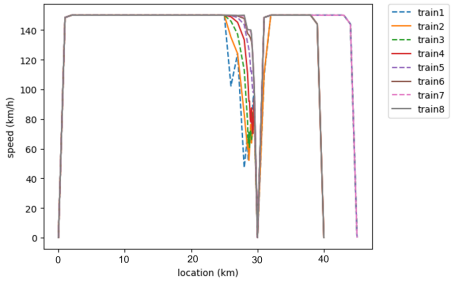

(a) Speed-location profile of 8 trains (in turns) (MB) (RTMIN model)

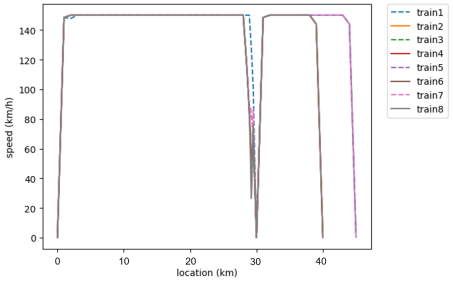

(b) Speed-location profile of 8 trains (in turns) (VC) (RTMIN model)

Figure B.14: Speed-location profile of 8 trains in turns (RTMIN model)

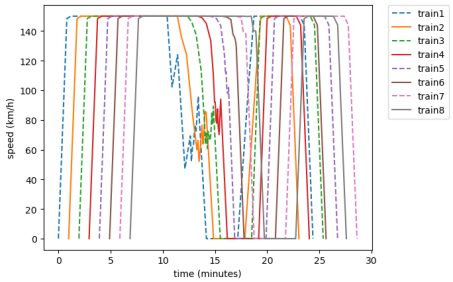

(a) Speed-time profile of 8 trains (in turns) (MB) (RTMIN model)

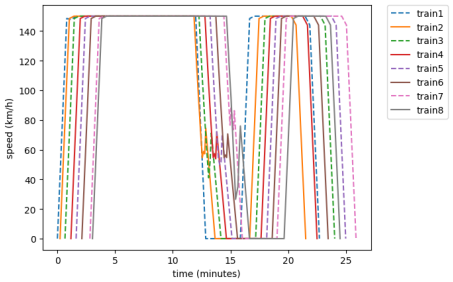

(b) Speed-time profile of 8 trains (in turns) (VC) (RTMIN model)

Figure B.15: Speed-time profile of 8 trains in turns (RTMIN model)

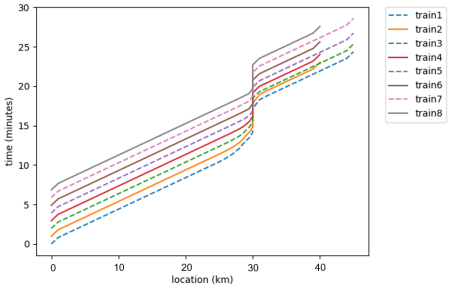

(a) Time-location profile of 8 trains (in turns) (MB) (RTMIN model)

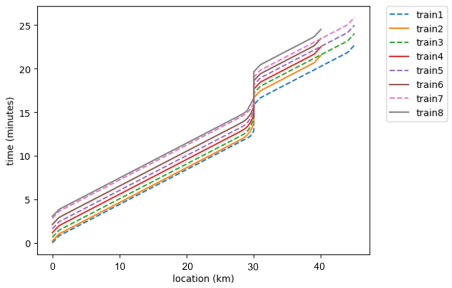

(b) Time-location profile of 8 trains (in turns) (VC) (RTMIN model)

Figure B.16: Time-location profile of 8 trains in turns (RTMIN model)

C ATMIN MODEL RESULT

C.1 RESULT OF TRAINS DEPARTING IN BATCH

Average headway and speed difference of trains departing in batch

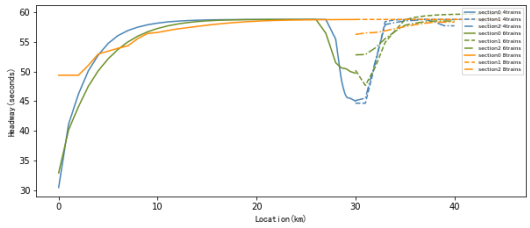

(a) Average headway of 4, 6, 8 trains (in batch) (MB) (ATMIN model)

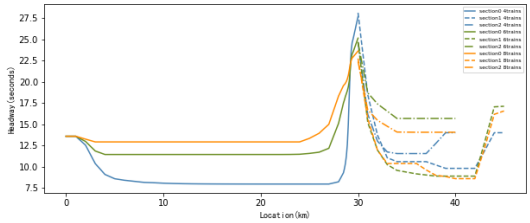

(b) Average headway of 4, 6, 8 trains (in batch) (VC) (ATMIN model)

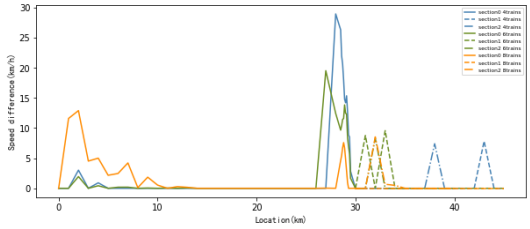

(c) Speed difference of 4, 6, 8 trains (in batch) (MB) (ATMIN model)

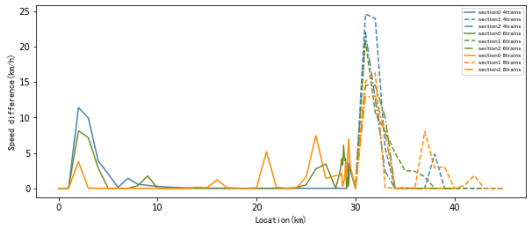

(d) Speed difference of 4, 6, 8 trains (in batch) (MB) (ATMIN model)

Figure C.1: Average headway and speed difference of 4, 6, 8 trains (in batch) (ATMIN model)

Result of 4 trains under moving block and virtual coupling

The headway, speed-location profile, speed-time profile and time-location profile are shown in the below.

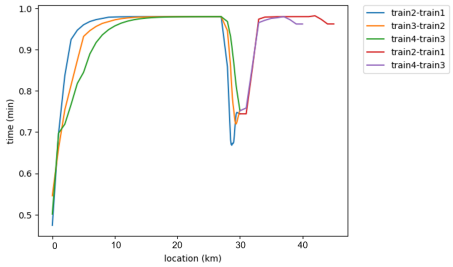

(a) Headway of 4 trains (in batch) (MB) (ATMIN model)

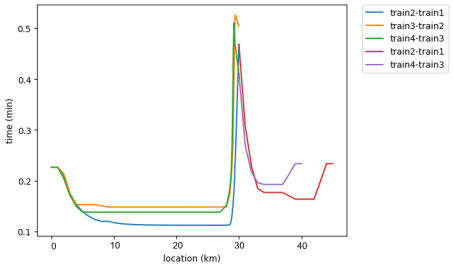

(b) Headway of 4 trains (in batch) (VC) (ATMIN model)

Figure C.2: Headway of 4 trains in batch (RTMIN model)

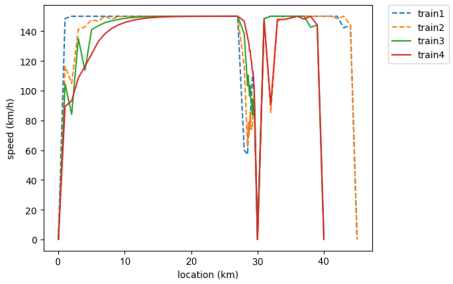

(a) Speed-location profile of 4 trains (in batch) (MB) (ATMIN model)

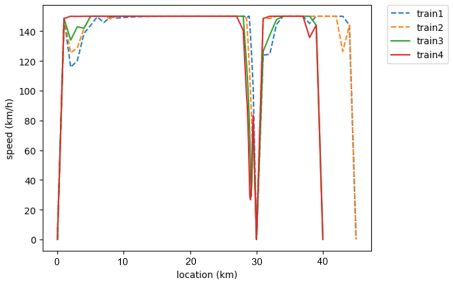

(b) Speed-location profile of 4 trains (in batch) (VC) (ATMIN model)

Figure C.3: Speed-location profile of 4 trains in batch (RTMIN model)

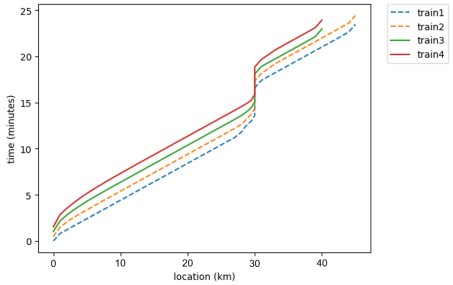

(a) Time-location profile of 4 trains (in batch) (MB) (ATMIN model)

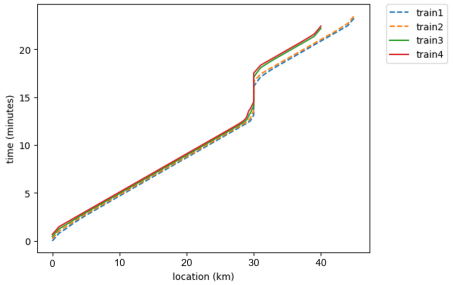

(b) Time-location profile of 4 trains (in batch) (VC) (ATMIN model)

Figure C.4: Time-location profile of 4 trains in batch (ATMIN model)

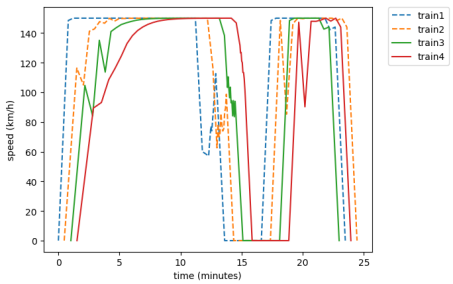

(a) Speed-time profile of 4 trains (in batch) (MB) (ATMIN model)

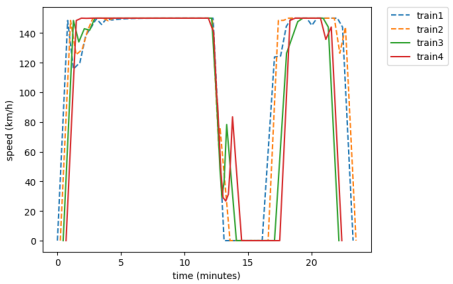

(b) Speed-time profile of 4 trains (in batch) (VC) (ATMIN model)

Figure C.5: Speed-time profile of 4 trains in batch (RTMIN model)

Result of 6 trains under moving block and virtual coupling

The headway, speed-location profile, speed-time profile and time-location profile are shown in the below.

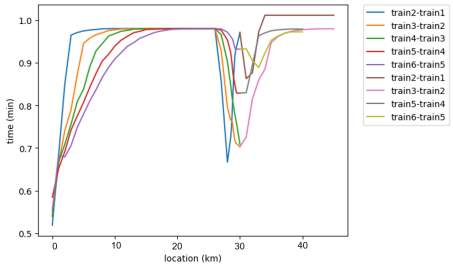

(a) Headway of 6 trains (in batch) (MB) (ATMIN model)

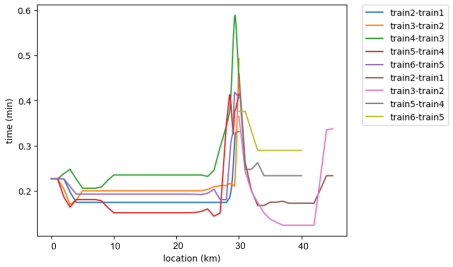

(b) Headway of 6 trains (in batch) (VC) (ATMIN model)

Figure C.6: Headway of 6 trains in batch (RTMIN model)

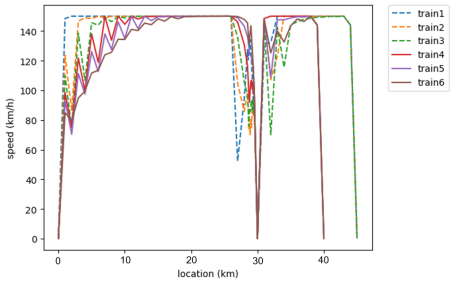

(a) Speed-location profile of 6 trains (in batch) (MB) (ATMIN model)

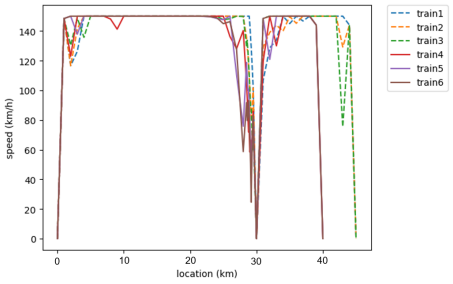

(b) Speed-location profile of 6 trains (in batch) (VC) (ATMIN model)

Figure C.7: Speed-location profile of 6 trains in batch (ATMIN model)

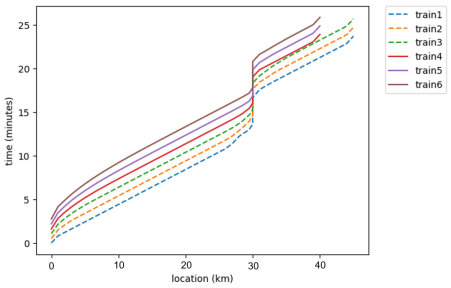

(a) Time-location profile of 6 trains (in batch) (MB) (ATMIN model)

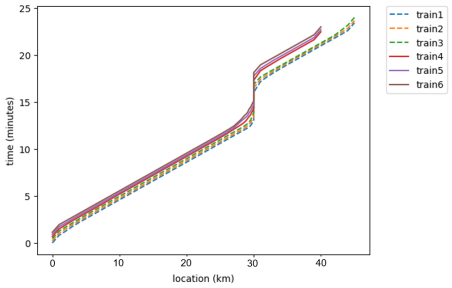

(b) Time-location profile of 6 trains (in batch) (VC) (ATMIN model)

Figure C.8: Time-location profile of 6 trains in batch (ATMIN model)

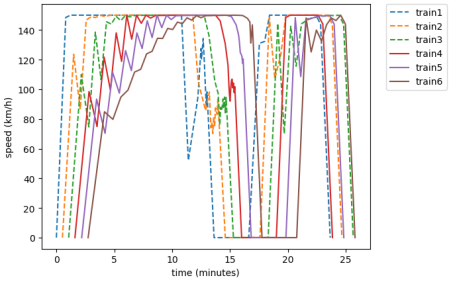

(a) Speed-time profile of 6 trains (in batch) (MB) (ATMIN model)

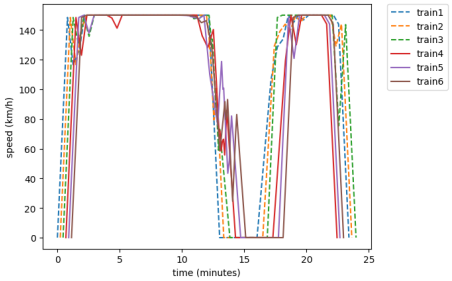

(b) Speed-time profile of 6 trains (in batch) (VC) (ATMIN model)

Figure C.9: Speed-time profile of 6 trains in batch (ATMIN model)

Result of 8 trains under moving block and virtual coupling

The headway, speed-location profile, speed-time profile and time-location profile are shown in the below

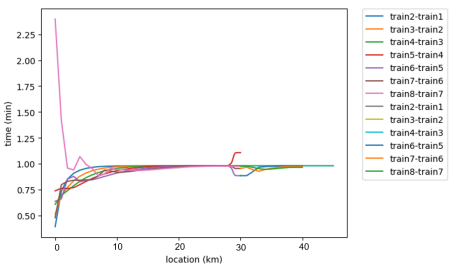

(a) Headway of 8 trains (in batch) (MB) (ATMIN model)

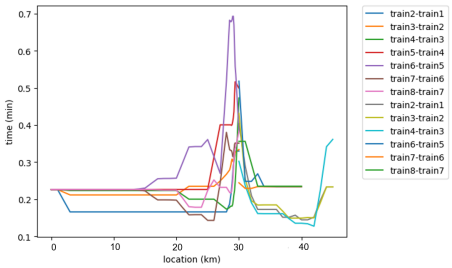

(b) Headway of 8 trains (in batch) (VC) (ATMIN model)

Figure C.10: Headway of 8 trains in batch (ATMIN model)

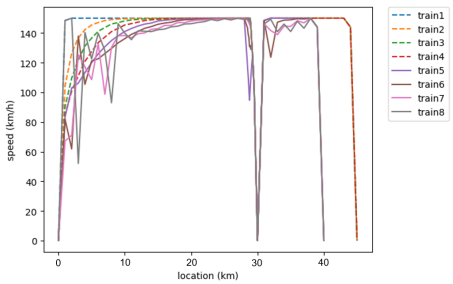

(a) Speed-location profile of 8 trains (in batch) (MB) (ATMIN model)

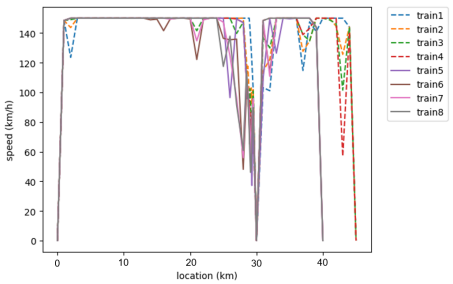

(b) Speed-location profile of 8 trains (in batch) (VC) (ATMIN model)

Figure C.11: Speed-location profile of 8 trains in batch (ATMIN model)

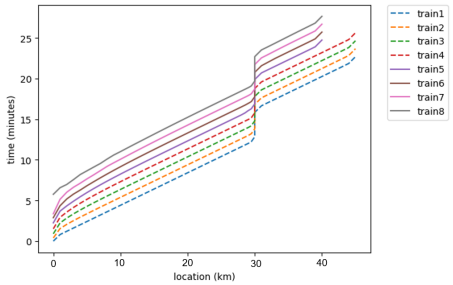

(a) Time-location profile of 8 trains (in batch) (MB) (ATMIN model)

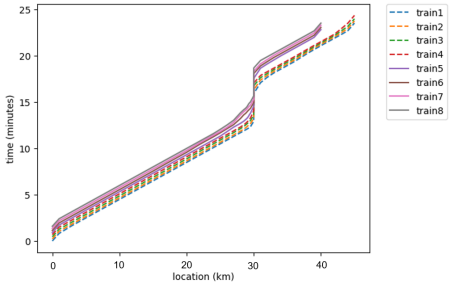

(b) Time-location profile of 8 trains (in batch) (VC) (ATMIN model)

Figure C.12: Time-location profile of 8 trains in batch (ATMIN model)

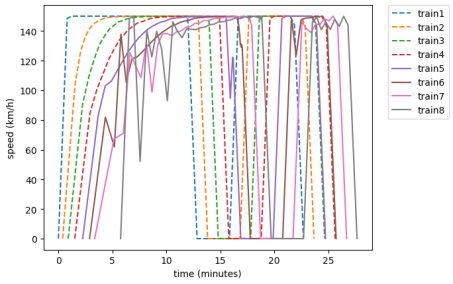

(a) Speed-time profile of 8 trains (in batch) (MB) (ATMIN model)

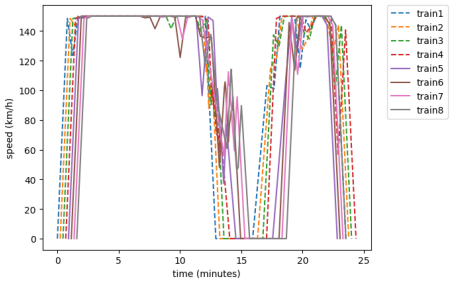

(b) Speed-time profile of 8 trains (in batch) (VC) (ATMIN model)

Figure C.13: Speed-time profile of 8 trains in batch (ATMIN model)

C.2 RESULT OF TRAINS DEPARTING IN TURNS

Average headway and speed difference of trains departing in turns

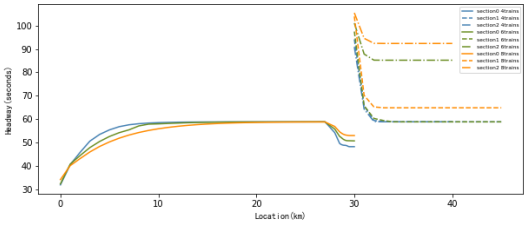

(a) Average headway of 4, 6, 8 trains (in turns) (MB) (ATMIN model)

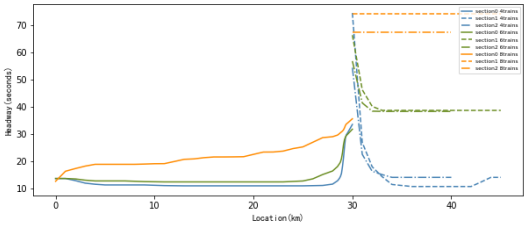

(b) Average headway of 4, 6, 8 trains (in turns) (VC) (ATMIN model)

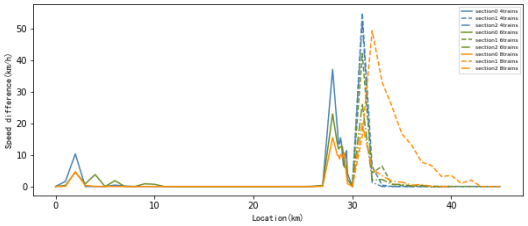

(c) Speed difference of 4, 6, 8 trains (in turns) (MB) (ATMIN model)

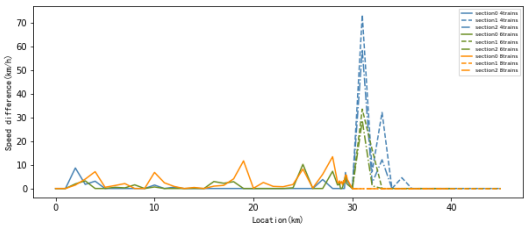

(d) Speed difference of 4, 6, 8 trains (in turns) (VC) (ATMIN model)

Figure C.14: Average headway of 4, 6, 8 trains (in turns) (ATMIN model)

Result of 4 trains under moving block and virtual coupling

The headway, speed-location profile, speed-time profile and time-location profile are shown in the below.

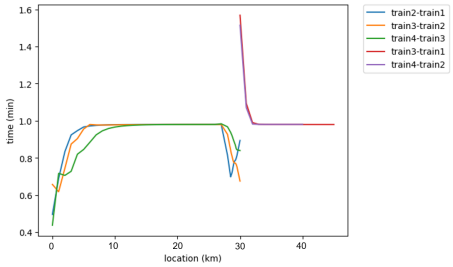

(a) Headway of 4 trains (in turns) (MB) (ATMIN model)

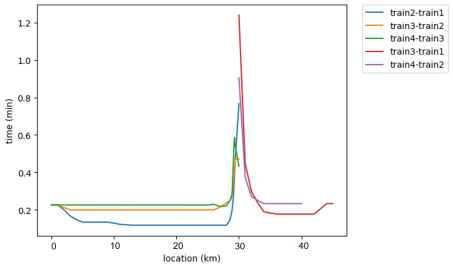

(b) Headway of 4 trains (in turns) (VC) (ATMIN model)

Figure C.15: Headway of 4 trains in batch (ATMIN model)

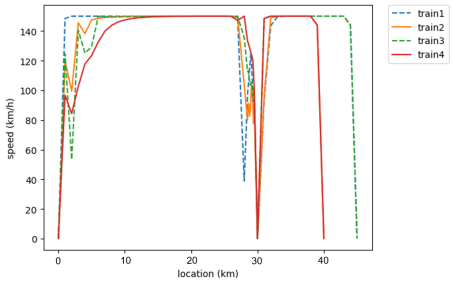

(a) Speed-location profile of 4 trains (in turns) (MB) (ATMIN model)

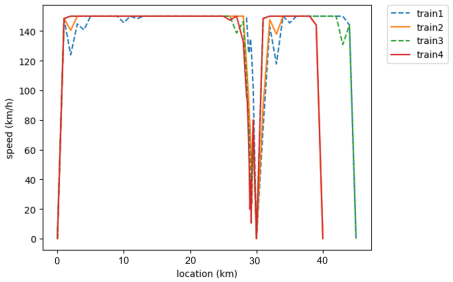

(b) Speed-location profile of 4 trains (in turns) (VC) (ATMIN model)

Figure C.16: Speed-time profile of 8 trains in batch (ATMIN model)

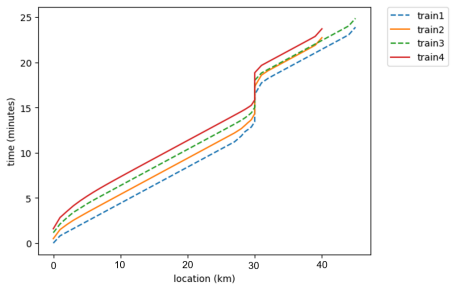

(a) Time-location profile of 4 trains (in turns) (MB) (ATMIN model)

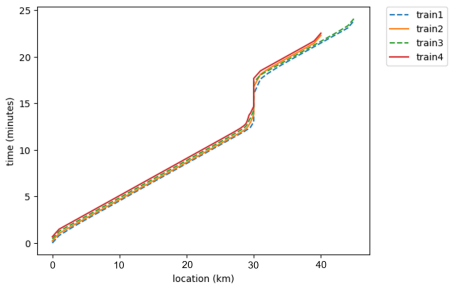

(b) Time-location profile of 4 trains (in turns) (VC) (ATMIN model)

Figure C.17: Time-location profile of 4 trains in batch (ATMIN model)

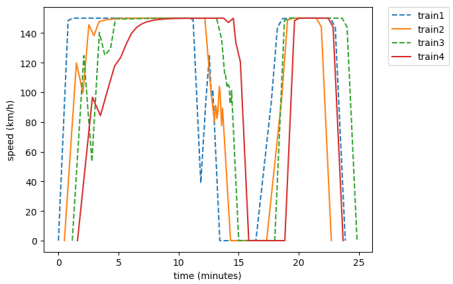

(a) Speed-time profile of 4 trains (in turns) (MB) (ATMIN model)

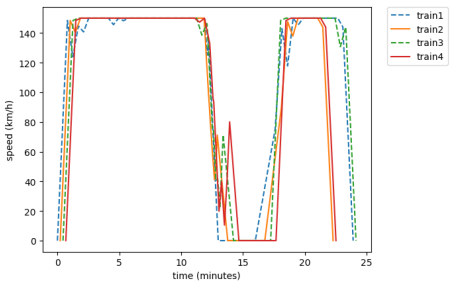

(b) Speed-time profile of 4 trains (in turns) (VC) (ATMIN model)

Figure C.18: Speed-time profile of 4 trains in turns (ATMIN model)

Result of 6 trains under moving block and virtual coupling

The headway, speed-location profile, speed-time profile and time-location profile are shown in the below.

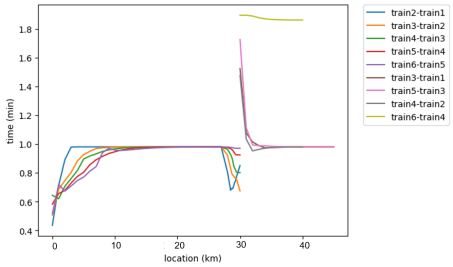

(a) Headway of 6 trains (in turns) (MB) (ATMIN model)

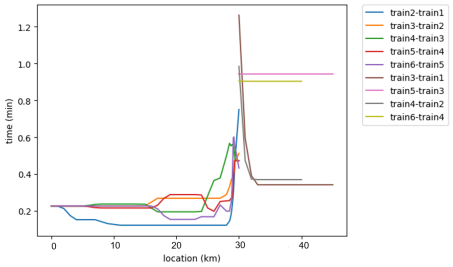

(b) Headway of 6 trains (in turns) (VC) (ATMIN model)

Figure C.19: Headway of 6 trains in turns (ATMIN model)

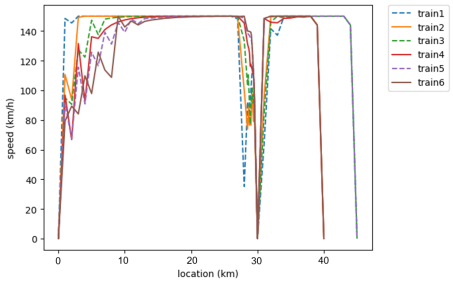

(a) Speed-location profile of 6 trains (in turns) (MB) (ATMIN model)

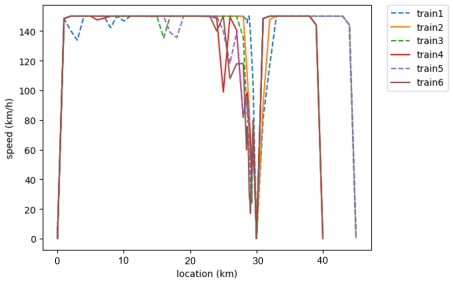

(b) Speed-location profile of 6 trains (in turns) (VC) (ATMIN model)

Figure C.20: Speed-location profile of 6 trains in turns (ATMIN model)

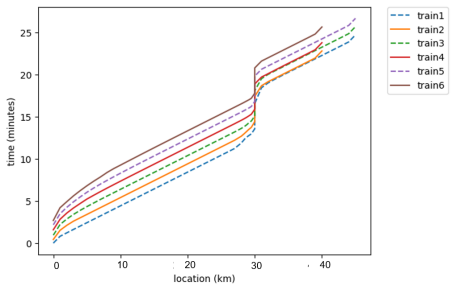

(a) Time-location profile of 6 trains (in turns) (MB) (ATMIN model)

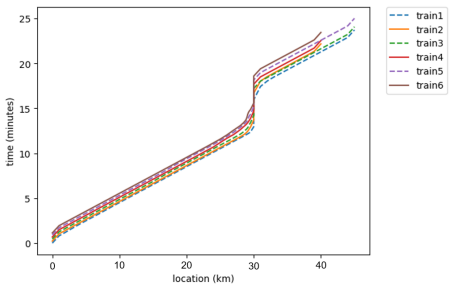

(b) Time-location profile of 6 trains (in turns) (VC) (ATMIN model)

Figure C.21: Time-location profile of 6 trains in turns (ATMIN model)

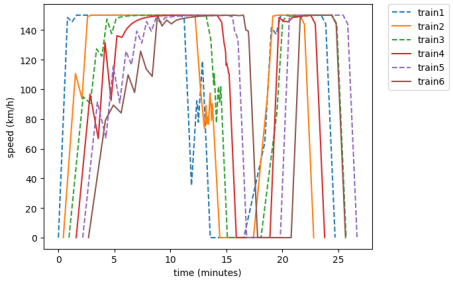

(a) Speed-time profile of 6 trains (in turns) (MB) (ATMIN model)

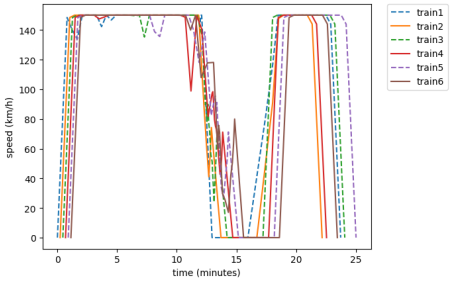

(b) Speed-time profile of 6 trains (in turns) (VC) (ATMIN model)

Figure C.22: Speed-time profile of 6 trains in turns (ATMIN model)

Result of 8 trains under moving block and virtual coupling

The headway, speed-location profile, speed-time profile and time-location profile are shown in the below.

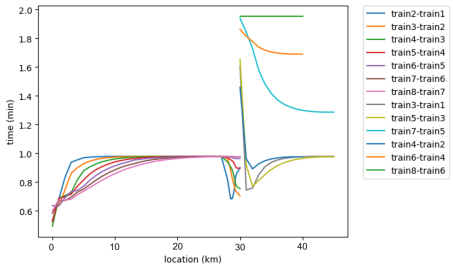

(a) Headway of 8 trains (in turns) (MB) (ATMIN model)

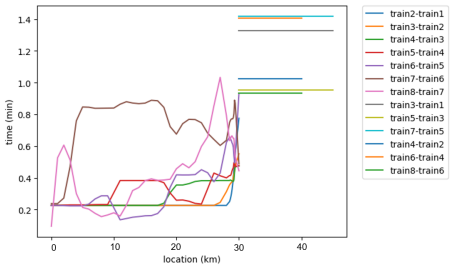

(b) Headway of 8 trains (in turns) (VC) (ATMIN model)

Figure C.23: Headway of 8 trains in turns (ATMIN model)

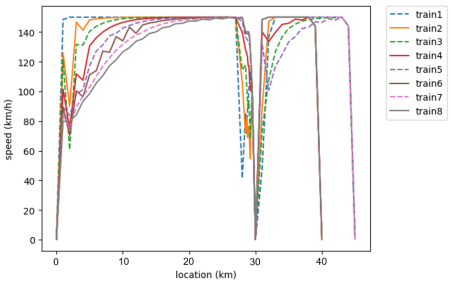

(a) Speed-location profile of 8 trains (in turns) (MB) (ATMIN model)

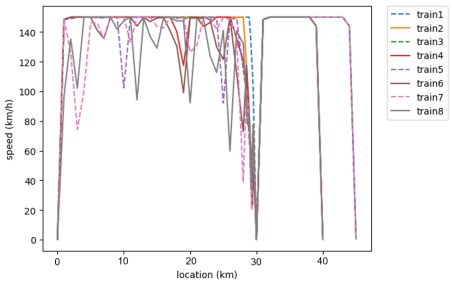

(b) Speed-location profile of 8 trains (in turns) (VC) (ATMIN model)

Figure C.24: Speed-location profile of 8 trains in turns (ATMIN model)

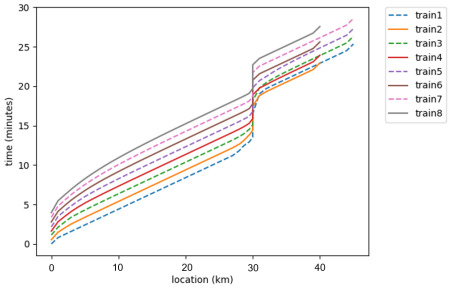

(a) Time-location profile of 8 trains (in turns) (MB) (ATMIN model)

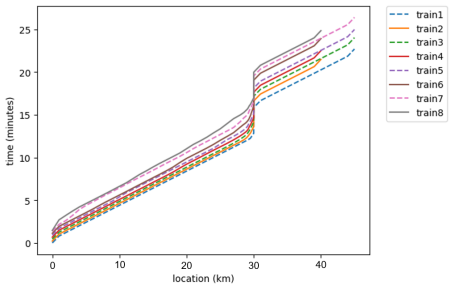

(b) Time-location profile of 8 trains (in turns) (VC) (ATMIN model)

Figure C.25: Time-location profile of 8 trains in turns (ATMIN model)

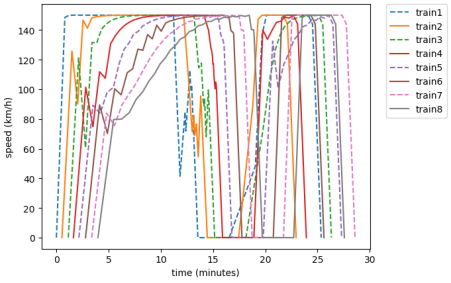

(a) Speed-time profile of 8 trains (in turns) (MB) (ATMIN model)

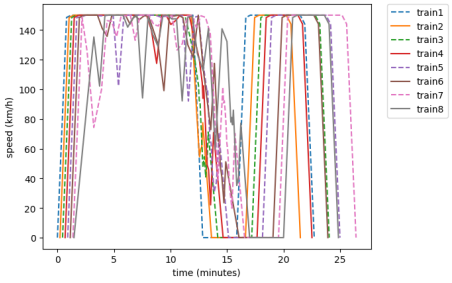

(b) Speed-time profile of 8 trains (in turns) (VC) (ATMIN model)

Figure C.26: Speed-time profile of 8 trains in turns (ATMIN model)

D NUMMAX MODEL RESULT

D.1 RESULT OF TRAINS DEPARTING IN BATCH

Average headway and speed difference of trains departing in batch

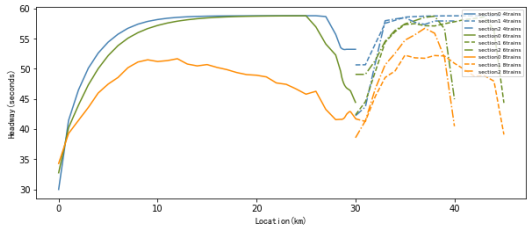

(a) Average headway of 4, 6, 8 trains (in batch) (MB) (NUMMAX model)

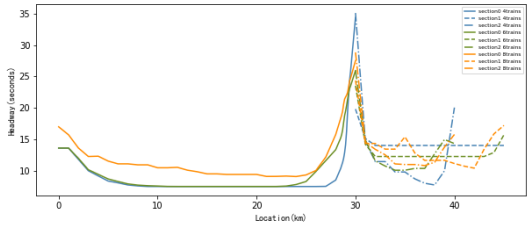

(b) Average headway of 4, 6, 8 trains (in batch) (MB) (NUMMAX model)

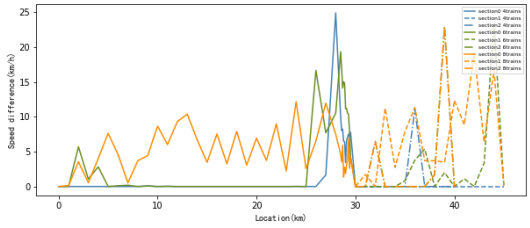

(c) Speed difference of 4, 6, 8 trains (in batch) (MB) (NUMMAX model)

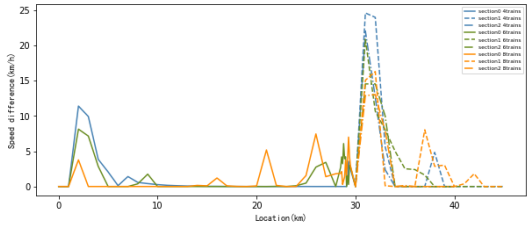

(d) Speed difference of 4, 6, 8 trains (in batch) (MB) (NUMMAX model)

Figure D.1: Average headway and speed difference of 4, 6, 8 trains (in batch) (NUMMAX model)

Result of 4 trains under moving block and virtual coupling

The headway, speed-location profile, speed-time profile and time-location profile are shown in the below.

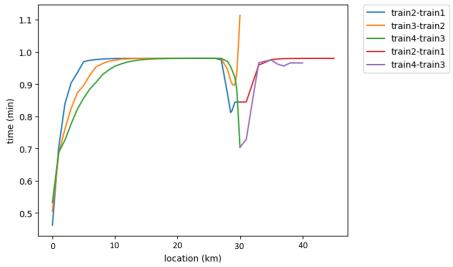

(a) Headway of 4 trains (in batch) (MB) (NUMMAX model)

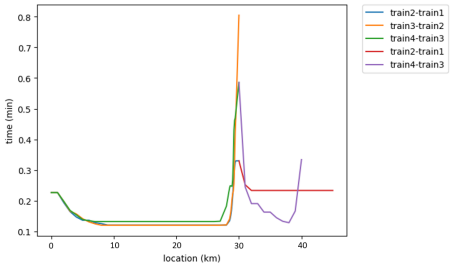

(b) Headway of 4 trains (in batch) (VC) (NUMMAX model)

Figure D.2: Headway of 4 trains in batch (NUMMAX model)

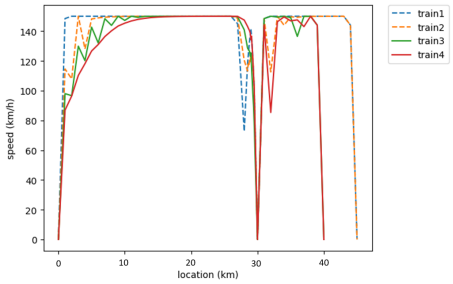

(a) Speed-location profile of 4 trains (in batch) (MB) (NUMMAX model)

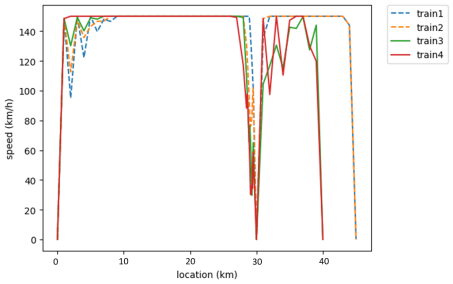

(b) Speed-location profile of 4 trains (in batch) (VC) (NUMMAX model)

Figure D.3: Speed-location profile of 4 trains in batch (NUMMAX model)

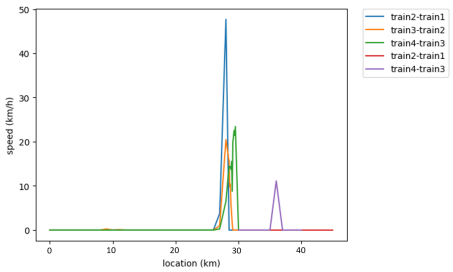

(a) Speed difference of 4 trains (in batch) (MB) (NUMMAX model)

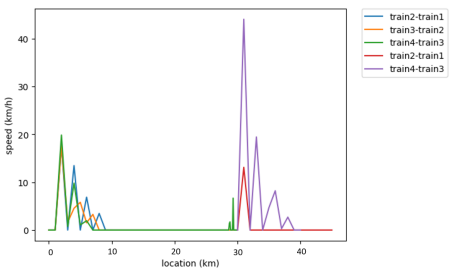

(b) Speed difference of 4 trains (in batch) (VC) (NUMMAX model)

Figure D.4: Speed difference of 4 trains in batch (NUMMAX model)

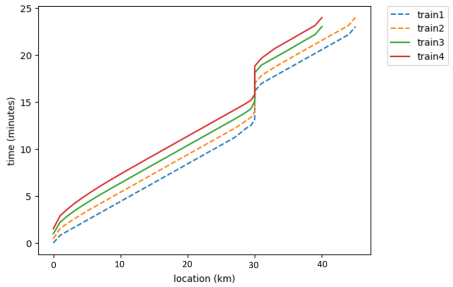

(a) Time-location profile of 4 trains (in batch) (MB) (NUMMAX model)

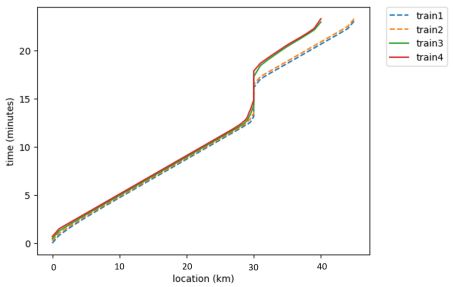

(b) Time-location profile of 4 trains (in batch) (VC) (NUMMAX model)

Figure D.5: Time-location profile of 4 trains in batch (RTMIN model)

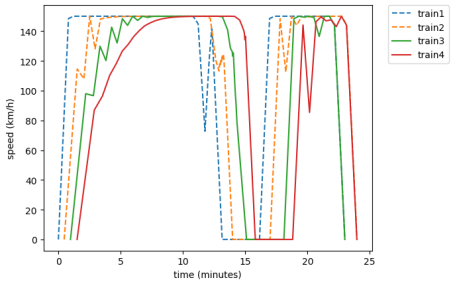

(a) Speed-time profile of 4 trains (in batch) (MB) (NUMMAX model)

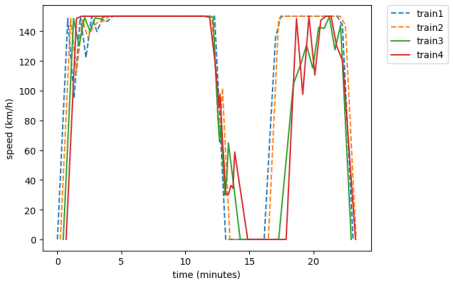

(b) Speed-time profile of 4 trains (in batch) (VC) (NUMMAX model)

Figure D.6: Speed difference of 4 trains in batch (NUMMAX model)

Result of 6 trains under moving block and virtual coupling

The headway, speed-location profile, speed-time profile and time-location profile are shown in the below.

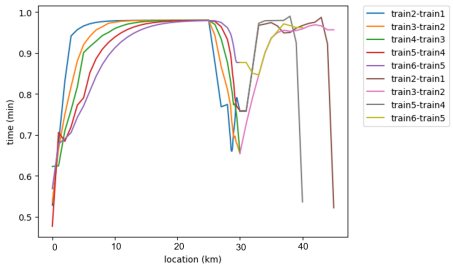

(a) Headway of 6 trains (in batch) (MB) (NUMMAX model)

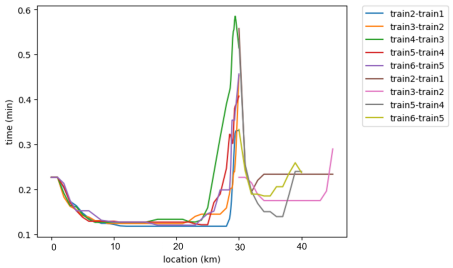

(b) Headway of 6 trains (in batch) (VC) (NUMMAX model)

Figure D.7: Headway of 6 trains in batch (NUMMAX model)

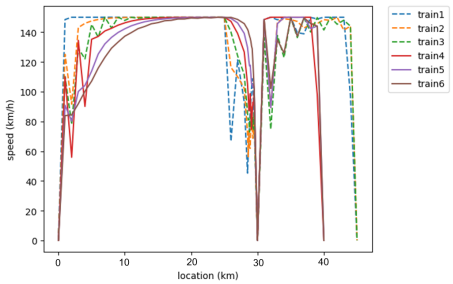

(a) Speed-location profile of 6 trains (in batch) (MB) (NUMMAX model)

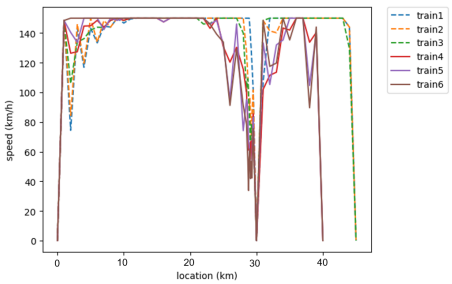

(b) Speed-location profile of 6 trains (in batch) (VC) (NUMMAX model)

Figure D.8: Speed-location profile of 6 trains in batch (NUMMAX model)

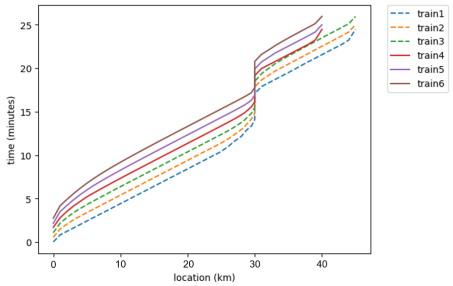

(a) Time-location profile of 6 trains (in batch) (MB) (NUMMAX model)

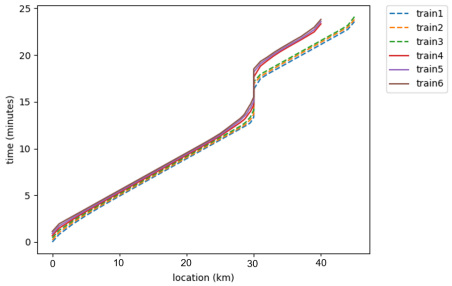

(b) Time-location profile of 6 trains (in batch) (VC) (NUMMAX model)

Figure D.9: Speed-location profile of 6 trains in batch (NUMMAX model)

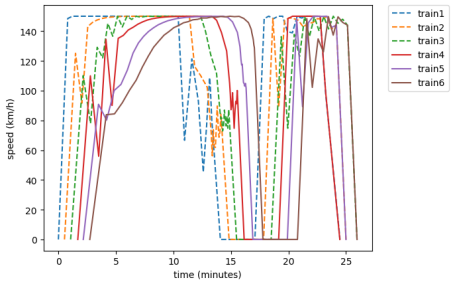

(a) Speed-time profile of 6 trains (in batch) (MB) (NUMMAX model)

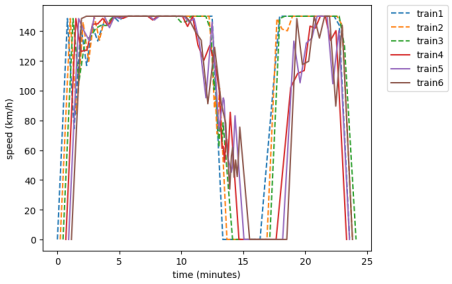

(b) Speed-time profile of 6 trains (in batch) (VC) (NUMMAX model)

Figure D.10: Speed-time profile of 6 trains in batch (NUMMAX model)

Result of 8 trains under moving block and virtual coupling

The headway, speed-location profile, speed-time profile and time-location profile are shown in the below.

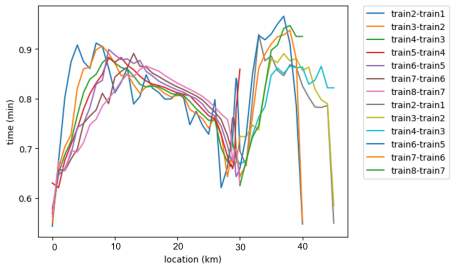

(a) Headway of 8 trains (in batch) (MB) (NUMMAX model)

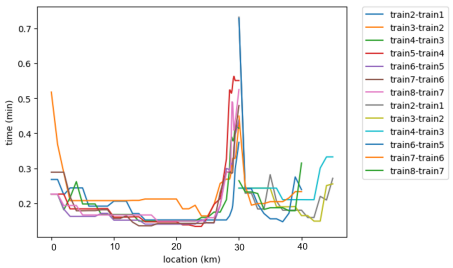

(b) Headway of 8 trains (in batch) (VC) (NUMMAX model)

Figure D.11: Headway of 8 trains in batch (NUMMAX model)

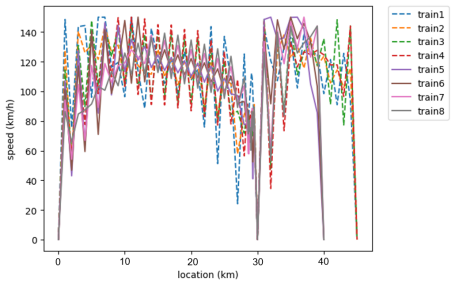

(a) Speed-location profile of 8 trains (in batch) (MB) (NUMMAX model)

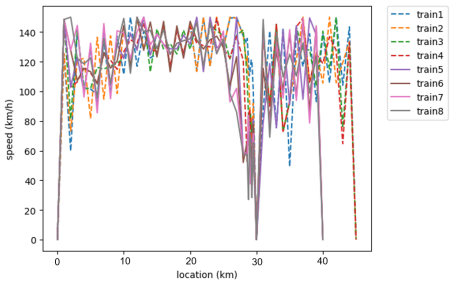

(b) Speed-location profile of 8 trains (in batch) (VC) (NUMMAX model)

Figure D.12: Speed-location profile of 8 trains in batch (NUMMAX model)

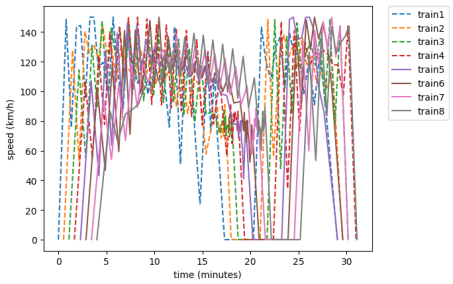

(a) Speed-time profile of 8 trains (in batch) (MB) (NUMMAX model)

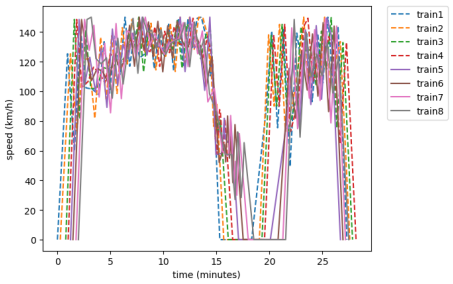

(b) Speed-time profile of 8 trains (in batch) (VC) (NUMMAX model)

Figure D.13: Speed-time profile of 8 trains in batch (NUMMAX model)

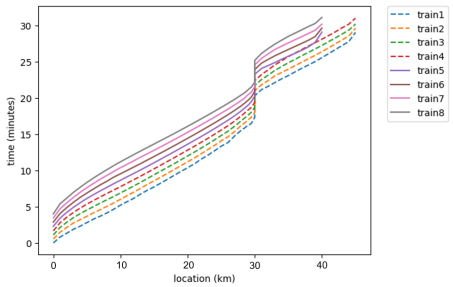

(a) Time-location profile of 8 trains (in batch) (MB) (NUMMAX model)

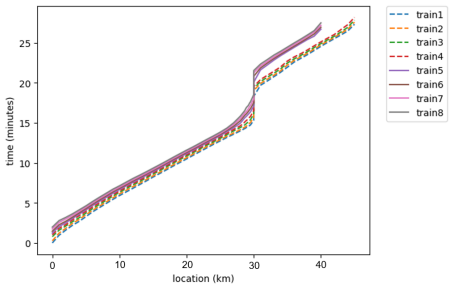

(b) Time-location profile of 8 trains (in batch) (VC) (NUMMAX model)

Figure D.14: Time-location profile of 8 trains in batch (NUMMAX model)

D.2 RESULT OF TRAINS DEPARTING IN TURNS

Average headway and speed difference of trains departing in turns

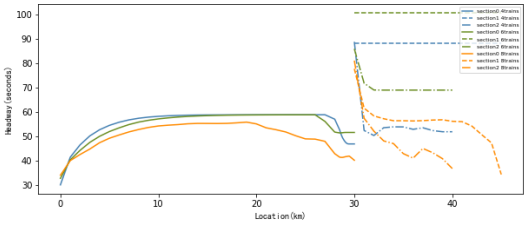

(a) Average headway of 4, 6, 8 trains (in turns) (MB) (NUMMAX model)

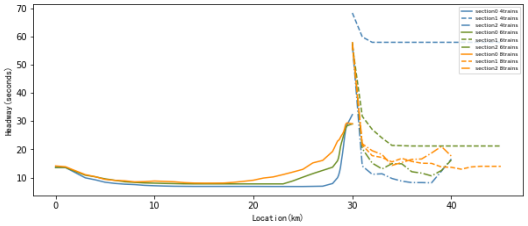

(b) Average headway of 4, 6, 8 trains (in turns) (MB) (NUMMAX model)

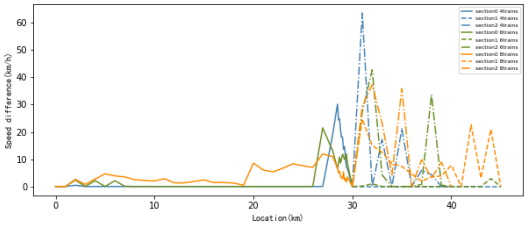

(c) Average speed difference of 4, 6, 8 trains (in turns) (MB) (NUMMAX model)

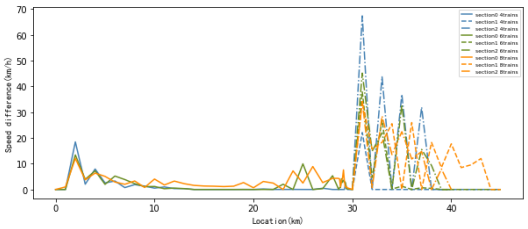

(d) Speed difference of 4, 6, 8 trains (in batch) (MB) (NUMMAX model)

Figure D.15: Average headway and speed difference of 4, 6, 8 trains (in turns) (NUMMAX model)

Result of 4 trains under moving block and virtual coupling

The headway, speed-location profile, speed-time profile and time-location profile are shown in the below.

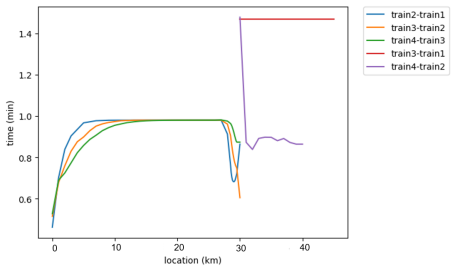

(a) Headway of 4 trains (in turns) (MB) (NUMMAX model)

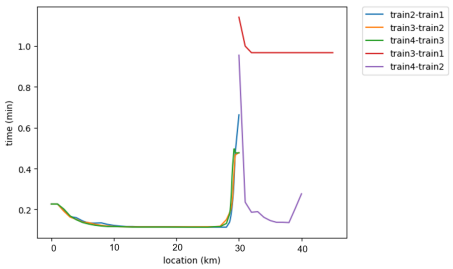

(b) Headway of 4 trains (in turns) (VC) (NUMMAX model)

Figure D.16: Headway profile of 4 trains in turns (NUMMAX model)

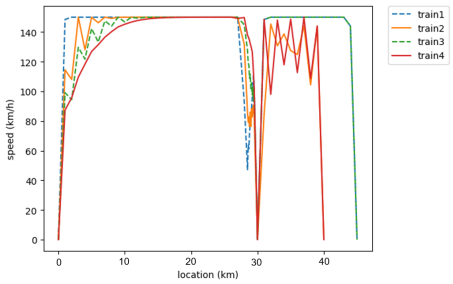

(a) Speed-location profile of 4 trains (in turns) (MB) (NUMMAX model)

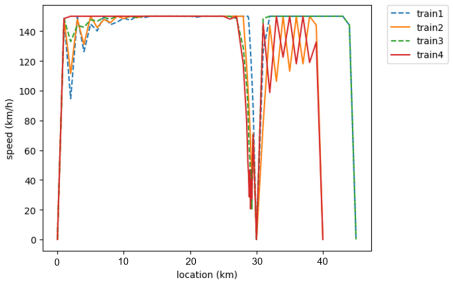

(b) Speed-location profile of 4 trains (in turns) (VC) (NUMMAX model)

Figure D.17: Speed-location profile of 4 trains in turns (NUMMAX model)

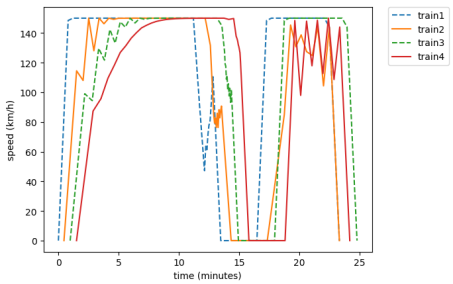

(a) Speed-time profile of 4 trains (in turns) (MB) (NUMMAX model)

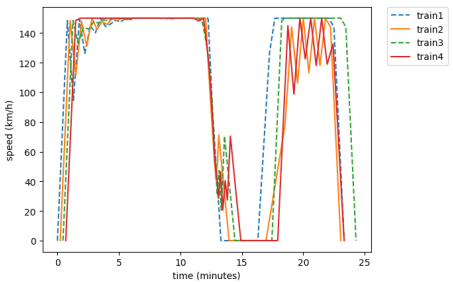

(b) Speed-time profile of 4 trains (in turns) (VC) (NUMMAX model)

Figure D.18: Speed-time profile of 4 trains in turns (NUMMAX model)

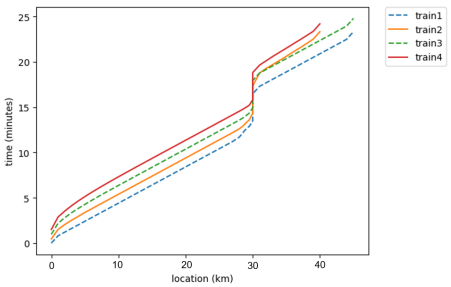

(a) Time-location profile of 4 trains (in turns) (MB) (NUMMAX model)

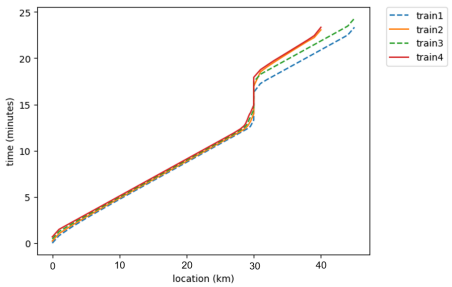

(b) Time-location profile of 4 trains (in turns) (VC) (NUMMAX model)

Figure D.19: Time-location profile of 4 trains in turns (NUMMAX model)

Result of 6 trains under moving block and virtual coupling

The headway, speed-location profile, speed-time profile and time-location profile are shown in the below.

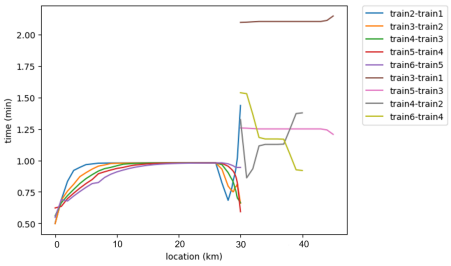

(a) Headway of 6 trains (in turns) (MB) (NUMMAX model)

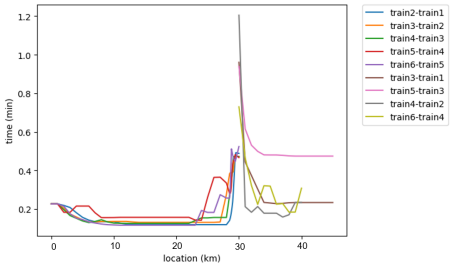

(b) Headway of 6 trains (in turns) (VC) (NUMMAX model)

Figure D.20: Headway of 6 trains in turns (NUMMAX model)

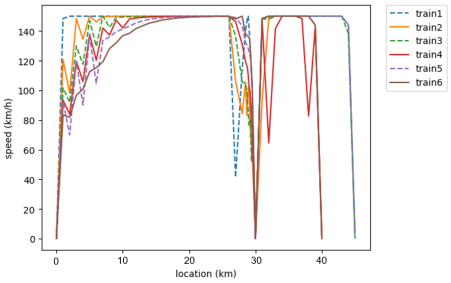

(a) Speed-location profile of 6 trains (in turns) (MB) (NUMMAX model)

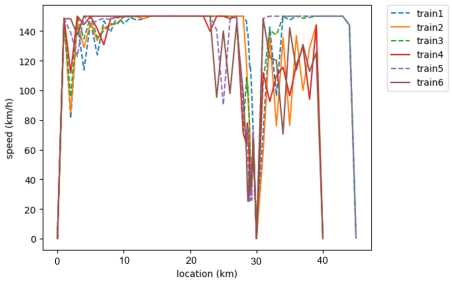

(b) Speed-location profile of 6 trains (in turns) (VC) (NUMMAX model)

Figure D.21: Speed-location profile of 6 trains in turns (NUMMAX model)

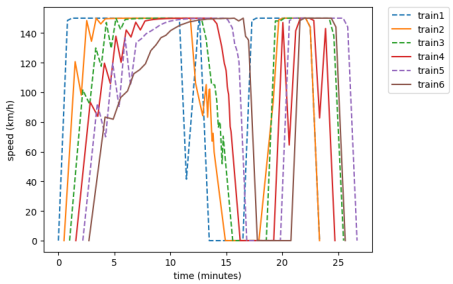

(a) Speed-time profile of 6 trains (in turns) (MB) (NUMMAX model)

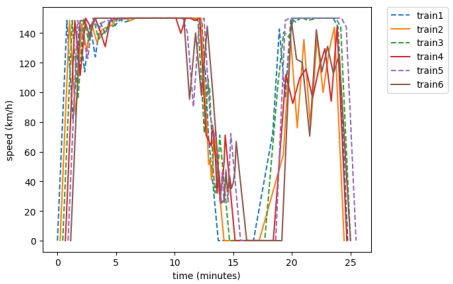

(b) Speed-time profile of 6 trains (in turns) (VC) (NUMMAX model)

Figure D.22: Speed-time profile of 6 trains in turns (NUMMAX model)

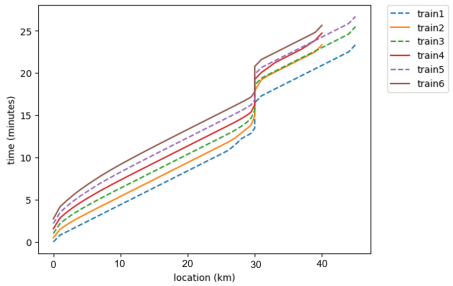

(a) Time-location profile of 6 trains (in turns) (MB) (NUMMAX model)

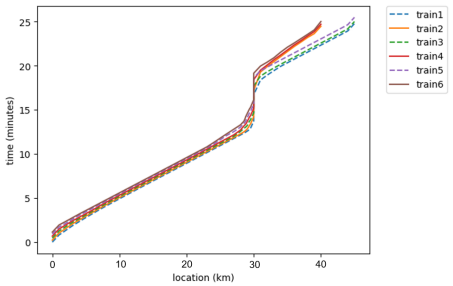

(b) Time-location profile of 6 trains (in turns) (VC) (NUMMAX model)

Figure D.23: Speed-location profile of 6 trains in turns (NUMMAX model)

Result of 8 trains under moving block and virtual coupling

The headway, speed-location profile, speed-time profile and time-location profile are shown in the below.

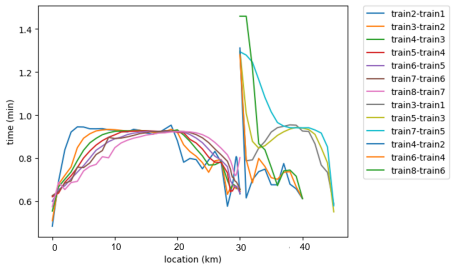

(a) Headway of 8 trains (in turns) (MB) (NUMMAX model)

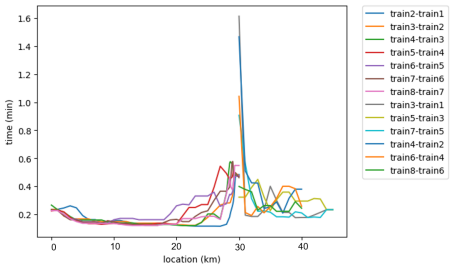

(b) Headway of 8 trains (in turns) (VC) (NUMMAX model)

Figure D.24: Headway of 8 trains in turns (NUMMAX model)

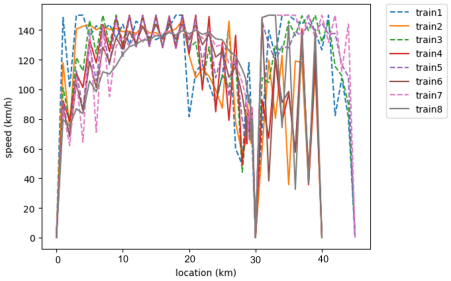

(a) Speed-location profile of 8 trains (in turns) (MB) (NUMMAX model)

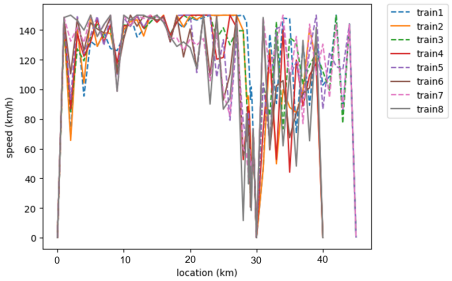

(b) Speed-location profile of 8 trains (in turns) (VC) (NUMMAX model)

Figure D.25: Speed-location profile of 8 trains in turns (NUMMAX model)

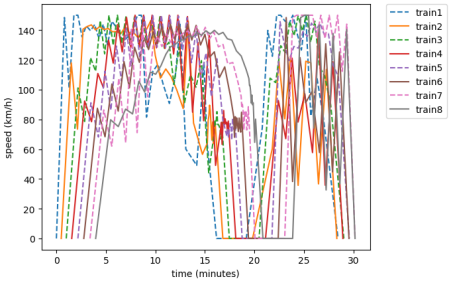

(a) Speed-time profile of 8 trains (in turns) (MB) (NUMMAX model)

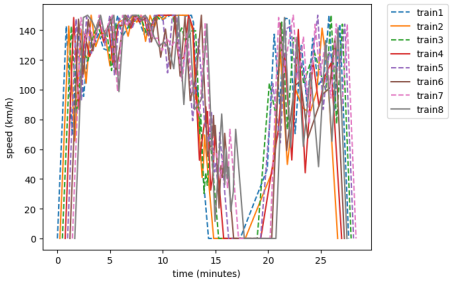

(b) Speed-time profile of 8 trains (in turns) (VC) (NUMMAX model)

Figure D.26: Speed-time profile of 8 trains in turns (NUMMAX model)

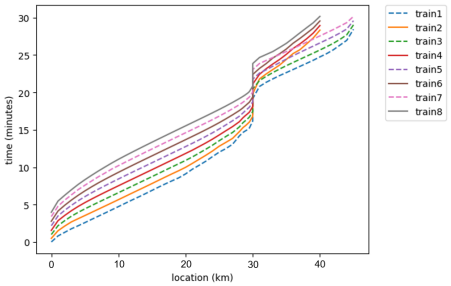

(a) Time-location profile of 8 trains (in turns) (MB) (NUMMAX model)

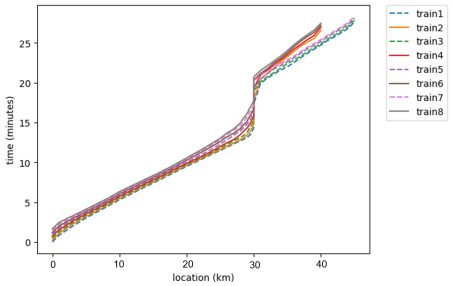

(b) Time-location profile of 8 trains (in turns) (VC) (NUMMAX model)

Figure D.27: Time-location profile of 8 trains in turns (NUMMAX model)

E OPTIMIZATION RESULT OF VARYING THE SERVICE BRAKING RATE

The location-speed profile of the 6 scenarios are shown below. Comparing the scenario 1-1 and 1-2 to 1-0, the leader of a convoy has less braking at the departing area.

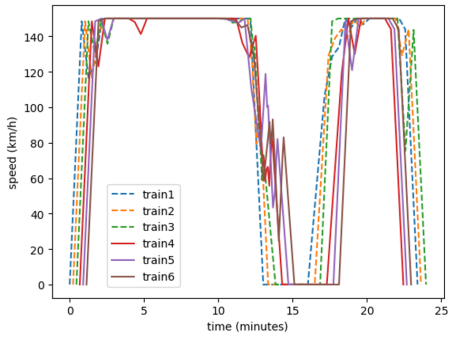

(a) Time-speed profile of scenario 1-0

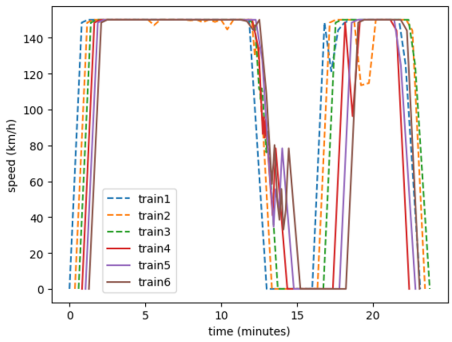

(b) Time-speed profile of scenario 1-1

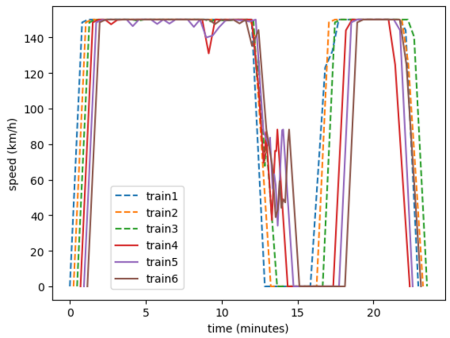

(c) Time-speed profile of scenario 1-2

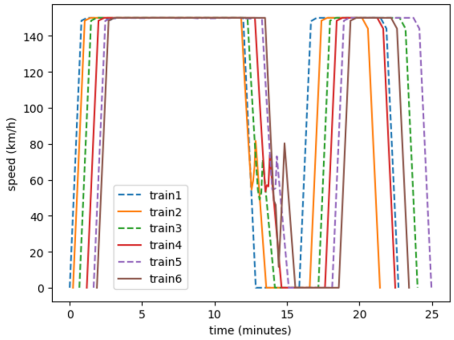

(d) Time-speed profile of scenario 2-0

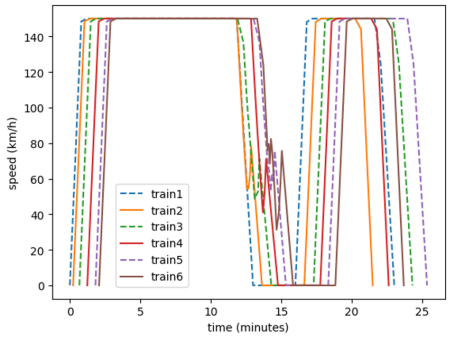

(e) Time-speed profile of scenario 2-1

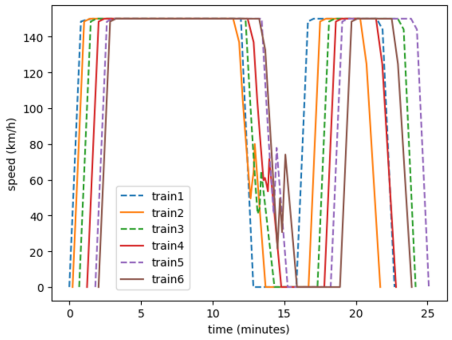

(f) Time-speed profile of scenario 2-2

Figure E.1: Time-speed profile

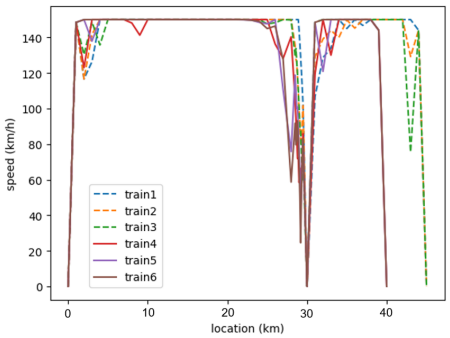

(a) location-speed profile of scenario 1-0

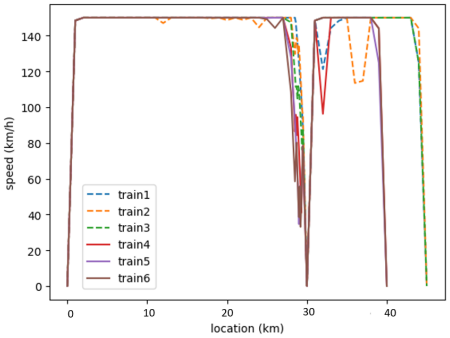

(b) location-speed profile of scenario 1-1

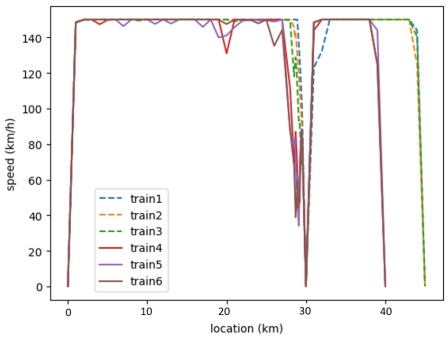

(c) location-speed profile of scenario 1-2

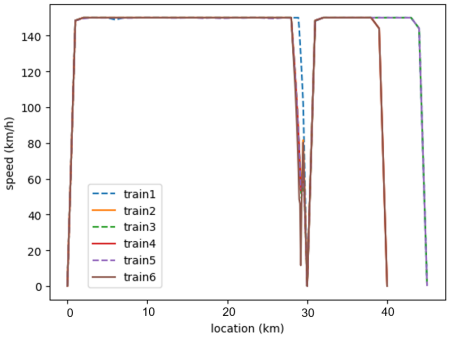

(d) location-speed profile of scenario 2-0

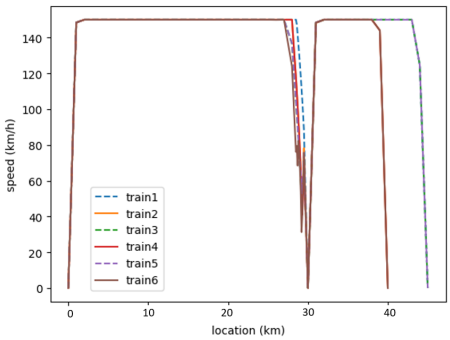

(e) location-speed profile of scenario 2-1

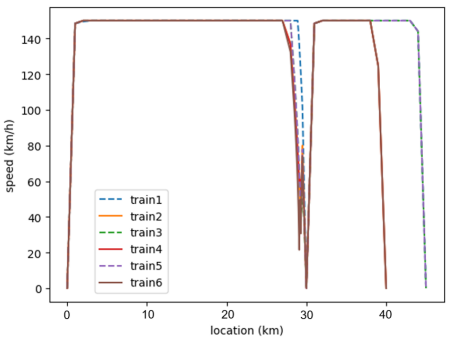

(f) location-speed profile of scenario 2-2

Figure E.2: location-speed profile

F OPTIMIZATION RESULT WITH SPEED LIMIT

The details of the trains operation including the speed-time profile and time-location profile are shown in below.

F.1 RESULT OF THE SPEED LIMIT TEST FOR TRAINS IN BATCH

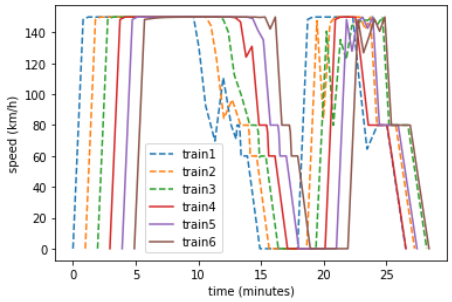

(a) speed-time profile of trains (in batch) (MB) (with speed limit)

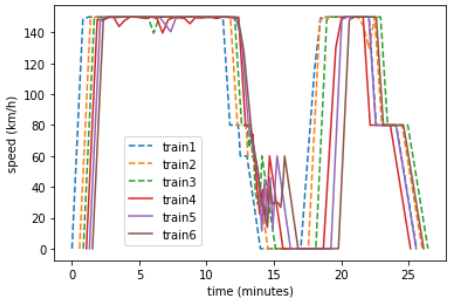

(b) speed-time profile of trains (in batch) (VC) (with speed limit)

Figure F.1: Speed-time profile of trains in batch (with speed limit)

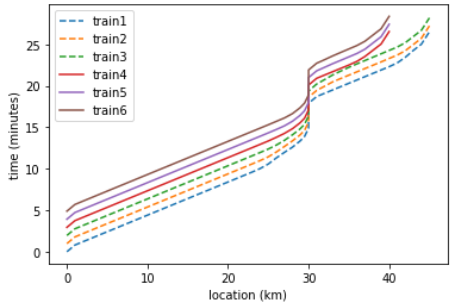

(a) Time-location profile of trains (in batch) (MB) (with speed limit)

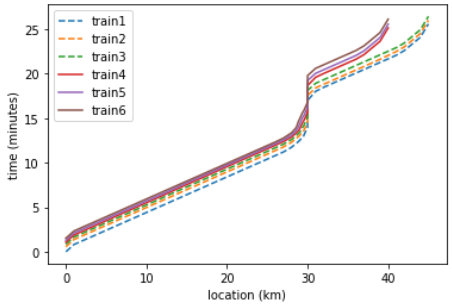

(b) Time-location profile of trains (in batch) (VC) (with speed limit)

Figure F.2: Time-location profile of trains in batch (with speed limit)

F.2 RESULT OF THE SPEED LIMIT TEST FOR TRAINS IN TURNS

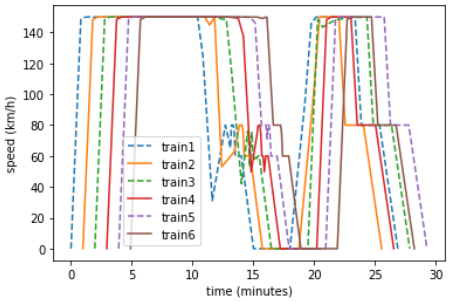

(a) Time-speed profile of trains (in turns) (MB) (with speed limit)

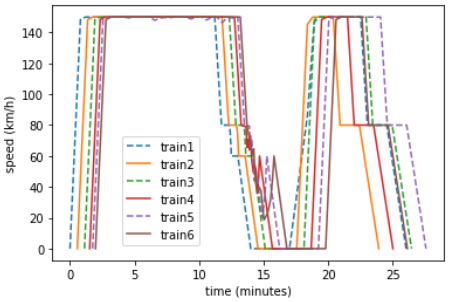

(b) Time-speed profile of trains (in turns) (VC) (with speed limit)

Figure F.3: Time-speed profile of trains in batch (with speed limit)

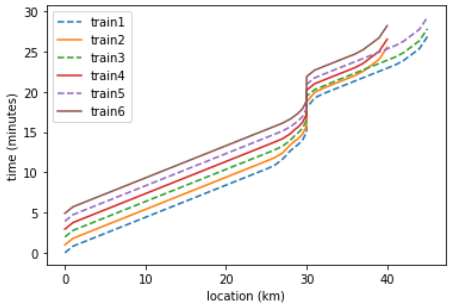

(a) Time-location profile of trains (in turns) (MB) (with speed limit)

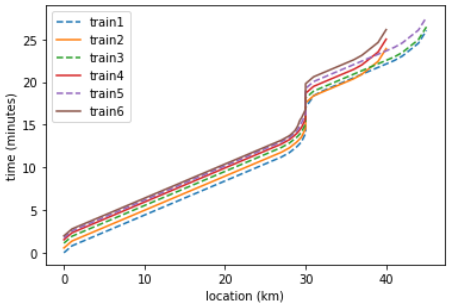

(b) Time-location profile of trains (in turns) (VC) (with speed limit)

Figure F.4: Time-location profile of trains in batch (with speed limit)